Effects of acid concentration on the extraction of rare earth elements from South African Coal Fly Ash.

UNIVERSITY *of the*
WESTERN CAPE

By

Kamohelo Mokoena

Supervisor: Dr Sumaya Clarke

Co-supervisor: Dr Lehlohonolo Sehai Mokhahlane

A thesis submitted in fulfilment of the requirement for the degree of Magister Scientiae

In

Environmental and Water Science in the Department of Earth Science
Faculty of Natural Sciences at the University of the Western Cape

2021

Declaration

I declare "Effects of acid concentration on the extraction of rare earth elements from South African Coal Fly Ash" is my own work, that it has not been submitted for any degree or examination in any other university, and that all the sources I have used or quoted have been indicated and acknowledge by complete references.

Full name: Kamohelo Mokoena

Signed:

Date: October 2021

Abstract

Coal is seen as a reliable and secure energy source in many countries around the world despite the development of a number of alternative sources of energy. A rise in global energy demand has led to an increase in coal consumption. Consequently, global coal fly ash (CFA) production has increased creating a pressing need for recycling and utilisation of coal fly ash. South Africa produces 50 million tons of ash per year from coal combustion with only about 10 % being utilised. There has been a rise in demand for REEs over the past decades due to their use in optics, automotive, electronics, energy, defence industries etc. These precious elements REE are known to be contained in CFA, making it a potential source.

The study aimed to investigate the effectiveness of alkali fusion-acid leaching for the recovery of REEs from South African CFA (Tutuka, Kendal and Duvha CFA). The approach involved (i) determining the mineral and elemental composition; (ii) optimization of REE recovery based on alkali fusion-acid leaching method (iii) determination of elements that are co-extracted to ascertain their environmental implications.

This study has determined that Tutuka, Kendal and Duvha CFA is characterized as Class F and was mainly composed of the major elements, silicon, aluminium and lower amounts of iron and calcium. The CFA also had a substantial amount of REEs and a range of other trace elements. Duvha CFA (573.77 ppm) had more REEs than Tutuka (526.35 ppm) and Kendal CFA (567.68 ppm). The study also determined that REEs occur in acid-resistant REE-bearing phases such as mullite, quartz, rutile and zircon found in the CFA. Thus, preconditioning of the CFA using alkali fusion was needed to break acid-resistant REE-bearing phases before being leached with a strong acid to recover REEs.

It was also determined that acid concentration has a significant effect on REE extraction and recovery from CFA using the alkali fusion-acid leaching method. REE extraction and recovery increased as HCl concentration increased from 1 to 2 mol/L and decreased as acid concentration increased to 3 mol/L. At 1 mol/L HCl concentration, the amount of HCl was insufficient for the requirements of the leaching process. As acid concentration increased to 2 mol/L there are more H^+ to react with the alkali fusion products, which in turn increased REE recovery. At 3 mol/L there is even more H^+ to react with the fusion products, however, the increase in H^+ increases the formation of silicic acid which forms a gel layer that inhibits contact of hydrogen ions (H^+) and with the solid particles Thus, decreasing REE recovery.

Therefore, an acid concentration of 2 mol/L was the optimal concentration for REE extraction and recovery using alkali fusion acid leaching for the CFA in this study. At the optimal acid concentration of 2 mol/L, Duvha CFA had a total rare earth element (TREE) recovery (34%) that was slightly more than the recovery of both Kendal and Tutuka CFA (33%). Duvha CFA also had a greater abundance of REEs than both Kendal and Tutuka CFA. Therefore, Duvha CFA is more viable than Kendal and Tutuka CFA for REE recovery using the alkali fusion acid leaching method. The study also showed that although the alkali fusion-acid leaching method was able to dissolve REE-bearing minerals (mullite, quartz, allanite zircon etc) these minerals were not dissolved completely. This could be one of the reasons why there were low REE recoveries and extractions from the CFA in the study using the alkali fusion-acid leaching method.

This study also determined that disposal of the lixiviant and solid residue after REE recovery using the alkali fusion-acid leaching method has environmental implications. The lixiviant of all the CFA has low pH with the presence of trace elements of major concern, lead (Pb), arsenic (As) chromium (Cr) and mercury (Hg) including the radionuclides thorium (Th) and uranium (U) were all present in lixiviant.

All the trace elements in the lixiviant that were documented by the Department of Water Affairs (DWAF) in 1996 had concentrations higher than their respective Target Water Quality Range (TWQR) for drinking water for all three CFA in the study except for Hg, Zn and Cu. Thus, the disposal of lixiviant without further treatment can be environmentally harmful. The solid residue still had all the trace elements found in the original CFA including Pb and Cr and radionuclides Th and U. However, the trace elements were less concentrated in the residue, making it safer to dispose of than the original CFA.

Dedication

I dedicate this work to my loving and supportive family.

Acknowledgements

What a beautiful journey.

I am so grateful that I got to experience this Master's journey. While I was filled with anxiety, excitement, exhaustion, joy, breakthroughs and sometimes near a breakdown, I grew. The late nights in the lab taught me perseverance, the days of uncertainty taught me the courage and the feedback, thickened my skin. This thesis might not be perfect but it's so much better than it was at the beginning this I acknowledge and I am so grateful for.

I raised my hands, tossing and turning, dancing at the cliff of my limitation, I cried, I prayed, I grew.

 And behold

Grace and all

He helped me.

List of abbreviations

ASTM	American Society for Testing and Materials
CFA	Coal Fly Ash
EC	Electrical Conductivity
EDX	Energy Dispersive X-Ray Analysis
Eskom	Eskom Holdings SOC Ltd
HCL	Hydrochloric Acid
HREE	Heavy Rare Earth Elements
ICP-MS	Inductively Coupled Plasma- Mass Spectrometry
LOI	Loss on ignition
LREE	Light Rare Earth Elements
MREE	Medium Rare Earth Elements
PPM	Parts Per Million
REE/s	Rare Earth Element/s
TIMA	TESCAN Integrated Mineral Analyzer
TREE	Total Rare Earth Elements
TWQR	Target water quality range
XRD	X-ray Powder Diffraction
XRF	X-ray Fluorescence Spectrometer

Table of contents

List of Figures

List of tables

UNIVERSITY *of the*

WESTERN CAPE

1 Introduction

The rapid rise in global energy demand has led to the development of various alternative sources of energy (hydropower, wind power, solar power etc.). However, the world still largely depends on coal-based energy (Gollakota et al., 2019). Despite the increases in the use of renewable sources, the global energy consumption of coal is expected to increase by 30% by 2035 (Wang et al., 2020). In 2016, coal accounted for 69% of South Africa's energy supply followed by crude oil (14%), renewables (11%), nuclear (3%) and natural gas (3%) (South African Department of Energy, 2019).

Eskom, the South African electricity public utility and national grid supplier that is responsible for 90% of the country's electricity had projected that in 2020, it would be operating 15 coal-fired power plants accounting for 85% of the installed capacity (Bohlmann et al., 2019). When coal is burned in coal-powered plants, it results in by-products of which the major fraction is coal fly ash (CFA). Therefore, the addition of new power stations will lead to an increase in the production of CFA. Large amounts of CFA are disposed of in landfills (Pan et al., 2020). This may result in an adverse environmental impact as CFA releases substantial amounts of trace metals. Trace elements such as molybdenum (Mo), manganese (Mn), zinc (Zn) and copper (Cu) along and a significant amount of other toxic elements (i.e. As, Cr, Co, Pb, Ni, Se) are a major source of soil and water pollution (Khan & Umar, 2019)

One of the major issues raised in literature is the limited space for disposing of CFA (Fatoba, 2010; Eze, 2014; Wagner & Matiane, 2018; Reynolds-Clausen & Singh, 2019). Eskom has given this issue more attention as it could potentially impact the security of the electricity supply. To avoid the issue of CFA disposal due to limited space and to maintain the security of electricity supply, Eskom has prioritised the re-use of the ash produced by power stations (Reynolds-Clausen & Singh, 2017).

In South Africa, CFA has been used as a cement extender, road base, soil ameliorant and for the neutralisation of acid mine drainage (Ripfumelo, 2012). All CFA applications make use of one or more of the unique properties of the material. The knowledge of the composition and chemistry of CFA aids in improving its utilization (Reynolds-Clausen & Singh, 2017).

CFA is considered to be a ferro-aluminosilicate, which is made up of glass spheres that largely consists of quartz and mullite (Petrik, 2004). CFA also contains traces of many valuable rare earth elements (REEs) that can be utilised for commercial purposes if handled appropriately (Gollakota et al., 2019). CFA potentially contains the full range of REEs and most conventional

REE mines extract only a few of these elements (Wagner & Matiane, 2018). Furthermore, REEs are critical to the automotive, energy electronics, and defence industries, they consist of 17 elements that are chemically similar to each other. These include 15 lanthanides as well as yttrium and scandium (Taggart et al., 2016).

The investigation of CFA as a potential source of REE is a new research area and it is attracting a fair amount of attention and investment globally (Taggart et al., 2016, 2018; King et al., 2018; Tang et al., 2019; Wang et al., 2019). Despite this, there is limited knowledge of REE occurrence in South African coals and CFA (Wagner & Matiane, 2018). This suggests a need to investigate the feasibility of this alternative source of REEs in a South African context.

1.1   Research problem

REE's have also been beneficial to many industries. They have been widely utilized in a variety of advanced materials and technologies such as alloys, optics, catalysts, electronic communications and renewable energy (Tang et al., 2019). Their demand has been increasing in the past decades due to their unique electrochemical, magnetic, and luminescent properties (Taggart et al., 2018). As a result of the increasing demand for REEs, there has been an investigation of secondary sources, including coal deposits and coal combustion residuals. CFA contains a full range of REEs, and most conventional REE mines extract only a few of these elements (Wagner & Matiane, 2018). There has been extensive research going into characterizing REEs in CFA (Ripfumelo, 2012; Franus et al., 2015; Taggart et al., 2016; Wagner & Matiane, 2018) but, little has been done to determine efficient extraction methods to recover REEs from CFA (King et al., 2018).

REEs reside in the aluminosilicate glass fraction of CFA (Taggart et al., 2016; Hower et al., 2019; Guo-qiang et al., 2020). Hence, hydrometallurgical leaching processes used to extract Al in bauxite ore can be used to recovery REEs in CFA since the chemical composition of CFA is similar to that of bauxite ore. Hydrometallurgical processes that have been used to recover alumina are broadly divided into two types, acidic and basic (Shemi, 2013). Acid leaching methods are generally preferred to extract aluminium from high silica non-bauxitic resources such as CFA (Taggart et al., 2016). There are two types of acid leaching, direct and indirect acid leaching. Direct acid leaching does not require intervention before the leaching process. While indirect acid leaching requires some material pre-conditioning before leaching (Shemi, 2013). Alkali fusion of CFA with an alkaline such as calcium oxide, sodium hydroxide, sodium carbonate or calcium sulphate is an example of preconditioning in preparation for acid leaching

2

(Taggart et al., 2018; Tang et al., 2019). Studies have shown that indirect acid leaching is generally more efficient at REE extraction than direct leaching methods (Taggart et al., 2018; Tang et al., 2019; Z. Wang et al., 2019) except for CFA with high in CaO and that is enriched with Ca-Fe in the glass phase (Taggart et al., 2018). However, there is still uncertainty that surrounds these methods in their efficiency for REE extractions and how different ashes characteristics could affect the leaching process (King et al., 2018). Furthermore, only a few studies are investigating the factors that affect the leaching process (Cao et al., 2018).

Acid concentration has been proven to be one of the most influential factors in REE acid leaching experiments (Taggart et al., 2018; Tang et al., 2019; Pan et al., 2020). However, the optimal acid concentration for the recovery of REEs from CFA differs for different CFA from different studies (Cao et al., 2018; Tang et al., 2019; Rybak & Rybak, 2021). The change in acid concentration also affects the leaching of trace elements including elements of potential environmental concern from CFA (Be, Cd, Co, Cu, Fe, Mg, Mn, Ni, Pb, Si, Sn, Th, Tl, U) (Izquierdo & Querol, 2012). There is more research that is needed to understand the environmental trade-offs of recovering metals from CFA (Taggart et al., 2018). Hence, this study explored how efficient the alkali fusion-acid leaching method is for the recovery of REEs from South African CFA at different acid concentrations.

1.2   Aim

The study aimed to investigate the effectiveness of alkali fusion-acid leaching for the recovery of REEs from South African CFA. This was achieved by the following objectives:

1.2.1   Objectives

- Determining the mineral composition, major elements and trace elements (including REEs) of South African CFA to understand the characteristics of the CFA. The major and trace elements and mineral phases of the CFA will be examined using the XRF, ICP-MS, XRD and TIMA analytical techniques respectively.

- Assessing the REE recoveries from South African CFA using the alkali fusion-acid leaching method and examine the relationship between REE recovery and acid concentration to determine the optimal acid concentration for the recovery of REEs from South African CFA.

- Examining the presence and concentrations of trace elements that are co-extracted with REEs in the lixiviant and solid residue after recovery of REEs from South African CFA to determine whether these elements are of environmental concern.

1.3   Significance of study

Research on the beneficiation of CFA has an industrial interest and environmental importance due to the large amount of CFA that is generated worldwide from coal combustion to meet energy demands (Eze, 2014). The study has the potential to contribute to the industrial and environmental beneficiation of CFA in South Africa. Multiple studies have characterized CFA (Ripfumelo, 2012; Franus et al., 2015; Taggart et al., 2016; Wagner & Matiane, 2018) however, there is limited research that has been done to determine efficient extraction methods of REE from CFA (King et al., 2018). This study intended to show how effective the alkali fusion-acid leaching method is for the recovery of REEs from South African CFA. Furthermore, the study has determined the effect of acid concentration on REE extraction in South African CFA. There is also limited research on the environmental hazards of recovering metals from CFA (Taggart et al., 2018). This study has examined the lixiviant and solid residue after REE recovery to determine the presence and concentrations of trace elements that could be environmentally hazardous.

1.4   Scope and delimitations of the study

The research used CFA from, Tutuka, Kendal and Duvha power stations as the base material for the investigation of the effectiveness of the alkali fusion-acid leaching method for the recovery of REEs from South African CFA. The study used an experimental method, where a lab experiment was set up to test the efficiency of the alkali fusion-acid leaching method on REE recovery from South African CFA at different acid concentrations.

The study was limited to the alkali fusion-acid leaching method that is modified from a USGS sodium peroxide (Na_2O_2) alkaline sintering method developed for the analysis of REEs in geological samples (Lichte et al., 1987; Meier et al., 1996; Meier & Slowik, 2002). The method has been further adapted using studies from Taggart et al. (2018) and (Tang et al., 2019) for the alkaline roasting stage and studies by Cao et al. (2018) and Tang et al. (2019) for the acid leaching stage. The study focused on the effect of acid concentration on REE recovery on South African CFA as it has proven to be very influential in REE recovery from CFA using acid leaching methods (Taggart et al., 2018; Tang et al., 2019; Pan et al., 2020). The study does not investigate downstream REE separation from lixiviant after alkali fusion-acid leaching due to lack of funds and time.

1.5   Chapter outline

- Chapter 1 Introduction*:* This chapter provides an overall introduction to the research, the problem statement, the aim, objectives, significance of the study and scope of the study.

- Chapter 2 Literature Review: This chapter sets out to review related literature on the extraction of REEs from CFA. The chapter includes general knowledge of CFA including the physical and chemical properties of the material. The controlling parameters and the environmental impacts of REE leaching are also mentioned in the chapter.

- Chapter 3 Research Methods: This chapter describes the materials and methods used in the study. The quality control and quality assurance measures taken in the study are also described.

- Chapters 4 Results and Discussion: In this chapter, the findings of the study were displayed, described and discussed.

- Chapter 5 Conclusion and recommendations: This chapter concludes the thesis with a summary of the findings and recommendations.

1.6   Chapter summary

The present chapter gave a general introduction to the study. The research questions, research problem together with aims and objectives were stated in this chapter. The significance of the study was described followed by the scope of the study and the chapter outline that concluded the chapter. The next chapter will review the literature relevant to the study.

2   Literature review of the occurrence and recovery of REEs

2.1   Introduction

Rare earth elements (REEs) have been recognised as critical raw materials that are an important part of many emerging technologies (Franus et al., 2015). Renewable energy technologies such as photovoltaic, fuel cells, and wind turbines make use of REEs (Alonso et al., 2012). REE deposits have been identified in 34 countries (Chen, 2011) however, their production and processing is energy-intensive, highly reliant on toxic chemicals, and can produce radioactive by-products, mostly from the radioactive element Thorium (An, 2014). This creates an increasing gap between the global demand and supply of REEs leading to the search for alternative resources (Franus et al., 2015). A promising alternative resource of REEs is coal fly ash (CFA), which is the main by-product of coal combustion that is enriched with REEs (Tang et al., 2019). The literature review will provide an overview of CFA, particularly from a South African context as a resource for REEs. The literature will describe the origins of REEs from coal and CFA. This includes the occurrence and abundance of REEs in coal and CFA. This will be followed by a discussion of the environmental concerns regarding REE extraction from both primary and secondary resources. Then REE extraction methods from CFA will be described with a focus on acid leaching methods and acids used in these methods. Finally, the controlling parameters of acid leaching of CFA for the recovery of REEs will be discussed.

2.2   Classification of REEs

According to Tang et al. (2019) "Rare earth elements are indispensable strategic resources which consist 17 elements that are chemically similar to each other, including 15 lanthanides as well as yttrium and scandium". These elements are scandium (Sc), lanthanum (La), cerium (Ce), praseodymium (Pr), neodymium (Nd), promethium (Pm), samarium (Sm), europium (Eu), gadolinium (Gd). terbium (Tb), dysprosium (Dy), holmium (Ho), erbium (Er), thulium (Tm), ytterbium (Yb), lutetium (Lu), and yttrium (Y) (An, 2014). REEs can be classified geochemically and according to the demand-and-supply relationship of individual REEs (see Table 2.1). According to geochemistry REEs can be divided into light REEs (LREEs), medium REEs (MREEs) and heavy REEs (HREEs) (Guo-qiang et al., 2020). HREEs are more valuable than LREEs and MREEs because HREEs are found at a lower concentration on the Earth's crust (An, 2014). Based on demand - and- supply relationship of individual REEs, REE's are divided into: critical, uncritical and excessive. This supply-and-demand classification of REEs evaluates the REE distribution that is more relevant to the REE industry (Franus et al., 2015).

The abundances of the individual REEs relative to each other do not correspond with their use. The supply challenges for REEs are mainly for the critical REEs, whereas excessive REEs are produced in surplus amounts.

Table 2.1: REE classifications according to Geochemical and Supply-Demand relationships.

Geochemical Classification	
LREEs	La, Ce, Pr, Nd, Sm
MREEs	Eu, Gd, Tb, Dy, Y
HREEs	Ho, Er, Tm, Yb, Lu
Supply-Demand Classification	
Critical	Dy, Nd, Eu, Er, Tb, Y
Uncritical	La, Pr, Sm, Gd
Excessive	Ce, Ho, Lu, Tm, Yb

It is worth noting that for both geochemical and supply-and-demand classifications Sc and Pm are not mentioned. This is because in terms of geochemistry Sc is seldom found with other REEs, either light or heavy (An, 2014), thus it is excluded altogether and in terms of supply-and-demand, Sc was removed from this list as it is considered uncritical in supply, even excessive, although the demand is high (Wagner & Matiane, 2018). Pm is also excluded from the classifications because it is not a naturally occurring element that can be extracted through mining but is rather synthetically produced for commercial use as a by-product of high-yield uranium processing. Due to this reason, Pm is not part of the conventional REEs mineral extraction supply and demand-supply chain and is commonly excluded from market analysis (An, 2014). There is a high demand for REEs because of their unique properties that make them crucial for modern technology (the advancement of the old technology that has new additions and modifications) (Seaman, 2010).

2.3   Role of REEs in the modern world

REEs have been widely utilized in a variety of advanced materials and technologies such as alloys, optics, catalysts, electronic communications and renewable energy (Tang et al., 2019). Their demand has been increasing in the past decades due to their unique electrochemical, magnetic, and luminescent properties (Taggart et al., 2018). These properties of REEs make them key role players in the manufacturing of materials from household to defence products,

that provide a modern standard of living (Seredin & Dai, 2012). REEs play an important part in the production of a variety of modern technologies including mobile phones, computers, plasma, LED and LCDs screens, microwaves, video and photo cameras; air conditioners, modern hybrid, electric and magnetic vehicles; power stations, nuclear reactors, lasers, and rockets (Seredin & Dai, 2012; An, 2014; Eze, 2014; Jha et al., 2016; Gollakota et al., 2019). REEs play a significant role in renewable energy and energy-efficient technologies. The automotive and the wind power industries are two areas where demand for REEs is significant and projected to increase (Seaman, 2010). REEs form important parts of super-power magnets. Super-power magnets such as neodymium magnets (NdFeB) and samarium cobalt (SmCo) magnets are irreplaceable components of industrial generators because they can effectively transform any kind of energy (wind, tidal, thermal etc.) into electricity (Seredin & Dai, 2012). Other REEs are also used for different renewable energy applications such as La that is used in long-life Nickel-metal hydride (NiMH) batteries that are needed for the production of hybrid vehicles. Ce is used as a catalyst to control emissions by filtering exhaust in renewable diesel technology and Gd is being used in magnetic refrigeration promising to revolutionise the market for refrigerators and eliminate the use of compression refrigeration systems (Seaman, 2010).

2.4　Rare earth element deposits

Since rare earth resources are randomly distributed, their supply is influenced by economic affairs and political situations. REE deposits have been identified in 34 countries, which shows that these elements are not extremely 'rare' (Franus et al., 2015). REEs are moderately abundant in the earth's crust, some even more abundant than copper, lead, gold, and platinum (Eze, 2014). REEs are primarily embedded in three types of rock-forming minerals: bastnäsite (CO_3F), monazite ($(Ce,La,Nd,Th)PO_4$), and xenotime (YPO_4) (An, 2014). Table 2.2 provides some insight into the abundance of REEs by principle countries according to the U.S. Geological Survey (2018). According to U.S. Geological Survey (2018), 33.33 % of the world's REE reserve is in China which is one-third of the world's reserve. Brazil and Vietnam both hold 16.67 % of the reserve. Russia accounts for 13.64 %, India 5.23 % and Australia 2.56 %. Additional reserves at smaller quantities are held in Greenland (1.14%), the United States of America (U.S) accounts (1.06 %). Malawi (0.11 %), South Africa (0.65%), Canada (0.63) and Malaysia (0,02).

Table 2.2: World reserves of REE by principal countries (U.S. Geological Survey, 2018)

Country	Reserves in tonnes (in terms of REO)	% Share
Australia	3,400,000	2.56
Brazil	22,000,000	16.67
Canada	830,000	0.63
China	44,000,000	33.33
Greenland	1,500,000	1.14
India	6,900,000	5.23
Malaysia	30,000	0.02
Malawi	140,000	0.11
Russia	18,000,000	13.64
South Africa	860,000	0.65
Vietnam	22,000,000	16.67
USA	1,400,000	1.06
World Reserve	132,000,000	
REO=Rare earth oxides		

China is an REE powerhouse because REEs reserves are spread throughout the country. The southern regions of the country have a high concentration of HREEs which are highly valuable (An, 2014). There are large iron-rich rare-earth-bearing deposits that exist outside of China like in Southern Africa, Canada, and Australia however a number of them are not exploited as no economically viable process exists to do so (Bisaka et al., 2017). Namibia has the second-largest reserve worldwide with about 20 Mt rare earth oxides (REOs), and South Africa has about 1 Mt. Despite the presence of large deposits, Africa's contribution to the global supply of REEs is insignificant (Gupta & Krishnamurthy, 2004). Furthermore, in recent years, the majority of countries that produce and export REEs like China, have reduced their export to other countries to protect their national downstream industries (Seaman, 2010). However, there is still a gap between REE's growing demand and decreasing supply, for this reason, it is extremely important to look for alternative resources for REEs (Franus et al., 2015).

To satisfy the growing industrial demand for REEs, new efforts have been put in place to reduce the risk of supply by developing an efficient process to recover REEs from secondary sources such as municipal solid waste, scrap magnet, spent catalyst, industrial process residues and CFA (Tang et al., 2019). CFA potentially contains the full range of REEs while most conventional REE mines extract only a few of these elements. Hence, there are research organisations and companies that are exploring methods to economically extract REEs from CFA (Wagner & Matiane, 2018). CFA is the fine ash that is carried out of the boiler with the

flue gases after coal combustion (Petrik, 2004). The REE content in CFA is dependent on the geological origin of the coal it was produced from (Taggart et al., 2016, 2018).

2.5   The abundance of REEs in South African Coal and CFA

In South Africa, coal is one of the major primary energy resources (Petrik, 2004). The coal deposit in South Africa is in the Main Karoo Basin. The Main Karoo Basin is within the Ecca Permian-aged sedimentary sequence of the Karoo Supergroup (Jeffrey, 2005; Wagner & Matiane, 2018). There are 19 coalfields in South Africa located mainly in KwaZulu-Natal, Mpumalanga, Limpopo, and the Free State, to a less extent Gauteng, the North West Province and the Eastern Cape provinces and all of them within the Main Karoo Basin. The Waterberg, Highveld and the Witbank coalfields contain most of South African's coal reserves with above 70% of the total reserves (Jeffrey, 2005). The predominant coal resource in the country is bituminous coal and it forms the core of the country's resources and reserves (Petrik, 2004). Coal is mainly composed of mineral and organic matter with the major elements, carbon, hydrogen, oxygen, nitrogen, and sulphur (Falcon, 1988). South African coals typically have low sulphur, nitrogen and phosphorus. The common mineral matter found in SA coalfields includes clays, sulphides, oxides, silicates, phosphates, and carbonates. Kaolinite and quartz are the most abundant mineral found in SA coals (Maledi, 2017). Trace elements such as arsenic (As), beryllium (Be), cadmium (Cd), cobalt (Co), chromium (Cr), fluorine (F), mercury (Hg), nickel (Ni), lead (Pb), antimony (Sb), selenium (Se), uranium (U), thorium (Th) and iron (Fe) reside in coal (Finkelman, 1999), as well as REEs (Seredin & Dai, 2012). The average sum of REE content of world coals, based on the calculation of average individual lanthanide and Y concentration is 68.5 ppm (Ketris & Yudovich, 2009) which is approximately 2.5 times lower than that in the rocks of the upper continental crust (UCC) (Seredin & Dai, 2012). There is very limited research that appears in the literature on REE occurrence in South African coals and related ash products (Wagner & Matiane, 2018). Table 2.3 shows the REE concentrations of South African coal (Tutuka coal and Witbank coalfield coal from seam 2) and CFA (Tutuka and Matla CFA) from available literature compared to the upper continental crust (UCC), coal Clarke values, Chinese coal and CFA from Jungar power station.

Table 2.3 Comparison of concentrations of REEs in the UCC, world coals and ash, coal and coal ash from China and South Africa (Wagner & Matiane, 2018).

REEs	a. Upper continental crust	b. Coal Clarke values		c. Jungar Power Plant, China			d. Tutuka Power station, S.A		e. Matla Power station, S.A	f. Witbank Coalfield, SA
	UCC	Hard Coal	Hard coal ash	Coal	Fly Ash, Economizer	Fly Ash (wet)	Coal	Ash	Ash	Coal (No 2 Seam)
Y	22	3.7 ± 0.2	24 ± 11	20.4	42.1	54.2	17.5	64.9	52.3	
La	30	11 ± 1	76 ± 3	41.2	85.4	104.3	39.9	91.4	81.55	9.72–34.16
Ce	64	23 ± 1	140 ± 10	71.8	141	178	91.61	182.4	189.78	
Pr	7.1	3.4 ± 2	26 ± 3	8.1	17.3	21.5	9.46	19.7	18.35	
Nd	26	12 ± 1	75 ± 4	27.6	58.5	72.5	30.84	71.8	63.5	
Sm	4.5	2.2 ± 0.1	14 ± 1	5.2	10.6	13.5	5.3	14.4	11.93	1.94–5.27
Eu	0.88	0.43 ± 0.02	2.6 ± 0.1	0.9	1.8	2.4	0.89	2.7	2.35	0.26–0.77
Gd	3.8	2.7 ± 0.2	16 ± 1	4.7	9.1	11.7	4.15	12.6	10.4	
Tb	0.64	0.31 ± 0.02	2.1 ± 0.1	0.7	1.4	1.8	0.57	1.9	1.6	0.25–0.66
Dy	3.5	2.1 ± 0.1	15 ± 1	4.2	8.6	10.8	3.31	11.9	9.5	
Ho	0.8	0.57 ± 0.04	4.8 ± 0.2	0.8	1.7	2.1	0.67	2.4	1.97	
Er	2.3	1 ± 0.07	6.4 ± 0.3	2.4	4.9	6.2	1.89	6.7	5.38	
Tm	0.33	0.3 ± 0.02	2.2 ± 0.1	0.3	0.7	0.9	0.27	1	0.77	
Yb	2.2	1.0 ± 0.06	6.9 ± 0.3	2.3	4.8	6	1.81	6.5	5.27	
Lu	0.32	0.2 ± 0.01	1.3 ± 0.1	0.3	0.7	0.9	0.25	1	0.72	
Sc	11	3.7 ± 0.2	24 ± 11				9.66	26.5	24.94	

Note: REE content in ppm

a. Taylor & McLennan (1985)
b. Ketris & Yudovich (2009)
c. Dai et al.(2010)
d. Akinyemi (2011)
e. Eze (2014)
f. Hart et al.(1982)

It should be noted that the Tukuka and Matla power stations receive coal from Highveld and Witbank coalfield in Mpumalanga respectively. The Clarke values determined by Ketris & Yudovich (2009) are a highly useful tool for geochemical comparisons on coals and coal ash globally, the authors estimated that on average world coals have 68.5 ppm REE concentration. The UCC data by Taylor & McLennan (1985) has been used in literature to normalize REE data (Taggart et al., 2016; Wagner & Matiane, 2018; Z. Wang et al., 2019). The coal that was combusted at the Tutuka power station generally had a higher REE concentration than the Jungar power station coal, the UCC and Clark values for hard coals. The Tutuka coal had a total REE (TREE) concentration of 218.08 ppm which is higher than 179.37 ppm in the UCC. The Tutuka power station coal had a higher TREE content than the Jungar power station coal even when excluding Sc with a concentration of 208.42 and 190.9 ppm respectively. The Tutuka coal also had a TREE concentration that is more than triple that of the average world coal (68.5). The Witbank coalfield coal from seam 2 had an REE concentrations range within the UCC data and the Clark coal values where data is available. The Witbank coalfield seam 2 coal and the Tutuka coal shows promising concentrations of REEs from South African coals however the concentration of REEs in the CFA is much higher. The Tutuka and Matla CFA both had TREE concentrations much higher than those found in the Tutuka and Witbank seam 2 coal with concentrations of 517.8 and 480.31 ppm respectively. This is an expected result because Ketris & Yudovich (2009) estimated that on an average global basis the REE concentration in CFA is 445 ppm. The Tutuka and Matla CFA also have a higher REE concentration than the average global basis and the CFA from the Jungar power station in China (388.6 - 486.8 ppm). This indicates that South African CFA has a high concentration of REEs and can compete with world CFA for REE extraction. Thus, it is recommended that South African CFA should be considered for further examination in terms of REE recovery.

2.6   The occurrence of REEs in CFA

The recovery REEs from CFA has attracted a lot of attention (Eze, 2014; Hower et al., 2017; King et al., 2018; Taggart et al., 2018; Tang et al., 2019) however, limited research appears for the occurrence and recovery of REEs in South African CFA (Wagner & Matiane, 2018). The recovery of REEs from CFA is dependent on the characteristics of the CFA (Rybak & Rybak, 2021). The characteristics of CFA are determined by the physical and chemical properties of parent coal, the coal particle size, combustion process, and the type of ash collector used (Eze, 2014).

2.6.1 Mineral characteristics of CFA

CFA is considered to be a ferro-aluminosilicate composed of small particle sized (20 – 80 μm) glass spheres with large surface areas and generally consists of quartz (SiO_4) and mullite ($3Al_2O_32SiO_2$) (Petrik, 2004). Due to the rapid cooling of the CFA from the flue gas, particles are composed mainly (50- 90%) of mineral matter in the form of glassy particles. The major mineralogical phases of South African CFA include glass, mullite, and quartz and to a lesser extent lime (CaO), portlandite ($Ca(OH)_2$), and the Fe oxides such as hematite (Fe_3O_4), maghemite (γ-Fe_2O_3) and magnetite (α-Fe_2O_3) (Campbell, 1999). REEs are mainly found in the glass phase (see Figure 2.1) meaning that aggressive extraction methods are required to break down the glass to extract the REEs (Taggart et al., 2018).
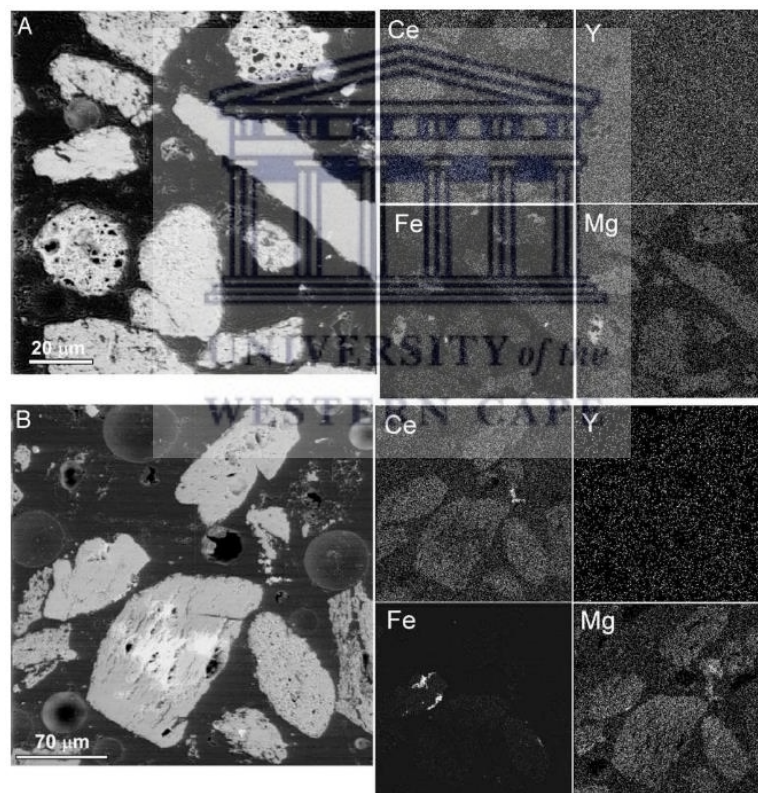
Figure 2.1: (A) Cerium, Fe, and Mg distribution in glassy fly ash particles from the Jungar power plant. Scale bar 5 10 mm. (B) Cerium, Fe, and Mg distribution in glassy fly ash particles from the Jungar power plant. Scale bar 5 50 mm (Hower et al., 2003).

Multiple studies have investigated the occurrence of REEs in CFA and found that REE resides in the aluminosilicate (Al_2SiO_5) glass fraction (Taggart et al., 2016; Kolker et al., 2017; Lin et al., 2018; Pan et al., 2018; Hower et al., 2019; Guo-qiang et al., 2020). With this understanding, a logical starting point for the recovery of REEs from CFA would be to use methods developed

for recovering alumina as they target the aluminosilicate glass where REEs reside (Taggart et al., 2018). To extract aluminium (Al) from high silica non-bauxitic resources such as CFA, acid leaching processes are generally preferred. Silica (Si) is substantially insoluble in acid solutions unlike in alkaline solutions. A strong acid or base and high temperatures are required to dissolve the amorphous phases in CFA and decompose acid-resistant mullite into soluble forms of Al (Taggart et al., 2016).

A study by Kolker et al. (2017) showed the distribution of REEs in CFA from the U.S. The study showed that although REEs are enriched in the aluminosilicate glass of CFA, the aluminosilicates without other main elements (such as Fe and Ca) usually have REE content similar or slightly lower than the REE content in the bulk CFA sample. Figure 2.2 shows the Fe-enriched aluminosilicate glasses are commonly REE enriched relative to the more common Al-Si glasses. Furthermore, the mineral quartz has REE contents less than both the aluminosilicate and the Fe-enriched aluminosilicate as well as the bulk CFA sample.
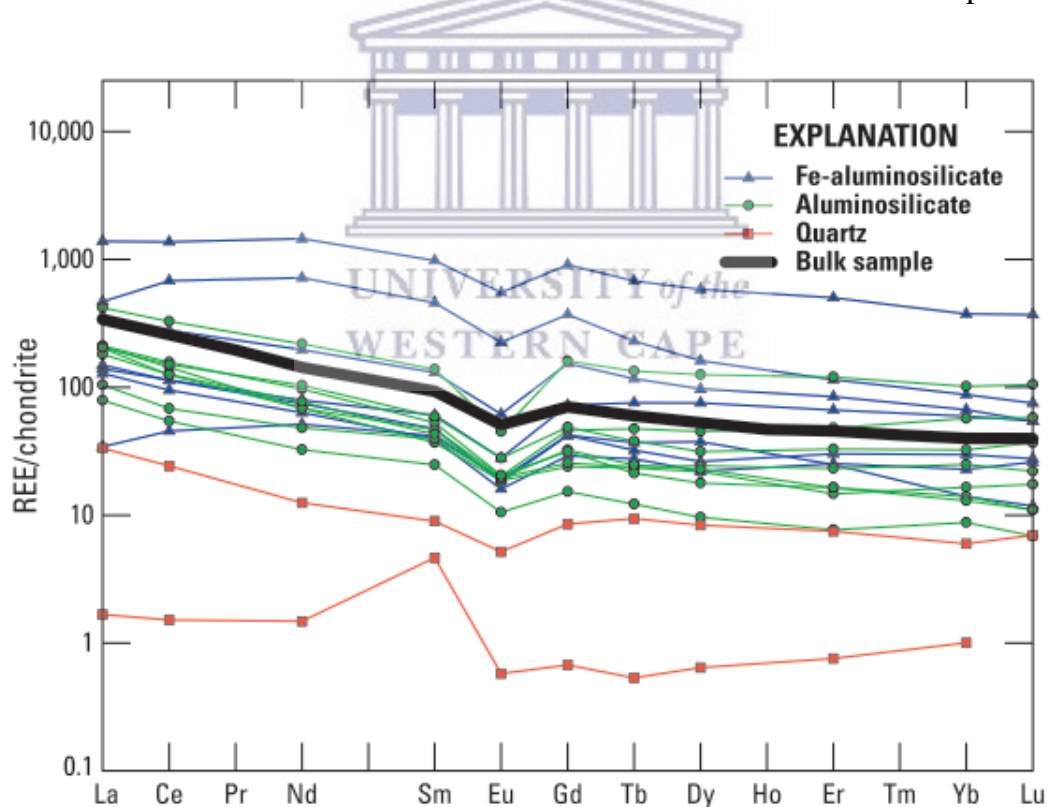
Figure 2.2: Chondrite-normalized plot showing the relative enrichment of REEs in iron-bearing aluminosilicate glass (Fe-aluminosilicate) relative to aluminosilicate glasses that lack iron or constituents other than aluminium and silicon. REE were concentrations were normalized to concentrations of REEs in chondrites (a group of stony meteorites) (Kolker et al., 2017).

14

The authors explained that this depletion of REEs in quartz was expected because there is a lack of minor element substitution into the quartz crystal structure. These results show that when recovering REEs from CFA the focus should mainly be on the aluminosilicate glass to obtain higher REE recoveries. Major elements also play a role in the REE enrichment of CFA despite REEs mainly residing in the aluminosilicate glass (Taggart et al., 2018). Thus, it is important to characterise CFA in terms of its chemical constituents.

2.6.2 The Chemical characteristics of CFA

The chemical composition of CFA mostly depends on the chemical composition of the coal, the combustion conditions and the removal effectiveness of air pollution (Eze, 2011). Although CFA varies in chemical composition, elemental analysis has shown that CFA mostly consists of the same fundamental chemical elements but in different concentrations (Eze, 2014). Chemical analyses have shown that most natural elements can be found in CFA. The major elements in CFA are iron (Fe), aluminium (Al) and silicon (Si) with significant amounts of calcium (Ca), potassium (K), sodium (Na) and titanium (Ti). The concentrations of these major elements are higher relative to those found in the parent coal. Trace elements such as arsenic (As), boron (B), lead (Pb), nickel (Ni), selenium (Se), strontium (Sr), vanadium (V), and zinc (Zn) including REEs are also found in higher concentrations in fly ash relative to coal (Eze, 2014; Izquierdo & Querol, 2012). The total and extractable REE content of coal fly ashes depended on the fractions of major elements in the CFA. A study by Taggart et al. (2016) investigated the trends in REE content of different CFA from the U.S. The study showed that the TREE content correlated strongly with the fraction of aluminium oxides (Al_2O_3) comprising the CFA ($r^2 = 0.71$). The study also showed that CFA with high calcium oxide (CaO) content had higher REE recoveries than those with lower CaO content when extracting REEs from CFA using nitric acid (HNO_3). The reason being that calcium-bearing particles were likely to be more soluble in HNO_3 than the other major oxides comprising CFA such as silicon and aluminium oxides. A study by King et al. (2018) found similar results when recovering REEs from U.S based CFA using hydrochloric acid (HCl) as a lixiviant, CFA with high CaO content had higher REE recoveries than CFA with lower CaO.

South African CFA generally has lower CaO which is expected because it is Classified as Class F CFA according to the American Society for Testing and Materials (ASTM) (Petrik, 2004). ASTM classifies CFA into two groups, Class F and Class C (see Table 2.4). The difference between Class F and Class C fly ash is based on the sum of the total silica, aluminium and iron

oxides ($SiO_2 + Al_2O_3 + Fe_2O_3$) in the CFA. When $SiO_2 + Al_2O_3 + Fe_2O_3$ is greater than 70 % CFA is classified as Class F. When $SiO_2 + Al_2O_3 + Fe_2O_3$ is between 50 % and 70 % the CFA is classified as Class C (ASTM C 618, 1993).

Table 2.4: ASTM C618 requirements for Class F and Class C CFA (ASTM C 618, 1993).

Chemical properties	Class F (%)	Class C (%)
Minimum $SiO_2 + Al_2O_3 + Fe_2O_3$ minimum %	>70	50-70%
Maximum SO_3 %	5	5
Maximum moisture content %	3	3
Maximum Loss on Ignition	6	6
Maximum Available alkalis (Na_2O)	1.50	1.50

Class F CFA has total calcium that typically ranges from 1 to 12%, mostly in the form of calcium hydroxide, calcium sulphate and glassy components in combination with silica and alumina. While Class C has calcium contents as high as 30 to 40% and the alkalis and sulphates are generally higher in Class C than in Class F CFA. Class F CFA, which is produced in South Africa, is produced from the burning of bituminous or anthracite coal (Petrik, 2004).

Since low CaO CFA has lower REE recoveries because it is not as soluble in acids as CFA with high CaO, preconditioning the CFA before acid extraction could improve the REE recoveries. A study by Taggart et al. (2016) analysed the influence of origin and composition of CFA on REE recovery using HNO_3 leaching. The maximum percentage recovery for CFA with low CaO was only 44.1% even with high leaching temperatures of 85−90 °C and HNO_3 concentrations as high as 15 mol/L. The authors introduced sodium peroxide (Na_2O_2) sinter pre-treatment and leached the CFA with a lower concentration of HNO_3 (4 mol/L) and REE recoveries were >80%. Since South Africa CFA has low CaO content it is a viable option to pre-treat the CFA to improve REE recovery. As mentioned in section 2.6.1 a strong acid or base used together with high temperatures are required to dissolve the amorphous phases where REEs occur in CFA to decompose acid-resistant mullite into soluble forms of Al for better REE recoveries. The use of strong acids may improve REE recovery however, they can also increase the solubility of other trace elements such as Be, Cd, Co, Cu, Fe, Mg, Mn, Ni, Pb, Si, Sn, Th, Tl, U and Zn from CFA. At normal environmental conditions (mildly acidic to alkaline pH) the leachability of these elements is low, however, in acidic CFA the mobility of the above-listed elements rises with decreasing pH (Izquierdo & Querol, 2012). When extracting REEs

16

from CFA it is important to be aware that the extraction process is non-selective, elements of concern can be mobilized along with REEs through the extraction process (King et al., 2018). While it is necessary to find optimal conditions to improve the efficiency of REE extraction in CFA, it is critical to determine the environmental hazard that remains after the extraction process (Taggart et al., 2018).

2.7   Environmental implications of REE recovery

The processing of REEs, directly and indirectly, affects the environment. The mining of REEs from their ores can produce a variety of waste products such as radionuclides, acids, fluorides etc. This process involves initial crushing and grinding of the ores to smaller particles, filtration and flotation to remove undesired minerals, and further conditioning before final metal purification. The exploration of secondary resources of REEs can aid in keeping the environment free from the effects of rare earth mining. REE recovery from a secondary resource such as CFA may be more efficient than ore processing since the physical form is more amenable to processing (Mayfield & Lewis, 2013; Jha et al., 2016).

In South Africa, Eskom, the major power utility company, produces nearly 37 Mt of CFA annually (Vadapalli et al., 2012). The majority of this CFA is stored as stockpiles or ash dams close to power stations (see Figure 2.3). CFA has a variety of metals (As, B, Pb, Ni, Se, V, Zn, REEs) in high concentrations and is therefore considered an environmental hazard in the country. These metals can leach from ash heaps through rainwater infiltration and may eventually reach the groundwater table and contaminate groundwater (Vadapalli et al., 2012). Furthermore, many power stations are currently running out of ash storage space. Expansion of the ash disposal facilities is required because this could impact the security of the electricity supply, due to limited ash disposal areas. To avoid this capital expenditure, Eskom has embarked on a process to increase the utilisation of the ash produced (Reynolds-Clausen & Singh, 2019). The recovery of REEs from CFA has the potential to remove hazardous elements from CFA making it safer for disposal (Taggart et al., 2018).

Figure 2.3: An image of a South African ash dump

Extraction techniques for recovery of REEs from CFA generally include initial acid leaching of the material, followed by removal (e.g., precipitation) of undesired minerals, and purification using solvent extraction. REE extraction and recovery, as described above, is a chemically intense process. Specifically, the metal separation steps will require the use of leaching acids, caustic precipitates, and organic solvents. The initial acid leaching process is generally non-specific to trace elements, therefore any remaining common elements will require recovery and disposal (Mayfield & Lewis, 2013). The mobility of trace elements from CFA is dependent on pH. Elements such as As, B, Cr, Mo, Sb, Se, V and W display the maximum leachability from CFA at the pH 7–10 range (neutral to alkaline conditions), out of the elements of concern are As, B, Cr, Mo and Se. At lower pH values (acidic conditions) elements such as Be, Cd, Co, Cu, Fe, Mg, Mn, Ni, Pb, Si, Sn, Tl and Zn are mobilized with REEs along with radioactive elements such as Th and U (Izquierdo & Querol, 2012). Th and U occur naturally alongside REEs in CFA. Thus, REE extraction methods for CFA also have the potential for generating radioactive wastes which are toxic to the environment (Taggart et al., 2018).

Therefore, the management of wastes remains a necessary component of REE resource development. Processes for extraction of REEs from CFA have yet to be commercialized, thus the understanding of future waste streams is limited. Furthermore, the potential for exposure (i.e., to workers, communities, or surrounding ecosystems) to any of the chemical contaminants

18

inherent in this process is unknown. Hence, monitoring of environmental exposures may be needed as CFA resources are reclaimed (Mayfield & Lewis, 2013).

CFA that is identified as being potentially economically viable should undergo a full chemical characterization to determine which contaminants may require specialized waste handling measures. There is more research required to understand the environmental trade-offs of recovering REEs from CFA. When removing hazardous elements like U and Th from CFA, the residual ash may be safer to dispose of. However, releasing hazardous elements like those mentioned above and concentrating them during the purification process may be more environmentally damaging (Taggart et al., 2018).

2.8 Rare Earth Element Recovery from Coal Fly Ash

As mentioned in section 2.6.1 to recover REEs from the aluminosilicate glass methods used for recovering alumina are used. Methods used to recover alumina target the aluminosilicate glass where REEs reside. Hydrometallurgical leaching processes used to extract Al in bauxite ore can be used in CFA since the chemical composition of CFA is similar to that of bauxite ore. Hydrometallurgical processes that have been used to recover alumina are broadly divided into two types, acidic and basic. There are several leaching methods for CFA processing that have been extensively researched using a variety of routes that are acidic, alkaline or a combination of acidic and alkaline (Shemi, 2013). The most significant ones are briefly discussed in the subsequent sections.

2.8.1 Bioleaching

One method of leaching aluminium from its sources is through bioleaching. Bioleaching uses bacterial microorganisms to recover metals from primary ores or secondary sources. The most common bacterial microorganism that is known to facilitate bioleaching reactions is the Thiobacilli species. Thiobacillus strains are capable of producing H_2SO_4 which leads to the solubilization of metals contained in CFA, such as aluminium, titanium, vanadium, selenium, boron, molybdenum, cobalt and others (Fass et al., 1994). The advantages of bioleaching are low cost, mild process conditions, low energy demand and landfill space. However, slow kinetics and insufficient selectivity concerning specific metals, specifically aluminium, outweigh the advantages of the CFA bioleaching process (Shemi, 2013).

2.8.2 Alkaline leaching

Alkaline leaching is another method used in hydrometallurgy to recover aluminium from primary and secondary sources. The Bayer process is a traditional method used for the recovery of alumina

from aluminium-bearing ores using alkaline leaching. The method involves alkaline leaching of aluminium-bearing ores like bauxite with a sodium hydroxide (NaOH) solution. Aluminium hydroxides from bauxite dissolve selectively at a high pH value, elevated temperature and pressure while most of the other compounds remain insoluble in the leachate or bauxite residue (red mud) (Kaußen & Friedrich, 2016). Pressure leaching with alkaline solutions is quite selective for Al and because Fe is almost insoluble in alkaline solutions. However, the dissolution of silicon dioxide (SiO_2) is of concern and can only be removed at the expense of extracted aluminium. The removal of silicon (Si) from aluminate solution before precipitation of aluminium hydroxide ($Al(OH)_3$) can become a major problem due to the formation of insoluble sodium aluminate silicates (Shemi, 2013).

2.8.3 Acid leaching

To extract aluminium from high silica non-bauxitic resources such as CFA, acid leaching processes are generally preferred. Silica is substantially insoluble in acid solutions unlike in alkaline solutions. A strong acid or base and high temperatures are required to dissolve the amorphous phases in CFA and decompose acid-resistant mullite into soluble forms of Al (Taggart et al., 2016).

The three commonly used acids are hydrochloric acid, sulphuric acid and nitric acid (Shemi, 2013). It is important to note that all three acids are hygroscopic (attract water molecules from the surrounding environment) and corrosive to (destroy or irreversibly damage) living tissue (Hagen & Järnberg, 2009). A brief review of the acids is given below. The knowledge of their characteristics is necessary for the selection of suitable conditions for acid leaching processes.

Hydrochloric (HCl) is the strongest of the three acids. The acid can be described as a clear, colourless aqueous solution of hydrogen chloride gas with a pungent irritating odour (Hagen & Järnberg, 2009; Shemi, 2013). HCl is highly corrosive however it is a strong monoprotic mineral acid that has many industrial uses. The acid is consumed in many mining operations for ore treatment, metal extraction, separation, purification, and water treatment. HCl is also very effective in extracting REEs from CFA. The acid reacts with basic compounds such as calcium carbonate or calcium sulphate to form soluble chlorides (Shemi, 2013). The disadvantage of using HCl besides that it is highly corrosive is that it also reacts rapidly with oxidants forming toxic chlorine. When in contact with air HCl emits corrosive fumes and hydrogen gas produced from HCl attacks nearly all metals (Hagen & Järnberg, 2009).

Sulphuric Acid (H₂SO₄) is a colourless to slightly yellow viscous liquid which is soluble in water at all concentrations, it is also a highly corrosive, strong mineral acid. H_2SO_4 is highly corrosive, due to its highly exothermic (generates heat) reaction with water (Hagen & Järnberg, 2009). However, unlike HNO_3 and HCl it is diprotic meaning it releases two protons (H^+) per molecule in an aqueous solution. H_2SO_4 has a wide range of applications such as metal extraction, chemical synthesis and production of copper sulphate solution used as an electrolyte in copper electro-refining and electro-winning processes (Shemi, 2013). The disadvantage of using the acid is that when in contact with metals the acid can release flammable hydrogen gas (Hagen & Järnberg, 2009).

Nitric Acid (HNO₃) is the weakest of the three acids and is also a highly corrosive, monoprotic, toxic and strong mineral acid with strong oxidizing characteristics (Hagen & Järnberg, 2009). The acid is normally colourless but can acquire a yellow cast due to the accumulation of oxides of nitrogen if stored for a long time. Normally nitric acid has a concentration of 68%, however, when concentration is more than 86%, it forms nitric acid fumes. The primary uses of nitric acid include the production of explosives, etching and dissolution of metals, especially as a component of aqua regia for the purification and extraction of gold, and in chemical synthesis (Shemi, 2013). The drawback of using HNO_3 is that it has a choking odour and in the presence of light or by heating, HNO_3 readily decomposes. When HNO_3 reacts with metals the reaction may produce nitrous gases and ammonia. Concentrated HNO_3 (~70 %) is a powerful oxidising agent and reacts with combustible, organic and readily oxidisable materials. The reactions are often highly exothermic and explosive. It is important to note that aqueous solutions of > 45 % HNO_3 may spontaneously ignite organic materials such as wood and straw (Hagen & Järnberg, 2009).

All the acids mentioned above have their advantages and disadvantages in terms of their safety and their use in industry. It is important to also discuss their efficiency in REE extraction to select the ideal acid to use for the present study. In a study by Yang, (2019) the leaching characteristics of REEs from bituminous coal-based sources in Kentucky in the U.S were studied. The author achieved total REE leaching efficiency of 80%, 76%, and 74% using 1 mol/L of HCl, HNO_3, and H_2SO_4 solutions respectively. HCl was not only the most efficient acid it also had the highest leaching rate followed by HNO_3 then H_2SO_4.

In another study, Kim et al, (2016) investigated the optimization of acid leaching of REEs from Mongolian apatite-based ore. At a concentration of only 2 mol/L, HCl and NHO_3 solutions

leached almost 100% of REEs. While with H_2SO_4, at 2 mol/L, only about 50% of REEs were leached and even after an increase in concentration up to 13 mol/L no greater than 80% of REEs were leached.

A study by Walawalkar et al, (2016) found that HNO_3 had the highest leaching efficiency out of all the three acids used during the investigation of the acid leaching of REEs from Canadian phosphogypsum. At 1.5 mol/ L, HCl, HNO_3 and H_2SO_4 had leaching efficiencies of 51%, 57% and 33% respectively.

In all the above-mentioned studies, H_2SO_4 had the lowest leaching efficiency. Both Kim et al, (2016) and Walawalkar et al, (2016) mention that the reason behind the low efficiency is in H_2SO_4 solutions is the reprecipitation of REEs via calcium sulphate ($CaSO_4$) formation. Calcium sulphate hydrates (gypsum, hemihydrate, and anhydrite) readily form wherever calcium and sulphate are present together in aqueous solutions. The formation of $CaSO_4$ resulted in a significant decrease in the average leaching efficiencies of REEs in H_2SO_4 solutions at different acid concentrations (Kim et al., 2016).In all the studies mentioned above the leaching of large amounts of Ca in solutions with HCl and NHO_3 was an issue of concern. The authors mentioned that large amounts of Ca in the leachate can cause complications during REE recovery by either precipitation or solvent extraction. Walawalkar et al. (2016) suggested increasing solid-liquid-ratios and decreasing acid concentration to lower Ca leaching efficiency. While Kim et al. (2016) used a two-stage leaching procedure to reduce the amount of Ca ions in the leachate. The leaching procedure involved pre-leaching with 1 mol/L of HCl to dissolve Ca then leach the sample with 2 mol/L to dissolve REEs. The reactions between HCl and CFA during acid leaching for the recovery of REEs can be explained by the following equations (Cao et al., 2018):

$$Al_2O_3 + 6HCl = 2AlCl_3 + 3H_2O \tag{2.1}$$

$$Fe_2O_3 + 6HCl = 2FeCl_3 + 3H_2O \tag{2.2}$$

$$CaO + 2HCl = CaCl_2 + H_2O \tag{2.3}$$

$$RE_2O_3 + 6HCl = 2RECl_3 + 3H_2O \qquad (2.4)$$
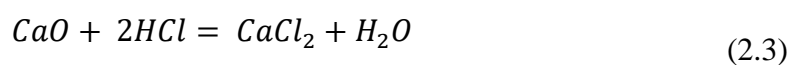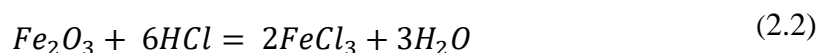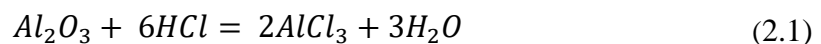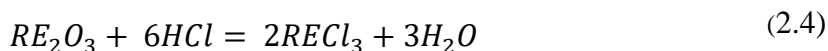
HCl is often preferentially reacted with the oxides of the major metal such as Al_2O_3, Fe_2O_3 and CaO in CFA as shown in Equations (2.1), (2.2) and ((2.3) and then the reactions between HCl and oxides of REEs (RE_2O_3) proceed as indicated in equation (2.4). This is because REEs tend to be encased within the Fe, Ca-rich aluminosilicate glass thus HCl first reacts with the major elements then reacts with REEs (Cao et al., 2018). This indicates that there needs to be an adequate amount to HCl so that there is enough to react with REEs even after reaction with major element oxides (Tang et al., 2019) however in some instances preconditioning of the CFA may be required to breakdown the aluminosilicate glass so that the acid has greater access to REE during acid leaching and improve REE recoveries (Taggart et al., 2018).

The shrinking core model

Leaching kinetics of REEs from CFA have been studied to understand influencing factors in leaching experiments (Cao et al., 2018). Seidel & Zimmels (1998) stated that "Leaching processes of CFA can be described in the framework of heterogeneous non-catalytic reactions in conjunction with the shrinking core model." In the shrinking core model (SCM) the reaction occurs from the outer layer of the particle to the inner layer (see Figure 2.4)
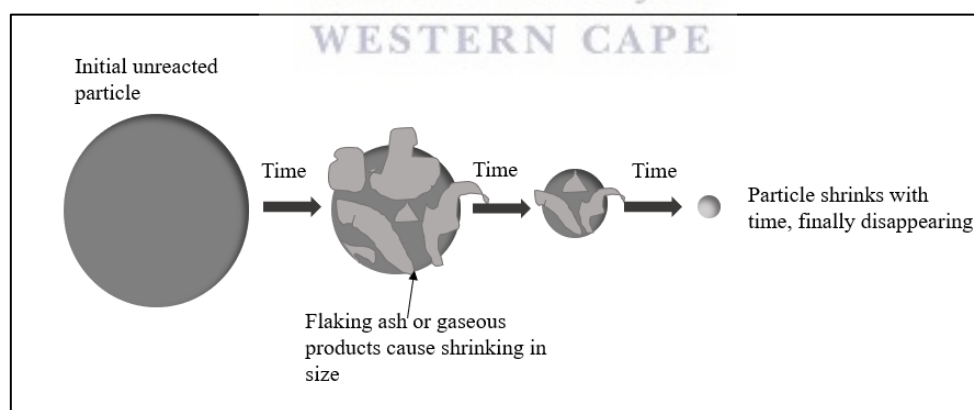
Figure 2.4: Shrinking core model modified from Ray & Ray (2018)

The effective reaction zone erodes into the solid and generates completely reacted material and an unreacted core. This core material presents and shrinks in size throughout the reaction time (Levenspiel, 1999). CFA particles can be seen as spherical particles which contain REEs. If the migration of H+ in the solution is not limited by solution concentration and the solid−liquid ratio, H+ reacts with the REEs at the surface of the CFA particle, and rare earth ions are dissolved out from the particle surface and diffuse into the solution. The REEs are encapsulated

in the body of CFA and they are dissolved and released layer by layer during the leaching process (Cao et al., 2018).

The SCM is based on the assumptions of pseudo-steady state diffusion and that the solid particle is spherical and reacts with the fluid isothermally (temperature of a system remains constant) (Shemi, 2013). According to these assumptions the surface reaction of solid-fluid systems can be considered to consist of the following steps (Wen, 1968):

(1) diffusion of the fluid reactants across the fluid film surrounding the solid,

 (2) diffusion of the fluid reactants through the porous solid layer

(3) adsorption of the fluid reactants at the solid reactant surface,

(4) chemical reaction with the solid surface,

(5) desorption of the fluid products from the solid reaction surface, and

(6) diffusion of the product away from the reaction surface through the porous solid media and through the fluid film surrounding the solid.

Depending on which step from the list above, is rate-controlling, three different types of reaction mechanisms may be obtained. These reaction mechanisms are, (1) diffusion control, (2) product layer control and (3) chemical reaction control. These steps take place consecutively, meaning that if any of the above steps is much slower than all the others, that step becomes the rate-determining step (Wen, 1968). This essentially means that SCM is controlled either by the diffusion process where the concentration of the substance on a solid surface plays an important role or by the chemical reaction of the solid and liquid (Yang, 2019).

The model equation to determine the rate constant of either process are as shown in equation 2.5 for diffusion, and equation 2.6 for chemical reactions (Gharabaghi et al., 2009; Levenspiel, 1999):

$$\left[1 - \frac{2}{3} - \propto -(1-\propto)^{\frac{2}{3}}\right] = \frac{2M_B\, DC_A}{\rho_B a r_0} = k_d t \qquad (2.5)$$

$$\left[1 - (1-\propto)^{\frac{1}{3}}\right] = \frac{kM_B\, C_A}{\rho_B a r_0} = k_r t \qquad (2.6)$$

Where α is the fraction that reacted; k the kinetic constant; M_B the solid molecular weight; C_A the acid concentration (% by weight); a the stoichiometric coefficient of the component in reaction; r_0 the initial radius of the particle; t the reaction time; D the diffusion coefficient in porous product layer; and k_d , k_r the diffusion rate constant and chemical reaction rate constant, respectively.

2.8.4 Direct and Indirect acid leaching

As discussed in the previous section, the type of acid used plays an important role in acid leaching for REEs. Another important role player in these leaching experiments is the type of acid leaching conducted in the experiment. There are two types of acid leaching, indirect and direct acid leaching. Figure 2.5 is a diagram showing the basic steps in direct and indirect acid leaching methods. Direct acid leaching does not require intervention before the leaching process. While indirect acid leaching requires some material pre-conditioning before leaching. (Shemi, 2013).
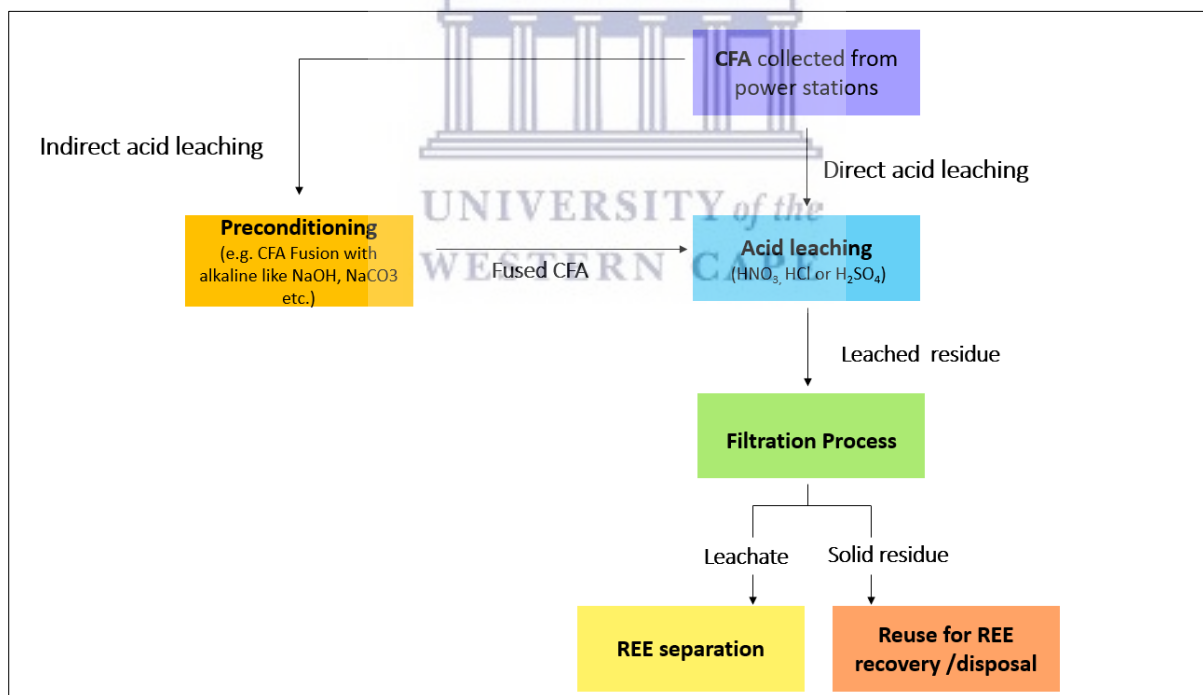
Figure 2.5: Direct and indirect acid leaching methods for recovery of REEs from CFA.

An example of pre-conditioning is sintering REE source material with an alkaline like calcium oxide (CaO), sodium hydroxide (NaOH), sodium carbonate (Na_2CO_3), calcium sulphate ($CaSO_4$), and/or ammonium sulphate (NH_4)2SO_4) followed by acid leaching (Taggart et al., 2018). Sintering activates the inert material from CFA based on the reaction with a sodium or calcium compound at high temperature, in which the phases of quartz and mullite can be

25

transferred into a series of soluble silicates such as nepheline, and noselite, to provide good materials for subsequent acid leaching (Taggart et al., 2018; Yao et al., 2014). The reaction between NaOH with mullite ($3Al_2O_3 \cdot 2SiO_2$) and quartz (SiO_2) in the CFA can be explained using the following equations (Pan, Hassas, et al., 2020):

$$6NaOH(s) + 3Al_2O_3 \cdot 2SiO_2(s) = 2NaAlSiO_4(s) + 4NaAlO_2(s) + 3H_2O(g)$$ (2.7)

$$2NaOH(s) + SiO_2(s) = Na_2SiO_3(s) + H_2O\ (g)$$ (2.8)
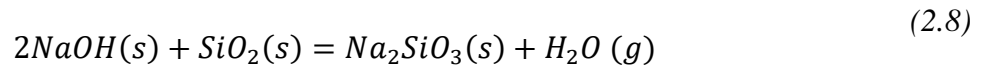
NaOH reacts with mullite and quartz in CFA to produce nepheline ($NaAlSiO_4$) and sodium silicate (Na_2SiO_3), which can then be readily dissolved in acid to improve the recovery of REEs during acid leaching. The leached residue can be filtered and separated into leachate and solid residue. Then the leachate can be taken for further processing where REE can be separated from the solution and the solid residue can be reused for REE recovery again or the residue can be disposed of (Pan et al., 2020). Taggart et al. (2018) studied the effects of roasting additives (alkalines) and leaching parameters on the extraction of REEs from CFA found in Powder River Basin and Appalachian, Illinois, USA. When Appalachian, Illinois CFA, was directly leached with acid, the CFA recovered < 50% of total REEs. The leaching efficiency of the CFA improved when it was sintered with NaOH before leaching, recovery was >70% REEs. However, from the Powder River Basin CFA, approximately 100% of REEs were recovered regardless of whether the sintering process was applied before acid leaching. This suggested that for Powder River Basin CFA, direct acid leaching was sufficient for recovering REEs. The authors of the study concluded that there are three reasons why CFA from Powder River Basin is more susceptible to acid leaching. The first reason is that Powder River Basin CFA has a higher CaO content than Appalachian, Illinois CFA. The Higher CaO content of CFA makes the particles more soluble thereby increasing REE extraction. Secondly, Ca-Fe in the glass phase of Powder River Basin CFA is more enriched, meaning REEs are present in higher concentrations relative to the bulk ash. Finally, high-Ca CFA is essentially subjected to alkali roasting conditions during combustion which makes them more susceptible to acid leaching.

Tang et al. (2019) found results similar to the Appalachian, Illinois CFA from the previous study by Taggart et al, (2018). The authors studied the extraction of REEs from Panbei coal-fired power plant CFA through alkali fusion–acid leaching. Alkali fusion-acid leaching involves roasting CFA with an alkaline then leaching the material with acid. CFA in the study

was subjected to direct and indirect leaching (alkali fusion -acid leaching). The concentration of each REE in leachate after alkali fusion was two times larger than that of direct leaching. REEs such as yttrium increased sharply from 8.93 ppm to 48.9 ppm and Ce increased from less than 43 ppm to 98 ppm.

The indirect leaching CFA also yielded better results than direct leaching in a study done by Wang et al. (2019). The authors studied the concentration, characterization and optimized extraction of REEs in CFA from the Luzhou power plant in Sichuan, Southwest China. In this study, CFA was directly leached with HCl alone and indirectly leached by NaOH then subsequently leached with HCl. The authors achieved average REE extraction efficiencies of 24.48% and 84.95% for direct and indirect leaching respectively.

The above studies have indicated that indirect acid leaching is more efficient at REE extraction than direct leaching except for CFA that has high CaO and Ca-Fe in the glass phase. Taggart et al. (2018) have suggested that for CFA that is high in CaO and that is enriched Ca-Fe in the glass phase, direct leaching is sufficient for REE extraction. To find optimum alkali fusion-acid conditions for REE leaching, the controlling parameters are discussed in the next section.

2.9   Controlling parameters

Alkali fusion-acid leaching is divided into two stages: the alkali fusion stage where an additive (flux) is roasted with CFA and an acid leaching stage, where the roasted mixture is subsequently leached with an acid to extract REEs. There are controlling parameters for both alkali fusion and acid leaching processes (Tang et al., 2019). To understand the effects of these parameters on the extraction of REEs from CFA three studies by Cao et al. (2018); Taggart et al. (2018) and Tang et al. (2019) have been discussed in the sections that follow. Taggart et al. (2018) conducted alkali fusion-acid leaching experiments on CFA found in Powder River (PRB), Appalachian (App) and Illinois (IL) basins in the U.S however the authors focused more on alkali fusion parameters. Cao et al, (2018) specifically conducted direct acid leaching experiments focusing on acid leaching parameters on CFA from the Panbei power station in China. Tang et al. (2019) conducted direct leaching and indirect leaching (alkali fusion- acid leaching) experiments focusing on both alkali fusion and acid leaching parameters also on CFA from the Panbei power station. Collectively, the parameters that these studies investigated are flux type, flux to CFA ratio, roasting temperature, acid concentration, leaching temperature, stirring speed, solid to liquid ratio and leaching time.

Alkali-fusion

A summary of the studies that investigated the controlling parameters of alkali fusion and their respective REE recoveries where available are shown in Table 2.5.

Table 2.5: Summary of alkali fusion controlling parameters investigated by different studies.

Parameter	study	Conditions	REE recovery
Flux type	(Taggart et al., 2018)	**Roasting**: $CaSO_4$, CaO, Na_2CO_3, NaOH, and Na_2O_2, 150, 250,350 and 450 °C; 1:1 and 1:6 ratio; 30 mins **Acid leaching**: 2 mol/L HNO_3	$CaSO_4$, CaO, Na_2CO_3 <50% NaOH, and Na_2O_2 >90%
Roasting temperature	(Taggart et al., 2018)	**Roasting**: NaOH, 150, 250,350 and 450 °C; 1:1 ratio, 30 mins **Acid leaching**: 1 mol/L HNO_3	150 and 250°C <60%, 350 and 450 °C >70%
	(Tang et al., 2019)	**Roasting:** $NaCO_3$, 680, 740, 800, and 860 °C; 1:1 ratio; 30 min **Acid leaching:** 2 mol/L HCl, 1:10 ratio, 200 rpm	
Flux to CFA ration	(Taggart et al., 2018)	**Roasting:** 1:1 and 1:6 ratio; $CaSO_4$, CaO, Na_2CO_3, NaOH, and Na2O2; 450 °C; 30 mins **Acid leaching:** 2 mol/L HNO_3	NaOH 1:05 50%, 1:1 80%, 1:6 90%
	(Tang et al., 2019)	**Roasting:** 1:05, 1:1, 1:1.2, 1:1.5 ratio, $NaCO_3$, 30 min **Acid leaching:** 2 mol/L HNO_3, 1:10 ratio, 200rpm	1:1.2 55.98%, 1:1.5 49.06%

2.9.1   Flux type

The study by Taggart et al. (2018) tested a variety of fluxes for the extraction of REEs from CFA. The authors selected low roasting temperatures in the experiments to directly compare roasting agents to the USGS Na_2O_2 sinter method and to avoid using high input energy during roasting. In the study, the only fluxes that had consistently high REE recoveries were NaOH and Na_2O_2. The authors explained that the effectiveness of Na_2O_2 and NaOH fluxes was due to their lower melting temperatures (460 °C and 318 °C, respectively) as compared to other fluxes tested (2613 °C for CaO, 851 °C for Na_2CO_3, and 1460 °C for $CaSO_4$). There were no fluxes besides Na_2O_2 and NaOH that recovered >50% of total REEs. The authors attributed the poor extraction efficiencies to the comparatively low roasting temperatures that were used in the study (150 to 450 °C). Na_2O_2 had the highest REE extraction efficiency however similar efficiencies were observed from NaOH. Consequently, the authors concluded that NaOH could be a less expensive alternative for an industrial-scale REE recovery operation since Na_2O_2 is more expensive. The authors were able to achieve REE recoveries > 90% using NaOH roasting, with the minimum flux-ash ratio is 1:1 and minimum acid strength is ~1–2 mol/L HNO_3.

2.9.2 Roasting temperature

Taggart et al. (2018) tested the effect of roasting temperature (at 150 °C, 250 °C, 350 °C, and 450 °C) on REE recovery. REE recovery when roasting at 450 °C and 350° was significantly greater than at 250 °C and 150 °C for App and IL Basin CFA. The PRB CFA was the only exception, REE recovery dropped at 250 °C and 350 °C but was near 100% at 450 °C and 150 °C. The authors explained that the extractability of PRB CFA was driven by acid-leaching rather than by roasting. The authors stated that the results suggested that for NaOH roasting, a temperature threshold exists between 250 °C and 350 °C, below which REE recoveries drop off. Furthermore, the optimal NaOH roasting temperature for REE extraction is 350 °C, though higher recoveries are possible at 450 °C., going beyond 450 °C is likely to result in diminishing returns for the energy expended to raise the temperature. The authors suggested that for future studies, longer roasting times (eg.2 h instead of 30 min) and a heated leaching step may improve REE recoveries while using less NaOH.

The study by Tang et al. (2019) also tested the effect of roasting temperatures for REE recovery. Then fusion mixture was roasted at 680 °C, 740 °C, 800 °C, and 860 °C. As observed in the study by Taggart et al. (2018) when the roasting temperature was relatively low (680 °C), some of the $NaCO_3$ does not react with CFA which produced low recoveries. When the roasting temperature increased, the $NaCO_3$ was further reacted so that the solid-state reaction was accelerated, and more minerals were transformed into nepheline (a soluble silicate) as the temperature rose to 860 °C. Thereby increasing REE recovery. REE leaching rate increased with increasing temperature. The optimal roasting temperature was found to be 860 °C. The optimal roasting temperature is much higher than the study by Taggart et al. (2018). It can be observed from these studies that the use of $NaCO_3$ requires high temperatures, which is a drawback due to the cost implications of the higher energy consumption at a larger scale. It is also important to study the effect of flux to CFA ratio because the amount of chemicals used in these experiments could also affect the feasibility of the REE extraction method at a larger scale (King et al., 2018).

2.9.3 Flux to CFA ratio

Taggart et al., (2016) stated that the processing of CFA for the recovery of metals such as REEs at an industrial scale requires economical use of reagents. Hence, the authors tested the 1:1 flux to CFA ratio on the different fluxes ($CaSO_4$, CaO, Na_2CO_3, $NaOH$, and Na_2O_2) to determine whether REE recovery depended on an excess of flux. The authors found that increasing the CFA to flux ratio from 1:6 to 1:1 resulted in lower TREE recoveries from both Na_2O_2 and

NaOH fluxes. However, REE recoveries for the 1:1 NaOH flux was consistently >70% and did not differ significantly from the mean of 1:5 NaOH, 1:6 Na_2O_2, or 1:1 Na_2O_2 REE recoveries. When leaching with 2 mol/L HNO_3, a six-fold reduction in NaOH (6:1 to 1:1 ratio) only slightly decreased REE recovery from 90% to 80%. The 1:1 ratio did not inhibit total REE recovery but improved it for the CaO and $CaSO_4$ roasts. The $NaCO_3$, recoveries at the 6:1 and 1:1 ratio did not differ significantly for any of the samples.

The study by Tang et al. (2019) found similar results when exploring the effect of the flux to CFA ratio on REE recovery. REE recovery first increased when CFA to flux ratio decreased from 1:0.5 to 1:1. However, REE recovery started decreasing when the ratio was further decreased from 1:1.2 to1:1.5. The authors stated that the reason for the increase in recoveries initially was due to a stronger reaction between CFA and Na_2CO_3 and the crystal structure of CFA being more activated but when the amount of Na_2CO_3 had continuously increased the leaching rate of TREEs reduced. The authors explained that the reduction was due to excessive Na_2CO_3. The Na_2CO_3 is left after the reaction, and some of the HCl is consumed to produce carbon dioxide gas. Both Taggart et al. (2018) and Tang et al. (2019) find that the optimal flux to CFA ratio was 1:1.

Acid leaching

A summary of the studies that investigated the controlling parameters of acid leaching and their respective REE recoveries where available are shown in Table 2.6.
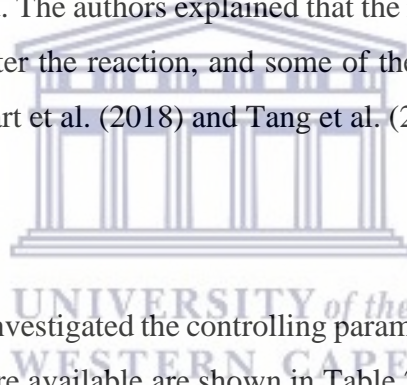
Table 2.6: Summary of acid leaching controlling parameters investigated by different studies

Parameter	study	Conditions	REE recovery
Leaching temperature	(Cao et al., 2018)	**Acid leaching:** 20, 30, 45, 60, 75, and 90°C; 2 mol/L HCl; 1:10 ratio; 200 rpm 120 min	Below 45°C <30%, 90°C 50%
Stirring speed	(Cao et al., 2018)	**Acid leaching:** 50, 100, 200, 300, and 500 rpm; 60°C; 2 mol/L HCl; 1:10 ratio; 120 min	
	(Tang et al., 2019)	**Acid leaching:** 100, 200, 300, 400, 500, 600 rpm; 2 mol/L HCl; 1:10 ratio	0 rpm < 36%, 400 rpm > 49%
Solid to liquid ratio	(Tang et al., 2019)	**Acid leaching:** 1:5, 1:10, 1:15, 1:20, and 1:30 ratio; 2 mol/L HCl; 400 rpm	1:5 < 50%,1:20 > 60%
	(Cao et al., 2018)	**Acid leaching:** 1:5, 1:10, 1:15, 1:20; 200 rpm, 60°C; 3 mol/L HCl; 120 min	1:5 40%; 1:10 60%
Leaching time	(Cao et al., 2018)	**Acid leaching:** 30, 60, 90, 120, 150, 180 min; 3 mol/L HCl; 60°C; 200 rpm; 1:10 ratio	30 min < 50%, 120 min > 60%
	(Tang et al., 2019)	**Acid leaching:** 0 to 120 min; 2 mol/L HCl; 1:10 ratio; 200 rpm	0 min < 40%, 120 min > 50%
Acid concentration	(Tang et al., 2019)	**Acid leaching:** 0.1, 0.5, 1, 2,4 mol/L HCl; 1:10 ratio; 400 rpm	0.1 mol/L 0.03%, 2 mol/L 59.78%
	(Cao et al., 2018)	**Acid leaching:**1, 2, 3, 5, and 7 mol/L; 200 rpm, 60 °C, 1:10 ratio; 120 min.	1 mol/L < 30%, 3 mol > 60%
	(Taggart et al., 2018)	**Acid leaching:** 0.0501–0.6001, 0.06–0.61, 0.366–0.916, 2 mol/L HNO₃, room temp	

2.9.4 Leaching temperature

The study by Cao et al. (2018) tested the effect of temperature on REE recovery from CFA. The authors intended to explore the possibility of recovering REEs from CFA under normal

pressure and low temperature (under 100 °C) conditions to save energy. At temperatures below 45 °C, the REE recoveries (La, Ce, Nd) were very low (<30%). The recoveries increased as the temperature increased. The authors explained that this is due to the accelerated process of the leaching reaction as temperature increases. However, the highest REE recovery achieved (obtained at 90 °C) was only about 50% within the scope of this experiment. The authors suggested that this could have been because the concentration of HCl used was not high enough. As the reaction continued, the acid depleted and the reaction was restricted. Therefore, it was necessary to find the optimal acid concentration. At 45−60 °C, REE recovery increased

rapidly. At 60−90°C REE recovery continued increasing but not as rapidly. Hence, 60 °C was selected as the optimal temperature for REE recovery.

Taggart et al. (2018) and Tang et al. (2019) leached roasted ash samples at room temperature however Taggart et al. (2018) suggested that having a heated leaching step may improve REE recoveries while using less NaOH in future studies.

2.9.1 Stirring speed

Cao et al. (2018) investigated the effect of stirring speed on REE recovery. The REE recovery tended to increase with the increase of the stirring speed. The authors stated that this is mainly attributed to the fact that the CFA particles are more dispersed in the acid solution as the stirring speed is increased, leading to an increase in the contact area between them and the acid. When the stirring speed was increased from 100 to 200 r/min REE recovery increased significantly. However, as stirring speed increased further, REE recovery increases only to a small degree. As the stirring speed increased from 200 to 500 r/min, REE recovery increased but not significantly. To improve REE recovery and save energy, the authors fixed the stirring speed at 200 r/min.

The influence of stirring speed on REE recovery was also investigated by Tang et al. (2019). As the stirring speed increased from 0 to 400 r/min, REE recovery increased significantly. The authors stated that the increase in REE recovery with stirring speed was primarily because this favours the liquid-solid reaction mass transfer in the reaction system. However, as the stirring speed continued to increase, the overall REE recovery showed a slight decline. They mentioned that this could have been because there were more silicon and iron that were leached into liquor, which contributed to the formation of a colloidal suspension. The consumption of the H+ in the solution aggravated this result, which impeded the leaching process.

The two studies show REE recovery increases with increasing stirring speed. Cao et al. (2018) stated that the REE recovery starts to decline at 300 r/min however Tang et al. (2019) found that the recovery declined after 400 r/ min. This could suggest that the optimal stirring speed is from 200 to 400 r/ min.

2.9.1 Solid to liquid ratio

Tang et al (2019) tested the effect of solid-liquid ratio on REE recovery. As the solid-liquid ratio decreased from 1:5 to 1:20, the REE recovery increased. Although the concentration of REEs in the liquor reduced with an increase in acid volume, the total of REEs in the liquor

increased. Consequently, the REE recovery was improved by increasing the solid-liquid ratio. Furthermore, the REE recovery was almost steady from 1:20 to 1:30. Considering the consumption of acid and the concentration of REEs in the leaching liquor the authors suggested the solid-liquid ratio of 1:20 was more appropriate.

Cao et al. (2018) also tested the effect of solid-liquid on REE recovery. As the volume of HCl increased, the recovery of REEs tended to increase. As the solid−solid ratio decreased from 1:5 to 1:10, the REE recovery rapidly increased from below 40% to above 60%. At lower solid−liquid ratios there is a higher contact probability between H+ and CFA particles, increasing REE recovery. However, as the liquid−solid ratio continued to decrease, REE recovery increased only a little. The authors stated that the reason for this was that there was already enough acid to react with the CFA powder so the solid-liquid ratio was no longer limiting REE recovery. The optimal liquid−solid ratio was 1:10.

2.9.2 Leaching time

The effect of leaching time on REE recovery was studied for both direct and indirect acid leaching by Tang et al. (2019). The study showed that REE recovery gradually increased with time. The optimal leaching time was 120 min.

Cao et al. (2018) tested the effect of leaching time on the REE recovery. REE recovery increased with the extension of leaching time. As the leaching time was extended from 30 to 60 minutes REE recovery increased significantly. At 60 to 90 minutes the REE recovery was almost unchanged. At 90−120 min, it increased significantly again. After 120 minutes, the rate of REE recovery was very slow. The authors' explanation for these results is as follows. There is a large concentration of H+ at the beginning (30 to 60 minutes), and there is a high content of rare earth compounds that are easily dissociated from CFA (mainly existing at the surfaces of CFA particles), prompting a rapid reaction process. As the reaction continues (60 to 90 minutes) the rare earth compounds on the surfaces of the particles are almost completely leached, and the unreacted part is mainly the part that is tightly packed inside the particle. The unreacted part of the CFA particles can be leached only after H^+ diffusion into the interior of the particles. As the reaction duration is further increased (90 to 120 minutes) the REE recovery rapidly increases again when H^+ comes into contact with the easily dissociated rare earth compounds inside the particles. After 120 min, there is only a slight increase in recovery because there is a decrease in the amount of H^+ in the solution, and the presence of unreacted rare earth compounds that are tightly packed in the CFA particles significantly reduce the

contact probability and contact area between the rare earth compound and HCl. Considering the potential savings in commercial costs the authors stated that 120 min can be selected as the optimal leaching time.

2.9.3 Acid concentration

The effect of acid concentration on REE recovery was tested by Tang et al. (2019). As the acid concentration increased, the REEs recovery increased rapidly. When the concentration of HCl was increased from 0.1 mol/L to 2 mol/L, the overall REE recovery increased distinctly from 0.03% to 59.78%. The authors stated that the primary reason for these results is that when the concentration of HCl was low, the amount of HCl was insufficient to meet the requirement of the leaching process, which lead to a surplus of alkali fusion products. However, as HCl concentration continued to increase, REE recovery declined slightly. The authors explain that the increase in concentration led to the increased dissolution of silicon and iron. Thus, a small amount of flocculation was formed on the surface of leach residue in suspension. This hindered the contact between H^+ and solid particles which lead to a drop in the leaching rate. The optimal HCl concentration was 2 mol/L. At optimal acid leaching conditions which are stirring intensity of 400 r/min and solid to liquid ratio of 1:20 (g/mL), Tang et al. (2019) found that the optimal acid concentration is 3 mol/L. When the authors tested the effectiveness of major acid leaching parameters (stirring intensity, acid concentration and solid to liquid ratio) against one another using orthogonal experimental analysis they found that acid concentration was the most influential parameter of the three. Acid concentration had a higher R-value (the difference between the maximum and minimum) for both REE leaching efficiency and concentration of REEs.

Cao et al. (2018) also examined the effect of HCl concentration on REE recovery. At relatively lower concentrations (1,2, 3 mol/L) HCl has a great influence on REE recovery. As the HCl concentration increased from 1 to 3 mol/L, the REE recovery sharply increased. However, when HCl concentration exceeds 3 mol/L REE recovery no longer increased significantly. The authors explained that at low acid concentrations, most of the acid was depleted by the major elemental oxide (Al_2O_3, Fe_2 and CaO) and only a small amount of acid was involved in the reaction with the rare earth compounds. As a result, there was a low REE recovery. At a higher acid concentration, there is enough acid to consume major elemental oxides and react with rare earth compounds. REE recovery no longer increases at concentrations higher than 3 mol/L because partially encapsulated REEs have no opportunity to contact the acid even though the recovery is no longer limited by the lack of hydrogen ions (H+). Therefore, Cao et al. (2018),

concluded that 3 mol/L was the optimal acid concentration for REE recovery from CFA. In a later study (Pan et al., 2020), the authors also had an orthogonal experimental analysis for acid leaching parameters (stirring rate, acid concentration, and solid-liquid ratio) and found that acid concentration had the highest R values, indicating that it was the most influential factor.

The effect of leachate pH on extractable REE percentage was tested by Taggart et al. (2018) at several NaOH-ash ratios using the Appalachian basin CFA. The author stated that leachate acidity had a greater impact on REE recovery than the flux-to ash ratio because the H+ concentration varied over a much wider range. They also observed that variation in total REE extracted with pH or NaOH-ash ratios was lower at high leachate pH values (pH 2.5 to 4). This suggests that acid concentration rather than NaOH-ash ratio controls REE recovery under these conditions. The authors suggested that to achieve >90% REE recovery using NaOH sintering, the minimum flux-ash ratio is 1:1 and the minimum acid strength is ~1–2 mol/L HNO_3.

In the study by Cao et al. (2018) the authors studied the leaching kinetics involved in the recovery of REEs from CFA using HCl and by fitting their leaching results in the SCM model equations and found that correlation values of the chemically controlled model were generally greater than those of the diffusion-controlled model. This meant that the leaching mechanism of REEs from CFA tends to be more controlled by chemical reactions. Efficiency is more affected by the reactant concentration than other process parameters in a chemical reaction, hence acid concentration is usually the most influential factor in acid leaching experiments. Thus, the present study will investigate the effects of acid concentration on the extraction of rare earth elements from South African CFA

2.10 Summary of literature

The literature has introduced REEs as critical raw materials that are an important part of many emerging technologies in the modern world. Rare earth elements (REEs) are indispensable strategic resources that consist of 17 elements that are chemically similar to each other, including 15 lanthanides as well as yttrium and scandium. These elements can be classified as light, medium or heavy depending on their geochemistry and critical, uncritical and excessive according to their demand-and-supply relationship. Heavy REEs are more valuable than light or medium REEs because they are rarer and critical REEs are more valuable because they are in high demand and are low in supply.

REEs have been widely utilized in a variety of advanced materials and technologies such as alloys, optics, catalysts, electronic communications and clean energy. Their demand has been

increasing in the past decades due to their unique electrochemical, magnetic, and luminescent properties. The automotive and the wind power industries are two areas where demand for REEs is significant and projected to increase. REE deposits are scattered around the world with China being the REE powerhouse. There are large iron-rich rare-earth-bearing deposits that exist outside of China like in South Africa however a number of them are not exploited as no economically viable process exists to do so. Furthermore, in recent years, the majority of countries that produce and export REEs like China, have reduced their export to other countries to protect their national downstream industry. This increases the gap between demand and supply of REEs, leading to the search for alternative sources of REEs such as CFA.

REEs are present in Coals all over the world including South African coals. South African coal deposits are from the Main Karoo Basin which hosts 19 coalfields. South African coals are potentially more enriched with REEs than the UCC and have REE contents higher than the hard coal Clarke values as well as Chinese coal from the Jungar power station. Furthermore, South African CFA is more enriched with REEs than the coal it produced from as well as the CFA that comes from the Jungar power station in China. This indicates that South African coals and CFA can compete with the world coal and CFA for REE recovery.

CFA is considered to be a ferro-aluminosilicate composed of glass spheres of small particle size (20 – 80 μm) with high surface areas and largely consists of quartz and mullite. REEs reside in the aluminosilicate glass of CFA. Aluminosilicate glasses that are enriched with major metals such as Fe and Ca are more enriched with REEs than aluminosilicate glasses that do not. Cao rich CFA yields higher REE recoveries than CFA with lower CaO content. South African CFA is characterised as class F CFA, meaning it is low in CaO. Preconditioning of the CFA may be required to make the CFA more soluble for the recovery of REEs. Strong acid or base used together with high temperatures are required to dissolve the amorphous phases where REEs occur in CFA to decompose acid-resistant mullite into soluble forms of Al for better REE recoveries. However, the use of strong acids can harm the environment.

Since REE extraction techniques generally include initial acid leaching, followed by removal of undesired minerals, using solvent extraction, it is also important to consider the environmental implications of these methods. When extracting REEs from CFA it is important to be aware that the extraction process is non-selective, elements of concern can be mobilized along with REEs through the extraction process (King et al., 2018).

Various studies have investigated REEs in CFA, but further research is needed to identify and refine scalable REE extraction. REEs reside in the alumina of CFA, hydrometallurgical processes can be used to extract aluminium of CFA enriched with REEs.

There are several leaching methods for CFA processing that have been extensively researched using a variety of routes that are acidic, alkaline or a combination of acidic and alkaline. Acid leaching methods had higher REE recoveries than alkaline methods. Literature has shown that HCl and HNO_3 produce high REE recovery, however, the in present study HCl will be used as a leachate for REE recovery because HCl is more economical.

The acid leaching processes in CFA can be described in the framework of heterogeneous non-catalytic reactions in conjunction with the shrinking core model. In the shrinking core model, the reaction occurs from the outer layer of the particle to the inner layer. The REEs are encapsulated in the body of CFA and they are dissolved and released layer by layer during the leaching process. If the migration of H^+ in the solution is not limited by solution concentration and the solid−liquid ratio, H^+ reacts with the REEs at the surface of the CFA particle, and rare earth ions are dissolved out from the particle surface and diffuse into the solution.

There are two types of acid leaching, these are direct and indirect acid leaching methods. Indirect acid leaching methods will be used in the current study for the extraction of REEs from CFA because indirect acid leaching methods produce higher REE recoveries than direct acid leaching methods.

Alkali fusion-acid leaching is controlled by the following parameters, flux type, roasting temperature, flux to CFA ratio, leaching temperature, stirring speed, solid to liquid ratio, leaching time and acid concentration.

NaOH and Na_2O_2 fluxes both had higher REE recoveries than the other fluxes studied by Taggart et al. (2018). Consequently, the authors concluded that NaOH could be a less expensive alternative for an industrial-scale REE recovery operation since Na_2O_2 is more expensive. The authors were able to achieve REE recoveries > 90% using NaOH roasting, with the minimum flux-ash ratio is 1:1 and minimum acid strength is ~1–2 mol/L HNO_3. Furthermore, the optimal NaOH roasting temperature for REE extraction is 350 °C, though higher recoveries are possible at 450 °C., going beyond 450 °C is likely to result in diminishing returns for the energy expended to raise the temperature. Taggart et al. (2018) and Tang et al. (2019) tested the flux to CFA ratio for the recovery of REEs using NaOH and Na_2CO_3 fluxes respectively. Both studies found that the optimal flux to CFA ratio was 1:1.

The study by Cao et al. (2018) tested the effect of leaching temperature on REE recovery from CFA. At 45−60 °C, REE recovery increased rapidly. At 60−90°C REE recovery continued increasing but not as rapidly. Hence, 60 °C was selected as the optimal temperature for REE recovery. Cao et al. (2018) investigated the effect of stirring speed on REE recovery. REE recovery tended to increase with the increase of the stirring speed. However, the authors found that when stirring speed increased beyond 200 r/min REE recovery increases only to a small degree. Therefore, 200 r/min was chosen as the optimal stirring speed. When the stirring speed was increased from 100 to 200 r/min REE recovery increased significantly. However, as stirring speed increased further, REE recovery increases only to a small degree. As the stirring speed increased from 200 to 500 r/min, REE recovery increased but not significantly. To improve REE recovery and save energy, the authors fixed the stirring speed at 200 r/min. Tang et al. (2019) also studied the influence of stirring speed on REE recovery. The study found that REE recovery only increased significantly from 0 to 400 r/min. Hence, the authors found that 400 r/min was the optimal stirring speed. Tang et al (2019) and Cao et al. (2018) tested the effect of solid-liquid ratio on REE recovery. The studies showed that leaching efficiency increases with decreasing solid to liquid ratio. At a solid to liquid ratio lower than 1:20 leaching efficiency started to decreases (Taggart et al.,2018) however, Cao et al. (2018) found that the leaching efficiency started to decrease at solid to liquid ratios lower than 1:10. This suggests that the optimal solid to liquid ratio exists from 1:10 to 1:20. Cao et al., (2018) and Tang et al. (2019) studied the effect of leaching time on REE recovery. The studies show REE recovery increases with leaching time. In the study by Tang et al. (2019), the leaching time only went up to 120 minutes. While in the study by Cao et al. (2018) the authors increased the leaching time to 180 minutes and they found that the leaching efficiency started to decline after 120 min. In both studies, the optimal leaching time is 120 minutes. The three studies by Tang et al. (2019), Cao et al. (2018) and Taggart et al. (2018) found that at concentrations lower than 1 mol/L the REE recovery drops and that increasing acid concentration can rapidly increase REE recovery. However, beyond 3 mol/L the REE recovery starts to decline. Furthermore, acid concentration has been proven to be the most influential factor in acid leaching experiments. This is because acid leaching for the recovery of REEs from CFA is a chemical reaction for which the efficiency is more affected by the reactant concentration than the other process parameters (Pan et al., 2020).

Cao et al. (2018) the authors studied the leaching kinetics involved in the recovery of REEs from CFA using HCl and by fitting their leaching results in the SCM model equations and

found leaching of REEs from CFA is more chemically controlled than diffusion controlled. Efficiency is more affected by the reactant concentration than other process parameters in a chemical reaction, hence acid concentration is usually the most influential factor in acid leaching experiments. Thus, the present study will investigate the effects of acid concentration on the extraction of rare earth elements from South African CFA.

3   Research methods

3.1   Introduction

REEs were recovered using the alkali fusion acid-leaching method using CFA from Tutuka, Kendal and Duvha power stations. The alkali fusion-acid leaching method is an indirect acid leaching method. Studies have shown that indirect acid leaching is generally more efficient at REE extraction than direct acid leaching methods (Taggart et al., 2018; Tang et al., 2019; Z. Wang et al., 2019). The CFA used in this study is produced by the combustion of coals that are found in the Highveld and Witbank coalfields. The Witbank and Highveld coalfields provide the majority of the coal sold in South Africa (Hancox & Götz, 2014). The power stations also dispose of the CFA using different methods (wet and dry disposal) which provides a good range of general ashing procedures in South Africa. This indicates that the samples collected in this study are representative of South African CFA.

3.2   Sampling location

Fresh CFA samples were collected from three South African power stations, Tutuka, Kendal and Duvha (see Figure 3.1). The power stations are all operated by Eskom, which generates 96% of South Africa's electricity (Hancox & Götz, 2014).
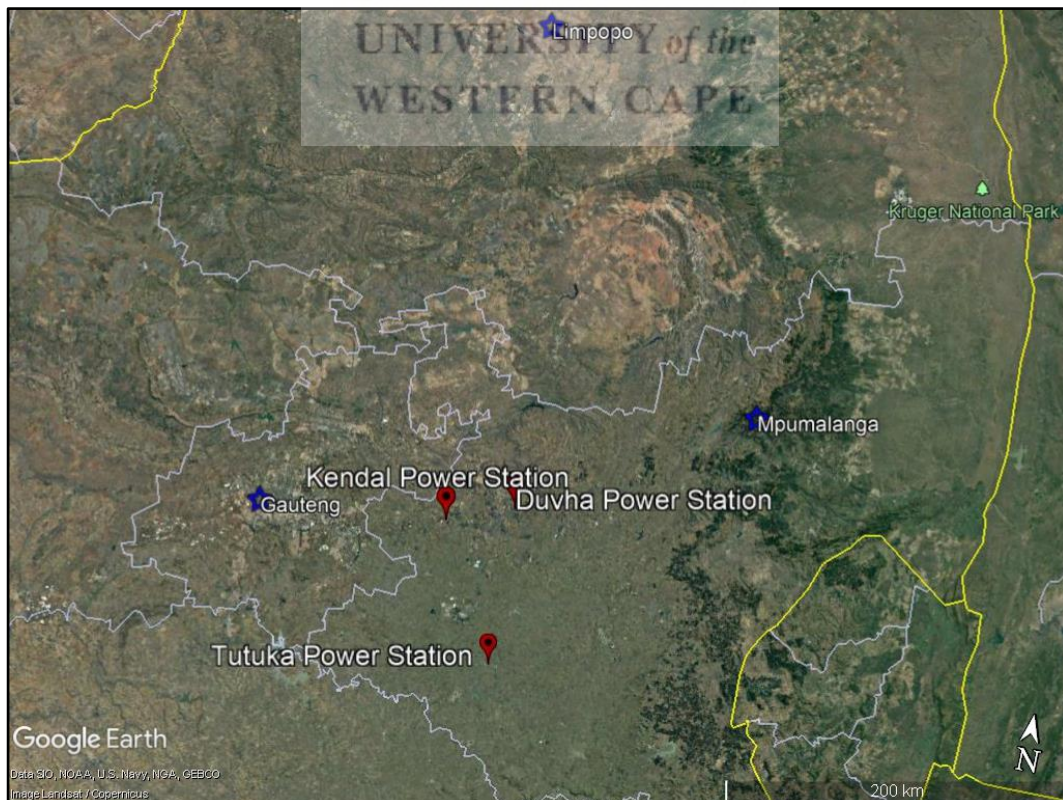
Figure 3.1: Location of power stations where CFA was sampled in the study

3.2.1 Tutuka

The Tutuka power station is located in between the towns of Standerton and Bethal, approximately 25 km from Standerton in the Mpumalanga province, South Africa. The power station consists of six 609 MW units at an installed capacity of 3 654 megawatts (Eskom Holdings SOC Ltd, 2020c). During power generation, the Tutuka power station disposes of dry ash (20% - 30% moisture content) through conveyors, a spreader and a stacker system from the station terrace to the ash disposal site (see Figure 3.2). The advantage of dry ash disposal is that there is reduced contact of ash with water, however, the disadvantage is the accumulation of dust and wind erosion as well as the instability of the ash pile when disposed of on the surface (Moolman, 2011).

Figure 3.2: Stacker being used for disposing of ash at the Tutuka Power Station (Lidwala Consulting Engineers (SA) (Pty) Ltd, 2014).

The AATC's New Denmark Colliery supplies the Tutuka power station with coal. The colliery is located in the Highveld Coalfield which is the second most productive coalfield in South Africa with ten operating collieries after the Witbank Coalfield (Jeffrey, 2005). The coalfield generally produced low-grade bituminous coal (Jeffrey, 2005). Akinyemi et al. (2012) studied the mineralogy and geochemistry of sub-bituminous coal and its combustion products from Mpumalanga Province, South Africa and found that Tutuka coal and coal ash have a total REE (TREE) concentration of 208.42 ppm and 517.8 ppm respectively. The coal and coal ash have a TREE concentration higher than that of the World hard coals (68.69 ppm) as determined by Ketris & Yudovich (2009) and the Upper Continental Crust (UCC) (168.37 ppm) as determined by Taylor & McLennan (1985). Thus, coal ash produced from the Tutuka power station should be considered as a viable option for REE recovery. Fresh CFA was collected on the conveyor belts at the Tutuka power station and poured into labelled 20-litre plastic buckets.

3.2.2 Duvha Power Station

Duvha is located approximately 15 km east of the town of Witbank in the Mpumalanga province, South Africa. The power station has six units that generate a combined capacity of the is 3 600 MW. The power station utilizes wet ash disposal during power generation (Eskom Holdings SOC Ltd, 2020a). The wet ash gets pumped into an ash dam. The settled water is then decanted to a low-level ash water return dam before it is pumped back to the station for reuse (Nemai Consulting, 2019). The advantage of wet ash is that it forms a pozzolanic layer which protects soil and groundwater, the disadvantage is the use of more water (Moolman, 2011). Duvha receives crushed coal from the neighbouring Duvha Opencast Mine (DOM) which is situated in the Witbank coalfield. The opencast coal mine is the largest in the Southern Hemisphere (Eskom Holdings SOC Ltd, 2020a). Wagner & Matiane (2018) studied REEs in the Main Karoo Basin (South Africa) coal and coal ash samples and found that coal from the Witbank coalfield had a TREE concentration of 141.08 ppm and also found that the CFA produced from burning the coal had an even higher TREE concentration of 587.53 ppm. The coal and coal ash have a TREE concentration higher than that of the World hard coals. However, the coal has a TREE concentration lower than that of the UCC. The coal ash sample, on the other hand, had a TREE concentration higher than the UCC, thus, coal ash produced from the combustion of Witbank coals like that of Duvha power station should be considered for REE recovery. Wet CFA samples were collected in the ash dams of the Duvha power station using labelled 20-litre buckets that were sealed after sample collection.

3.2.3 Kendal

The Kendal power station is found approximately 40km southwest of Witbank, Mpumalanga. The power station is the largest indirect dry-cooled power station in the world, which generates six 686MW units of power (Eskom Holdings SOC Ltd, 2020b). Kendal, like Duvha, receives coal from the Witbank Coalfield (Hancox & Götz, 2014). The power station also produces dry ash like Tutuka, during power generation (Zithole Consulting, 2000). The ash is partially wetted at the power station before being transported by conveyor belt to the ash disposal dump (Moolman, 2011). Kendal power station should also be considered for REE recovery because as stated in the previously coal ash produced from the combustion of coals from the Witbank coalfield should be considered for REE recovery because of their high REE concentration. The CFA was collected on the conveyor belts of the Kendal power station and poured into 20-litre labelled plastic buckets.

3.3 Sample preparation

The plastic buckets that contained the CFA samples were tightly closed to prevent the ingress of air and stored at room temperature for subsequent analysis. The samples were then dried in an oven at 105 °C for 24 hrs. before analysis at the University of the Western Cape.

3.4 Mineral and major and trace element analysis

The samples were characterized chemically and mineralogically using XRD, XRF and ICP-MS analytical techniques.

3.4.1 XRF

The X-ray Fluorescence spectrometer (XRF) analytical technique was used to characterize the CFA of the study by determining the major elements of the CFA. XRF analysis was conducted at the University of the Witwatersrand. XRF is generally used for the qualitative and quantitative elemental analysis of major elements in solid environmental, geological, biological, industrial and other samples (Eze, 2014). The principle of XRF analysis is based on the excitation of electrons by incident X-ray radiation. The ejection of electrons from the inner atomic shells creates vacancies that are filled by electrons falling back from the outer shells, whereby an excess of energy is emitted as a pulse of secondary X-ray radiation. The emitted fluorescence energy and wavelength spectra are characteristic for atoms of specific elements; this allows for the estimation of their relative elemental abundances (Weltje & Tjallingii, 2008).

Sample preparation

Clean Pt crucibles and porcelain loss of ignition (LOI) dishes were placed in a furnace at $1020^{o}C$ for half an hour to remove any organic residues. Once clean and cool approximately 1g of each sample was placed into each LOI dish. The LOI dish ID number and the weight of the LOI dish before and after the addition of the sample was recorded on a weight chart. The samples were ignited at $1020^{o}C$ for 40 minutes. Once ignition has completed the samples were removed from the furnace and allowed to cool in a desiccator (sealable enclosures used for preserving moisture-sensitive material). Approximately 1.75g of flux (Spectroflux 105) was placed into each Pt crucible. The Pt crucibles ID number and the weight of the Pt crucible before and after the addition of flux was recorded on a weight chart. The samples were also ignited at $1020^{o}C$ for 40 minutes. Once ignition has completed the samples were removed from the furnace and allowed to cool in a desiccator. A hot plate was switched on for a minimum of an hour. Once both the LOI and the Pt crucibles were cooled the after-ignition weights of the

LOI dishes were measured and recorded to determine the samples LOI. Similarly, the after-ignition weights of the Pt crucibles were measured and recorded to obtain the actual flux weights. Approximately 0.34g of pre-ignited sample was placed into each corresponding Pt crucible. The samples were ignited at 1020ºC for 50 minutes. Once ignition was completed the crucibles were removed from the furnace and allowed to cool in a desiccator. When solid particles were still present in the fused mixture once cooled, the mixture was reignited for an additional half an hour. After ignition, the weight of the Pt crucibles was recorded then returned into the furnace at 1020ºC. The fusion beads were individually poured from the Pt crucibles and pressed on a hot plate, making sure to lay the Pt crucibles in the same order as the beads are poured. If there were any beads containing bubbles or solid material they were broken and re-poured. The crucibles were then left to cool for 24 hours. The crucible IDs were then mapped for the labelling of the beads. The beads were allowed to sit for 90 minutes on the hot plate. Then the hot plate was switched off to allow the beads to anneal overnight.

XRF analysis

The prepared samples were ready for XRF analysis for the determination of major elements. Major elements were determined using the Norrish Fusion technique (Norrish & Hutton, 1969) using in-house correction procedures and using a Panalytical X-ray fluorescence spectrometer. CFA samples were fused using Johnson Matthey Spectrolflux 105 at 1000°C and raw data corrected using in-house software. Standard calibrations were made up using synthetic oxide mixtures and international standard rocks as well as in-house controls. The sample weight used was 0.35 gm and flux weight 2.0 gm. Calibration standards were primary International Reference Materials USGS series (USA) and NIM series (South Africa). Precision is taken as 1% for elements in an abundance of greater than 5% by weight, and 5% for elements in abundance less than 5%. The limitations of the XRF are that it only detects elements heavier in atomic weight than fluorine and that a large amount of sample (5g) is required for analysis due to the sample preparation method. In addition, the XRF technique cannot compete in accuracy with other well-established techniques for trace element analysis (Eze, 2014).

3.4.2   XRD

X-ray powder diffraction (XRD) analytical technique was used to determine the crystalline phases of the CFA in the study because REE occurrence has been associated with the aluminosilicate glass phase of CFA (Taggart et al., 2018). The XRD analysis was conducted at the iThemba labs. XRD analytical technique is widely used in chemistry and biochemistry to

determine the structures of an immense variety of molecules, including inorganic compounds, DNA, and proteins (Eze, 2014). XRD peaks are created by constructive interference of a monochromatic beam of X-rays scattered at specific angles from each set of lattice planes in a sample of material. The peak intensities are determined by the distribution of atoms within a lattice. As a result, the XRD pattern is the fingerprint of periodic atomic arrangements in a given sample of material (Bunaciu et al., 2015).

XRD analysis

The samples did not have to go through sample preparation because they were already in powder form. XRD measurements were taken using a multi-purpose X-ray diffractometer D8-Advance from Bruker operated in a continuous ϑ-ϑ scan in locked coupled mode with Cu-Kα radiation. The sample was mounted in the centre of the sample holder on a glass slide and levelled up to the correct height. The measurements were run within a range in 2ϑ defined by the user with a typical step size of 0.034° in 2ϑ. A position-sensitive detector, Lyn-Eye was used to record diffraction data at a typical speed of 0.5 sec/step which is equivalent to an effective time of 92 sec/step for a scintillation counter. The data was background subtracted so that the phase analysis was carried out for diffraction patterns with zero background after the selection of a set of possible elements from the periodic table. Crystalline phases were identified from the match of the calculated peaks with the measured ones until all phases were identified within the limits of the resolution of the results. The limitation of XRD is that it is much more accurate for measuring large crystalline structures. Small structures that are present in trace amounts can often go undetected which can result in skewed results (Johnson, 2021).

3.4.3 TIMA

The TESCAN Integrated Mineral Analyzer (TIMA) analytical technique was used to determine primary mineral phases in the CFA of the study. The TIMA analysis was conducted at the University of Witwatersrand. TIMA is a new generation of automated mineral analysers that incorporates many novel features to increase the capabilities and flexibility of the technology. The technology has been applied to a large number of commodities and industries such as base & precious metals, heavy minerals, coal, cement and oil & gas. It is used by mining companies at central and on-site laboratories, by service providers of mineralogical and metallurgical testing, by plant equipment and consumable suppliers and by earth science academic & research institutions (Gottlieb & Dosbaba, 2015).

Sample preparation

The CFA samples were prepared into ore blocks. The samples were split into smaller, representative portions of approximately 2g. The split sample was then placed into a plastic mould. Resin and hardener were mixed in one container, the ratio of a mixture was 7:1, 7 being resin and 1 a hardener. Approximately 7 ml of the resin mixture was poured into the plastic mould with the sample. The resin and the sample were mixed until bubbles disappeared. Then the sample was left to cure to room temperature, which would approximately take 8 hours. A sample label was placed in the cured sample then another mixture of resin and hardener was poured into the sample. The sample was left to cure for another 8 hours under room temperature. The sample was then removed from the mould and polished. Then the sample was ground using a 220grit grinding disc for 30 seconds. Then the sample was ground with a 1200grit for 1 minute. Then the sample was polished with 6micron diamond suspension and blue lubricant for 10 minutes with an MD_Dur polishing cloth. The sample was polished again using 3 microns of diamond suspension + blue lubricant for 10 minutes with an MD_Mol cloth. Finally, the sample was polished once more with a 1micron diamond suspension +blue lubricant for 10 minutes using an MD_fur cloth. Once the polishing is completed samples (ore block) are cleaned with water and dried with acetone and dispatched for TIMA analysis (see Figure 3.3).

Figure 3.3: Image of CFA samples prepared for TIMA analysis.

TIMA analysis

TIMA combines Energy Dispersive X-Ray (EDX) and backscattered electron (BSE) signals to identify minerals and create mineral images that are analysed to determine mineral concentrations, element distributions, and mineral texture properties such as grain-size, association, liberation and locking parameters. Image analysis in TIMA was performed simultaneously with SEM backscatter electron images and a suite of X-ray images. The level of hardware integration of the SEM and EDX allows for unprecedented acquisition speeds for fully automated data collection, resulting in fast, accurate, repeatable and reliable results.

3.4.4 ICP-MS: Solid samples

The inductively coupled plasma-mass spectrometry (ICP-MS) analytical technique was used to determine REE concentration in the CFA. The ICP-MS analysis was conducted at the University of Witwatersrand for the solid samples. The ICP-MS systems are widely used in the inorganic analysis landscape. The system continues to make inroads into laboratories that are requiring the lowest detection limits and the greatest level of productivity. When using ICP-MS samples are introduced into an argon plasma as aerosol droplets. The plasma dries the aerosol, dissociates the molecules, and then removes an electron from the components. Thereby forming singly charged ions, which are directed into a mass filtering device known as the mass spectrometer. Once the ions exit the mass spectrometer, ions strike the first dynode of an electron multiplier, which serves as a detector. The impact of the ions releases a cascade of electrons, that are amplified until they become a measurable pulse (PerkinElmer, 2011).

Sample preparation

The CFA samples were digested as follows. A mass of 50mg of sample was weighed and digested (decomposing a solid sample into a liquid state by dissolving it using reagents such as strong acids, alkalis, or enzymes) in an open hotplate. The open beaker/hotplate method begins with a 50mg sample which was placed directly into the 15ml Savillex beaker with 3mls of Ultra High Purity 2:1 HF: HNO_3 and placed on the hotplate at 70^OC to allow the acid to be evaporated off. Once dry 3mls of HF: HNO_3 was added and the beaker was capped and placed on the hotplate at 70° for a further 72 hours. The sample is then dried down at 70^OC and 3mls HNO_3 was added and evaporated off. Another 3mls HNO_3 was added and the beaker capped and placed on the hotplate at 70^OC for 24hours. The acid was then evaporated off and 3mls of HNO_3 was added again and allowed to evaporate off, samples were stored in this state until ready for analyses.

ICP-MS analysis

The Thermo Scientific iCAP RQ instrument was used for ICP-MS analysis (Figure 3.4). The solid samples were diluted to 50mls (Dilution Factor 1:1000) with 5% HNO_3, 100ppb rhenium (Re) and rhodium (Rh) as well as 50ppb Indium (In) and Bismuth (Bi), these elements are Internal Standards and are monitored throughout the analyses. Fluorides were minimised by allowing minimal contact between the sample and HF while still accomplishing total digestion. Samples were visually inspected for fluorides which occur as a precipitate once diluted. Calibration Standards were made at 5 different concentrations (10, 30, 50, 75 and 100ppb) with all the elements to be analysed present from purchased International Certified Reference Materials (CRM). The Thermo Scientific iCAP RQ was optimised for maximum counts on In and oxide levels set to less than 2% as well as doubly charged ions set to less than 2%. All measurements were done in triplicate by the instrument and averaged, replicate deviation greater than 2% was flagged.

Figure 3.4: An image of the Thermo Scientific iCAP RQ instrument used for ICP-MS analysis

The CRMs were digested and analysed with all unknowns, usually BCR-1, BHVO-2 and BIR-1. The CRMs must return to less than 10% deviation from known concentrations for all elements to pass the Quality Controls, they are usually within 5%. A Total Procedural Blank (TPB) was analysed with all unknowns, this entails a beaker with no sample but taken through the whole sample digestion procedure. This indicated Blank levels and how clean the preparation lab was. ICP-MS is limited by the matrix effects and instrument drift. Matrix

effects are enhancements and suppression of an analyte signal due to properties of the sample matrix. Instrument drift occurs when dissolved solids in samples deposit in the nebuliser and/or interface cones which leads to signal suppression (Wilschefski & Baxter, 2019).

3.5   Alkali fusion-acid leaching

A flow diagram of the alkali fusion-acid leaching is shown in Figure 3.5. The alkali fusion-acid leaching method that was used was modified from a USGS sodium peroxide (Na_2O_2) alkaline sintering method developed for the analysis of REEs in geological samples (Lichte et al., 1987; Meier et al., 1996; Meier & Slowik, 2002). The method has been further adapted using studies from Taggart et al. (2018) and Tang et al. (2019) for the alkaline fusion stage and studies by Cao et al. (2018) and Tang et al. (2019) for the acid leaching stage.
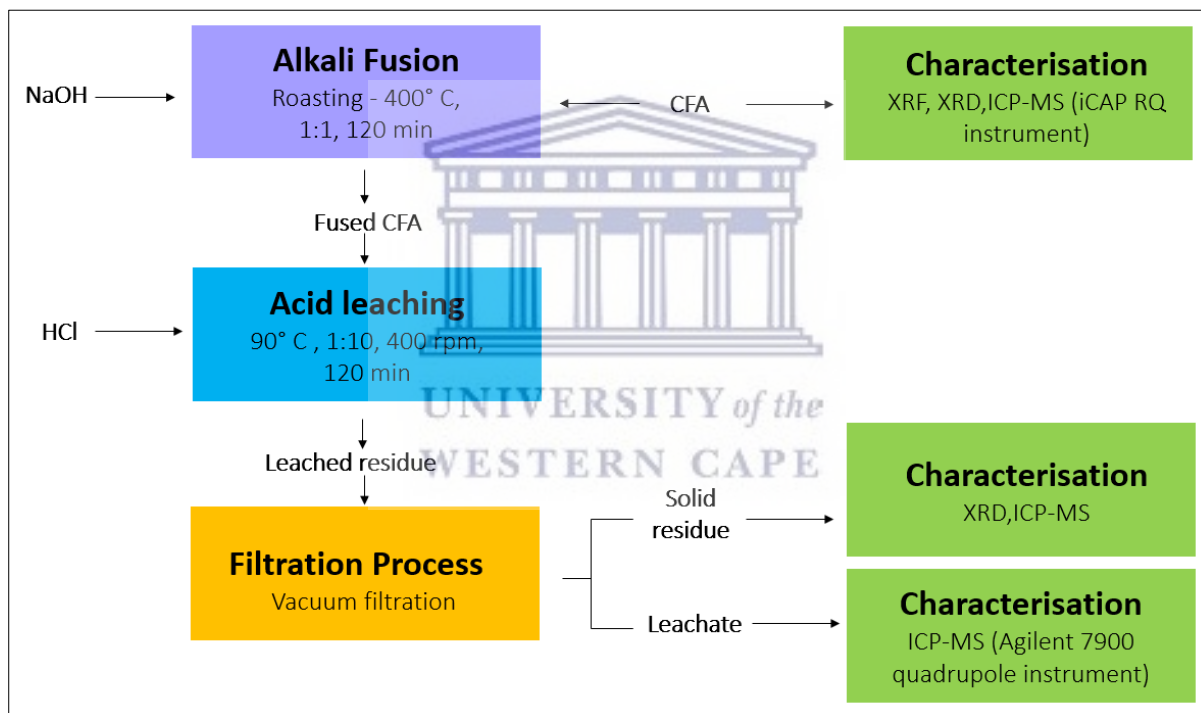
Figure 3.5: Flow diagram showing alkali fusion-acid leaching method.

3.5.1   Alkali fusion

In preparation for fusion, oven-dried CFA samples were mixed with NaOH pellets that were ground to a powder using a mortar and pestle. A mass of 10 g of CFA and 10 g NaOH (1:1 ratio) were weighed and mixed in a 30 ml crucible. 10 crucibles were prepared for each of the three power stations used in the study. The crucibles were placed in the Labofurn furnace to be roasted at 400 °C for 120 min (refer to Figure 3.6). Once roasted, the samples were left to cool to room temperature. Then the samples were subjected to grinding with mortar and pestle in

49

Figure 3.6: Image of alkali fusion samples which were roasted at a 1:1 ratio, 400 °C for 120 min.

preparation for acid leaching. Alkali fusion activates the inert material from CFA by reacting with NaOH at a high temperature to assist REE recovery during acid leaching.

3.5.2 Acid preparation

The following Equation was used to prepare acid for leaching:

$$C_1 V_1 = C_2 V_2$$

(3.1)

Where C_1 is the concentration of the stock acid, V_1 is the volume of acid that was added to the solvent (deionised water) and C_2 is the concentration of the solution after dilution and V_2 is the volume of the flask that will contain the solution.

To find the volume of stock acid that was required to prepare a specific concentration of acid, equation (3.1) can be rearranged to:

$$V_1 = \frac{C_2 V_2}{C_1}$$

(3.2)

3.5.3 Acid leaching

The acid leaching experimental apparatus as seen in Figure 3.7 was divided into a heating and stirring system, a reactor and a reflux condensing system. The magnetic stirrer hot plate provided heat to the water bath and a rotating magnetic field to stir the sample with the aid of

magnetic bars. A bar was placed in the water bath and another was placed in the 500 ml round bottom flask that serves as a reactor containing the acid leached CFA.
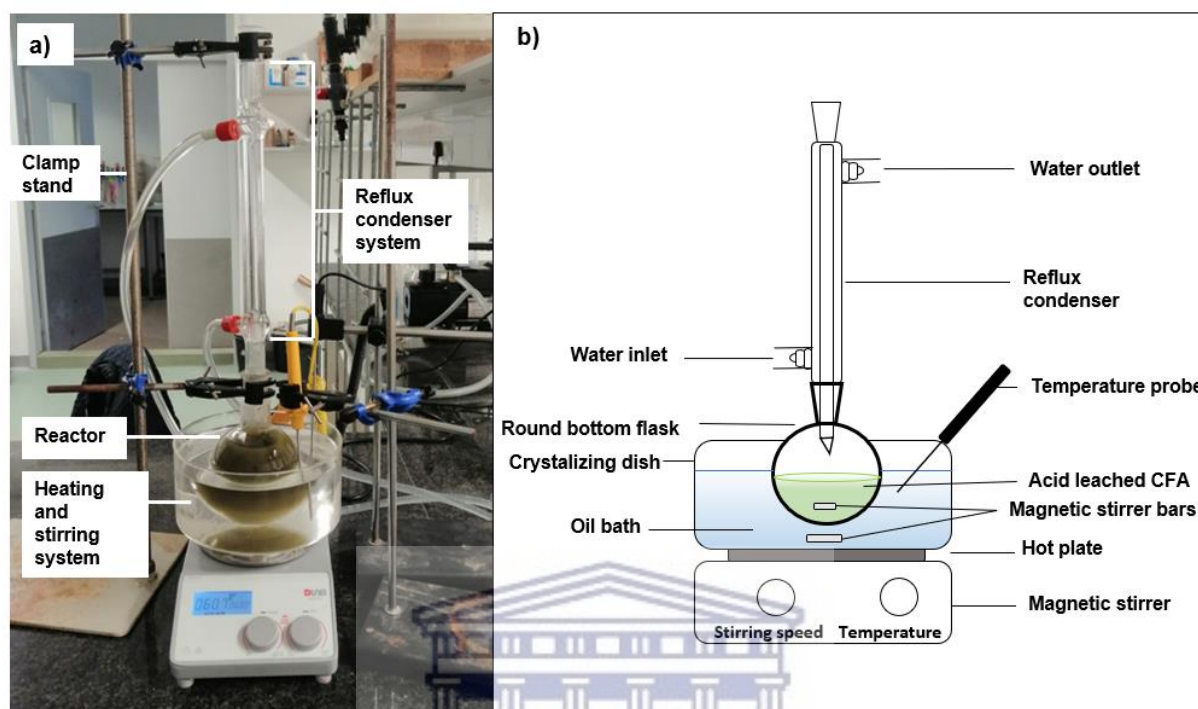
Figure 3.7: An overview a) and a detailed depiction b) of acid leaching of CFA at 1:10 solid to liquid ratio, 90 °C temperature, 400 rpm stirring speed and 120 min leaching time.

The flask neck was attached to the reflux condenser to prevent any liquid loss during the reaction. Cool tap water was continuously injected into the jacket of the condenser through the inlet of the condenser through to the outlet to reflux evaporated liquid. The evaporate above the reaction continuously condensed returning to the flask as condensate, this also ensures that the temperature of the reaction remains constant (Eze, 2014; Yang, 2019). The CFA of each power station was leached according to these conditions: 1:10 solid-liquid ratio (20g of CFA with 200 ml of HCl), stirring speed of 400 rpm and leaching time of 120 minutes. The acid concentration was set 1, 2 and 3 mol to test the effect of acid concentration on the extraction of REEs from the three-power stations. A duplicate sample was prepared for each sample taken at 1, 2 and 3 mol/L acid concentrations. A blank sample was prepared for each of the three power station CFA by leaching the CFA with deionized water. A total of 21 samples were taken for filtration.

3.5.4 Vacuum filtration

The vacuum filtration setup is shown in Figure 3.8. The setup was comprised of a Buchner funnel fitted with filter paper where the leching product was placed. The funnel was connected to a filtration flask with a rubber stopper. The flask collected the filtered leachate from the funnel. The flask was connected to a vacuum pump through a vacuum tube. When the vacuum pump was turned on it sucks out air from the filtration system, creating a vacuum.
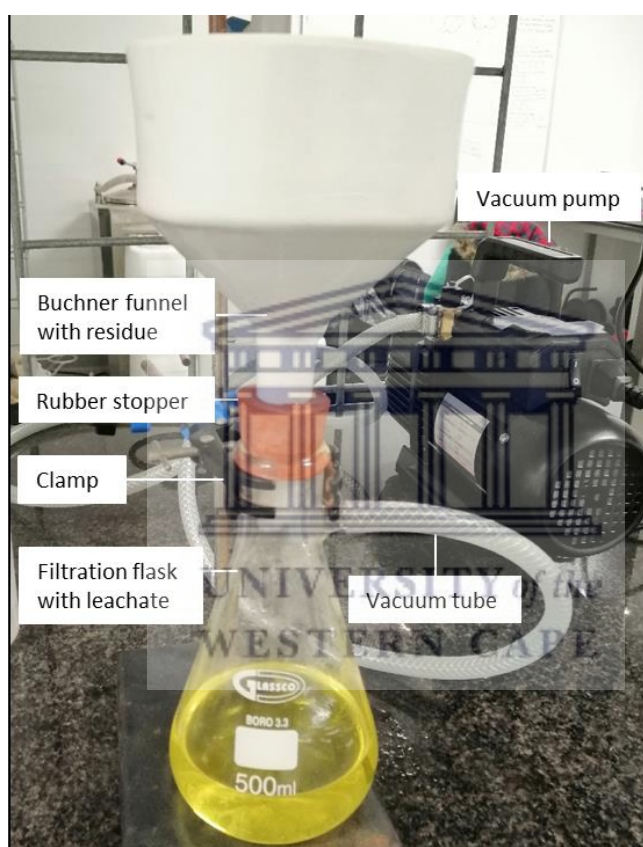
Figure 3.8: Vacuum filtration setup**.**

The vacuum creates pressure that allows the leachate to be filtered through the funnel. The solid residue was collected from the funnel after filtration and dried for 24 hours. The dried solid residue was then packed into labelled Ziploc bags then sent for analysis. The leachate was transferred into sampling bottles and stored in the fridge at 4 °C before being sent for analysis

3.5.5 ICP-MS: Leachate

The ICP-MS analysis for leachates was conducted at the Stellenbosch University. Trace element analysis of the leachates samples was performed on an Agilent 7900 quadrupole ICP-MS instrument equipped with a High Matrix Introduction (HMI) system to minimize matrix

loading during sample introduction. This reduces the effect of high matrix ions on analyte measurement by first minimizing instrument drift over time (resulting from salt deposition on the interface parts), while the ionization efficiency in the plasma is also increased through the reduction of easily ionized matrix elements. The sample was introduced through a ~0.2ml/min concentric nebulizer into a Peltier cooled spray chamber, after which the argon dilution gas from the HMI configuration is added before introduction into the high-temperature plasma. A 4th generation Octopole Reaction System (ORS), with helium (He) as collision gas and (hydrogen) H^2 as reaction gas was used to remove polyatomic interferences from the analytes of interest. To evaluate if the selected digestion methods were efficient in collecting the extractable mineral content from the samples and can be accurately and reproducibly measured by ICP-MS, suitable reference materials were processed in the same way as the samples. The accuracy of the method was reported along with the results. Sample duplicates were included when enough material was available. For the samples in this study, the following reference materials were used, Blood: Seronorm L2.

3.6   Rare earth element recovery

The REE recovery was determined using the following equation (Cao et al., 2018):

$$\propto = \frac{VC_2}{MC_1} \times 100\ \% \tag{3.3}$$

where $\propto$ is the recovery, V is the volume of leachate in mL, M is the mass of CFA sample in g, C_1 is the element content in CFA sample in µg/g, and C_2 is the element concentration in leachate in µg/ml. The efficiency of the alkali fusion-acid leaching method at different acid concentrations was examined by using statistical techniques.

3.7   Statistical Analysis

Statistical analyses were conducted using the IBMS, SPSS statistical analysis software. Three statistical analyses were conducted using the SPSS software: the Shapiro-Wilk test to determine normality of REE recovery data, Kruskal-Wallis H test was used to determine if there were significant differences between REE recoveries at different acid concentrations and the Mann-Whitney U test was used to determine which acid concentrations differed significantly in terms of REE recoveries.

Normality tests

There are numerous statistical procedures including correlation, regression, t-tests, and analysis of variance, namely parametric tests, that are based on the assumption that the data follow a normal distribution. Thus, it is important to determine the distribution of data to use the correct statistical techniques for the present study.

The Shapiro-Wilk test was used to determine whether REE recovery data from the CFA of each power station at each acid concentration was normally distributed. The Shapiro–Wilk test is a test of normality in frequentist statistics. The test was published in 1965 by Samuel Sanford Shapiro and Martin Wilk (Shapiro & Wilk, 1965). The Shapiro-Wilk test uses a single number to quantify the similarity between the observed and normal distributions. The test superimposes a normal curve over the observed distribution of data. It then computes which percentage of the sample overlaps with the normal curve (similarity percentage). The null hypothesis of this test is that the population is normally distributed. Thus, if the critical value (p) for the test statistic (W) is less than the alpha (α) level ($p < 0.05$) then the null hypothesis is rejected because there is evidence that the data is not normally distributed. In contrast, if the p-value is greater than the chosen α level ($p > 0.05$), then the null hypothesis (that the data came from a normally distributed population) cannot be rejected. The test statistic W is calculated as follows:

$$W = \frac{(\Sigma_{i=1}^{n} a_i x_{(i)})^2}{\Sigma_{i=1}^{n} (x_i - \bar{x})^2}$$

(3.4)

x_i is the ordered random sample values, a_i are constants generated from the covariances, variances and means of the sample (size n) from a normally distributed sample. The test is limited by sample size. The larger the sample, the more likely you'll get a statistically significant result. Although the Shapiro–Wilk test can handle larger sample sizes, the test is a more appropriate method for small sample sizes (<50 samples).

Normality can also be checked visually with frequency distribution (histogram), boxplot, and Q-Q plot (quantile-quantile plot). Normally distributed data creates a bell-shaped histogram, the lack of symmetry (skewness) and pointiness (kurtosis) are two main ways in which a distribution can deviate from normal. The skewness and kurtosis values of normally distributed data should be between -1.96 to +1.96. A boxplot that is symmetric with the median line at approximately the centre of the box and with symmetric whiskers that are slightly longer than

the subsections of the centre box suggests that the data may have come from a normal distribution. If the data are normally distributed, the result would be a straight diagonal line on a Q-Q plot (Ghasemi & Zahediasl, 2012).

Kruskal-Wallis H test

The Kruskal-Wallis H test is a non-parametric test that serves as an alternative to the One-Way ANOVA parametric test (Kruskal & Wallis, 1952). The H test is used when the assumptions for ANOVA are not met, like the assumption of normality. The test determines if the medians of two or more groups are different. The H static is the test statistic used in the Kruskal-Wallis H test. The null hypothesis of the test is that the medians of a population are equal. Thus, if the significance value (p) is less than the alpha (α) level ($p < 0.05$) then the null hypothesis is rejected because there is evidence that the medians of the groups are not equal. In contrast, if the p-value is greater than the chosen α level ($p > 0.05$), then the null hypothesis cannot be rejected. The Kruskal-Wallis H test assumes that there is/are:

- One independent variable with two or more levels (independent groups).
- Dependent variables can be in ordinal scale, ratio scale or interval scale.
- There should be no relationship between groups meaning that observations should be independent.
- All groups should have the same shape distributions.

The H statistic can be calculated as:

$$H = \left[\frac{12}{n(n+1)} \sum_{j=1}^{c} \frac{T_j^2}{n_j} \right] - 3(n+1) \tag{3.5}$$

Where n is the sample size for all samples, c is the number of samples, T_j is the sum of ranks in the jth sample and n_j is the size of the jth sample. The Kruskal-Wallis H test is limited because it determines if there are differences between groups, however, the test will not tell which groups are different for that a post-hoc test is required (Xia, 2020). The Mann-Whitney U test is a post hoc test (for non-parametric data) which is often an alternative to the t-test (for parametric data), which compares differences between two independent groups.

Mann-Whitney U test

The Mann-Whitney U test is a non-parametric test used to compare differences between two independent groups when the dependent variable is either ordinal or continuous, but not normally distributed (Mann & Whitney, 1947).

The assumptions of a Mann-Whitney U test are:

- The dependent variable should be measured at an ordinal or continuous level.
- The independent variable should consist of two categorical, independent groups.
- There should be independence of observations, which means that there is no relationship between the observations in each group or between the groups themselves.
- The distribution of the independent groups has to have the same shape.

The U statistic can be calculated as:

$$U = R_1 - \frac{n_1(n_1 + 1)}{2} \ or \ R_2 - \frac{n_2(n_2 + 1)}{2} \qquad (3.6)$$

Either of these two formulas is valid for the Mann Whitney U Test. *R* is the sum of ranks in the sample, and *n* is the number of items in the sample.

The limitations of using non-parametric tests such as the Kruskal-Wallis H test and the Man-Whitney U test is that they are not as powerful as parametric tests which means they are less likely to find a truly significant effect. However non-parametric tests can perform well with non-normal continuous data if there is a large enough sample size (generally 15-20 items in each group) (Sheskin, 2011). If there are significant differences in REE recoveries at different acid concentrations then the optimal concentration for the recovery of REEs from South African CFA can be established.

3.8 Chapter summary

This chapter has briefly described the power stations that have been sampled for CFA in the study. The sample preparation has been described followed by an explanation of the mineral and major and trace element analyses methods of CFA. The alkali fusion-acid leaching method and REE analysis have also been explained. The statistical analysis techniques used in the study have also been outlined. In conclusion, quality assurance measures that were taken in the study were as follows. The CFA collected from the selected power stations was placed in sealable

containers to prevent the ingress of air. The containers were labelled and the samples were documented appropriately. The pH and EC meters that were used were calibrated to ensure accurate readings. While quality control measures included taking blank samples for CFA from each power station and taking a duplicate for each acid leaching experiment. The next chapter will display and described the results of the study.

4   Results

4.1   Introduction

The composition of South African CFA from Tutuka, Kendal and Duvha power stations are examined through the analyses of major, minor and trace elements including rare earth elements (REEs) and mineral phases of the CFA. The major elements were determined using the XRF (X-ray Fluorescence spectrometry) analytical technique. The trace elements (including REEs) were determined using the ICP-MS (Inductively coupled plasma-mass spectrometer) analytical technique. The mineral phases were determined using the XRD (X-ray diffraction) and the TESCAN Integrated Mineral Analyzer (TIMA) analytical techniques. Furthermore, the chapter presents the findings of the REE extraction and recoveries at different acid concentrations from the CFA of the selected power stations. Finally, the concentration of trace elements in the leachate and solid residue after REE extraction were determined and compared to the target water quality ranges TWQR of South Africa to determine if there were any trace elements of concern.

4.2   Characteristics of African CFA South

4.2.1   Major elements

The elemental composition of Tutuka, Kendal and Duvha CFA used in this study was determined by XRF and the finding are shown in Figure 4.1 (see Appendix A- Table A1).
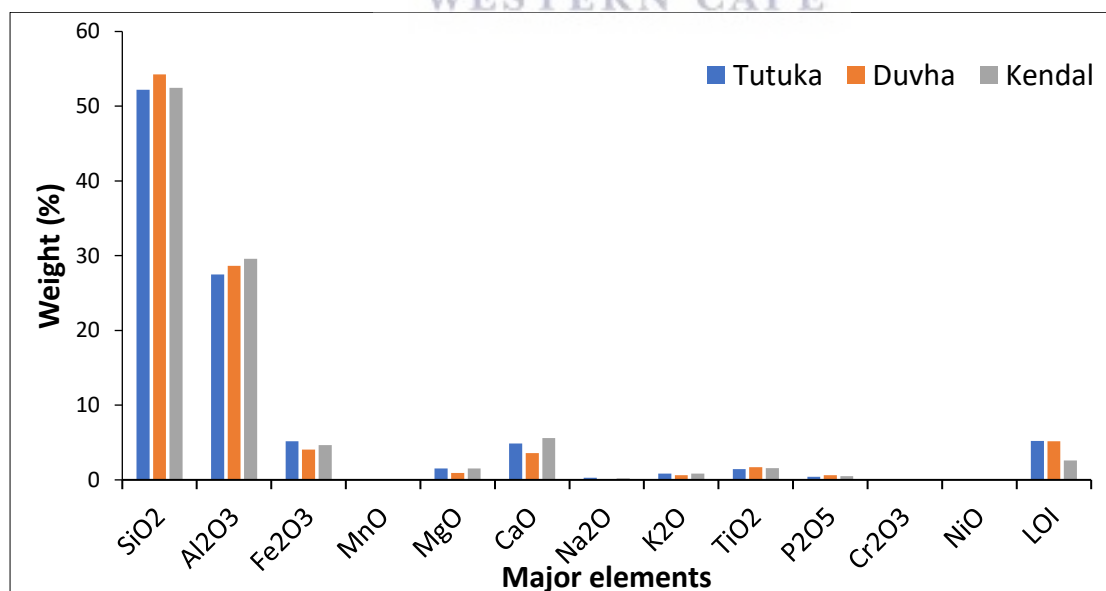
Figure 4.1: Major elements in Tutuka, Kendal and Duvha CFA as determined by XRF analytical technique.

The predominant major elements in all three CFAs were silicon dioxide (SiO_2), aluminium oxide (Al_2O_3), ferric oxide (Fe_2O_3) and calcium oxide (CaO) and they followed a similar trend. SiO_2 was the most abundant major element in all three CFAs. The loss of ignition (LOI) for all three CFA was very low (2.59-5.22%).

4.2.2 Trace Elements

The trace element composition of the Tutuka, Kendal and Duvha CFA as determined by the ICP-MS analytical technique is presented in Table 4.1 . The trend in the concentration of all the trace elements was similar for all the CFAs from the three power stations, with titanium (Ti) being the highest and Antimony (Sb) and Thallium (Tl) with the lowest concentrations.

Table 4.1: Concentration of trace elements in ppm for Tutuka, Kendal and Duvha CFA as determined by the ICP-MS analytical technique.

ppm	Tutuka	Kendal	Duvha
Li	146.62	219.45	189.00
P	1482.22	1831.75	2724.02
Ti	6923.69	7644.72	11456.88
V	123.73	113.34	131.49
Cr	152.85	142.87	166.77
Co	21.28	11.03	29.63
Ni	64.27	40.38	74.88
Cu	46.64	43.18	47.70
Zn	59.41	33.58	76.47
Ga	44.32	45.64	59.87
Rb	39.27	44.86	40.83
Sr	981.10	1333.09	1114.25
Zr	267.38	294.73	333.76
Nb	33.06	37.53	41.14
Sn	18.33	19.73	14.96
Sb	2.15	2.23	1.54
Cs	7.46	11.44	8.56
Ba	1084.05	1342.49	1173.24
Hf	7.81	8.70	8.08
Ta	2.93	3.32	2.81
W	5.25	5.12	6.66
Tl	2.22	1.56	2.01
Pb	47.02	36.08	74.29
Th	33.76	39.23	43.44
U	10.90	11.85	12.02

The toxic trace elements in CFA normally include arsenic (As), chromium (Cr), cadmium (Cd), lead (Pb) and mercury (Hg) uranium (U), thorium (Th) (Munawer, 2018). Pb, As, Cr and Hg

are usually regarded as the most toxic to humans and animals due to their neurotoxic and carcinogenic actions (Eze, 2014). Pb, Cr and the radioactive trace elements Th and U were detected from the CFAs. These highly toxic elements were found in high concentrations in all the CFAs, with Duvha CFA having higher concentrations of these elements than both Kendal and Tutuka CFA. In Tutuka CFA, Pb, Cr, Th and U were measured to have concentrations of 47.02 ppm, 152.85 ppm, 33.76 ppm and 10.90 ppm respectively. Similarly, in Kendal CFA Pb, Cr, Th and U had concentrations of 36.08 ppm, 142.87 ppm, 39.23 ppm and 11.85 ppm respectively. The concentrations of Pb, Cr, Th and U in Duvha CFA were 74.29 ppm, 166.77 ppm, 43.44 ppm and 12.02 ppm respectively.

4.2.3   Rare Earth Element Analysis on South African CFA

The concentrations of REEs in the Tutuka, Kendal and Duvha CFA as determined by ICP-MS follow the same trend, see Figure 4.2 (Appendix A-Table A2). The REE with the highest concentration was Ce in all the CFAs. The concentration of Ce in Tutuka, Kendal and Duvha CFA was 194.53, 216.56 and 216.98 ppm respectively. The REE with the lowest concentration was Lu in the CFA. The concentration of Lu in Tutuka, Kendal and Duvha CFA was 0.83, 0.80 and 0.87 ppm respectively. According to the geochemical classification (An, 2014) the light REEs (LREEs) which include, La, Ce, Pr, Nd and Sm are generally in higher concentration than Medium REEs (MREEs), which are Eu, Gd, Tb, Dy, Y and the Heavy REEs (HREEs), which are Ho, Er, Tm, Yb, Lu. Sc which is neither light, medium nor heavy according to geochemical properties is also in high concentration.
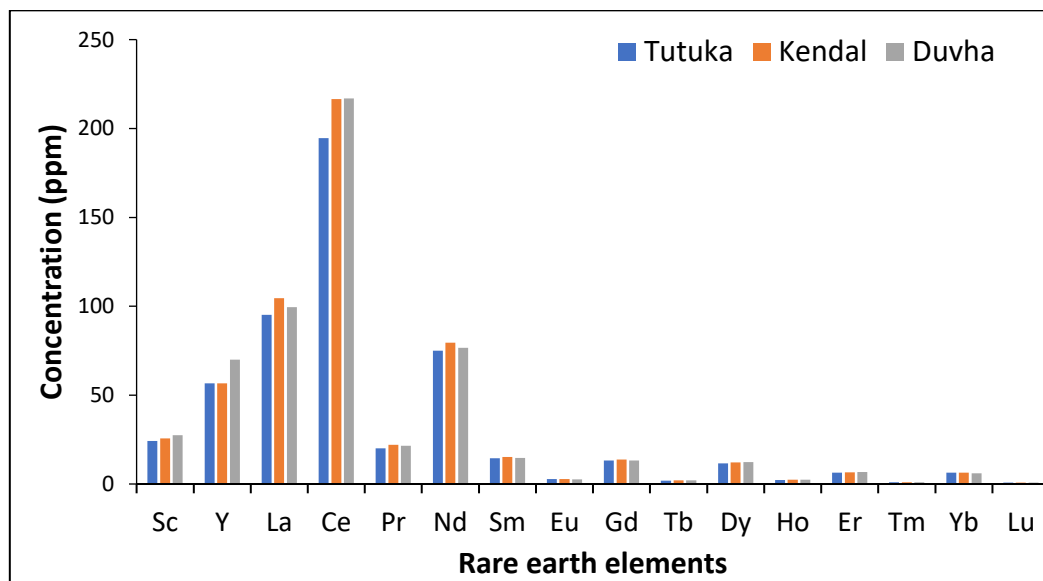
Figure 4.2: Concentration of REEs in ppm for Tutuka, Kendal and Duvha CFA as determined by the ICP-MS analytical technique.

Based on the demand-and-supply classification (Franus et al., 2015) the excessive REEs (Ce, Ho, Tm, Yb and Lu) were more abundant than the critical (Nd, Y, Dy, Er, Tb and Eu) and uncritical (La, Pr, Sm and Gd) REEs in the CFA of the study.

The Total Rare Earth Element (TREE) concentration for Tutuka, Kendal and Duvha CFA was 526.35, 567.68 and 573.77 ppm respectively. Duvha CFA had the highest TREE content of all the three power stations and Tutuka had the lowest.

4.2.4 Mineralogical analysis

The XRD pattern presented in .

Figure 4.3 shows the major crystalline phases of the CFA in the study. All three CFAs were observed to have quartz (SiO_2) and mullite ($Al_44Si.2O_9.6$) as major crystalline phases. Magnetite ($FeFe_2O_4$) appeared to a lesser extent in all the CFAs. Low amounts of calcite ($CaCO_3$) appeared in the Tutuka and Kendal CFA alone and even lower amounts of microcline ($KAlSi_3O_8$) appeared in the Duvha CFA alone.
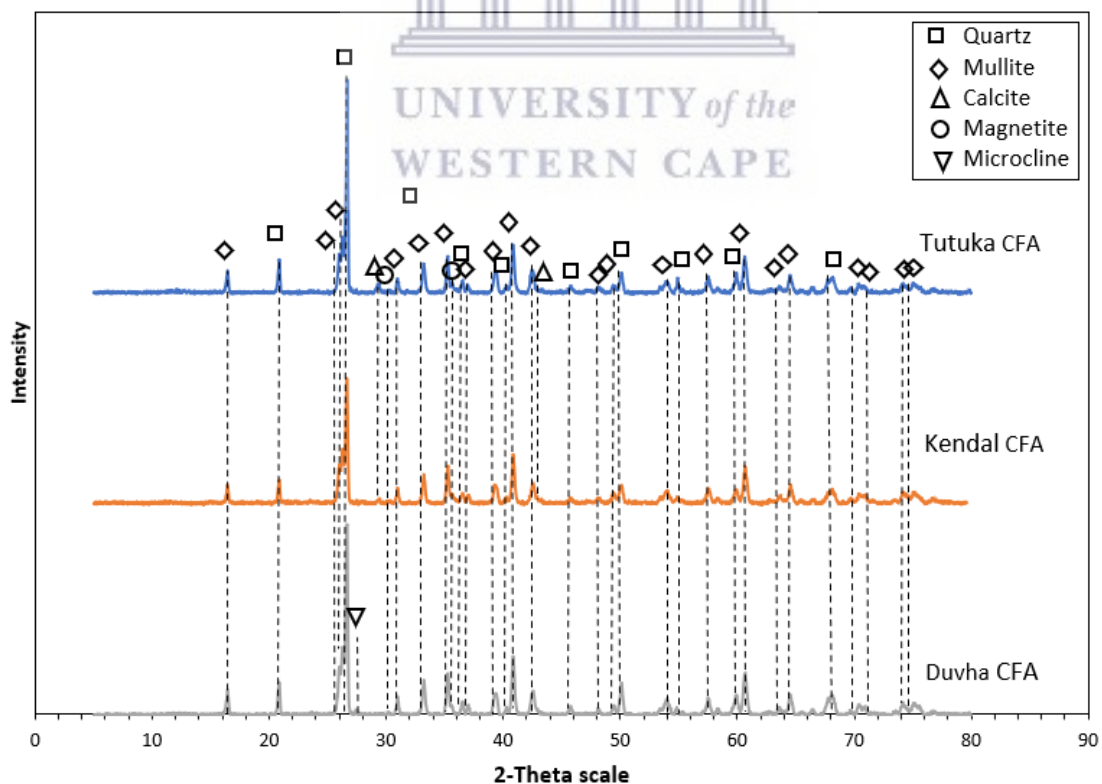
Figure 4.3: XRD pattern showing major and minor crystalline phases in Tutuka, Kendal and Duvha CFA.

The TIMA analytical technique was also used to find the primary mineral phases in Tutuka, Kendal and Duvha CFA. The primary phases found in the Tutuka, Kendal and Duvha CFA using the TIMA analytical technique are shown in Figure 4.4, Figure 4.5 and Figure 4.6 respectively (see Appendix A Table-A3). The most abundant minerals in Tutuka CFA were plagioclase followed by kaolinite, quartz then Schorl. While in Kendal CFA it was kaolinite followed by plagioclase, quartz then schorl. In the Duvha CFA, the most abundant minerals were kaolinite followed by quartz, plagioclase, schorl then aluminosilicate.

REEs were detected in abundance in different phases. Ilmenite, allanite and rutile had an abundance of LREEs (e.g., Ce, La and Pr) (see Figure 4.7). MREEs (e.g., Eu) and HREEs (e.g., Lu) were more abundant in mineral phases such as goethite, hematite and almandine (see Figure 4.8). Zircon had an abundance of Y (see Figure 4.9) while calcite had an abundance of Sc (see Figure 4.10) (see Appendix A-Table A 4-7).
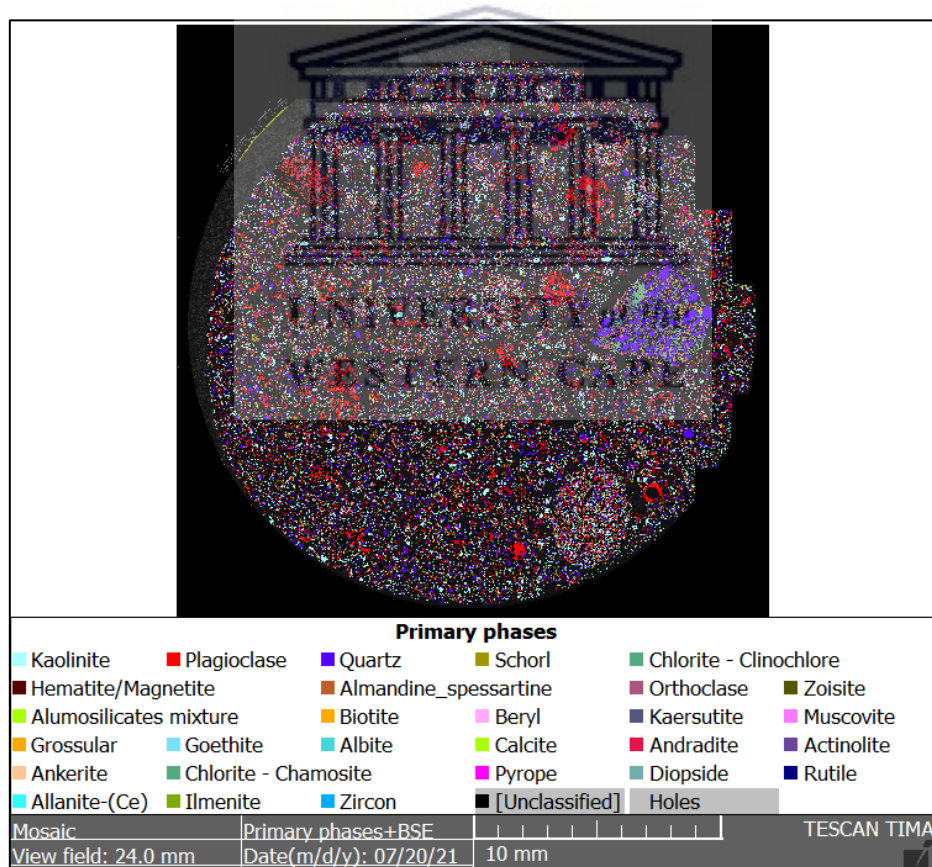
Figure 4.4: Primary mineral phases in Tutuka CFA as determined by the TIMA analytical technique.
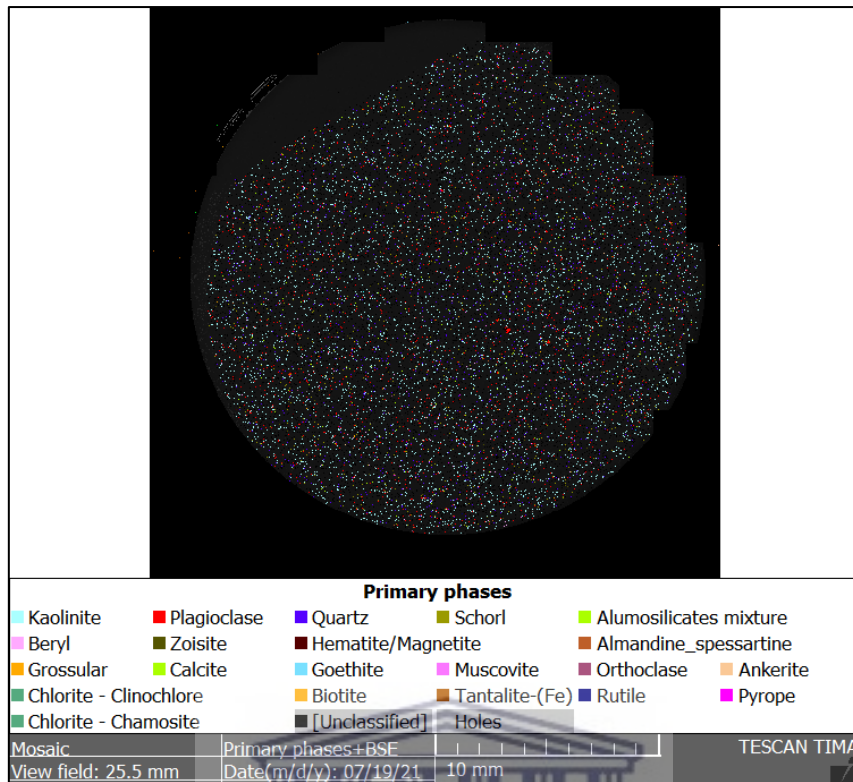
Figure 4.5: Primary mineral phases of Kendal CFA as determined by the TIMA analytical technique.
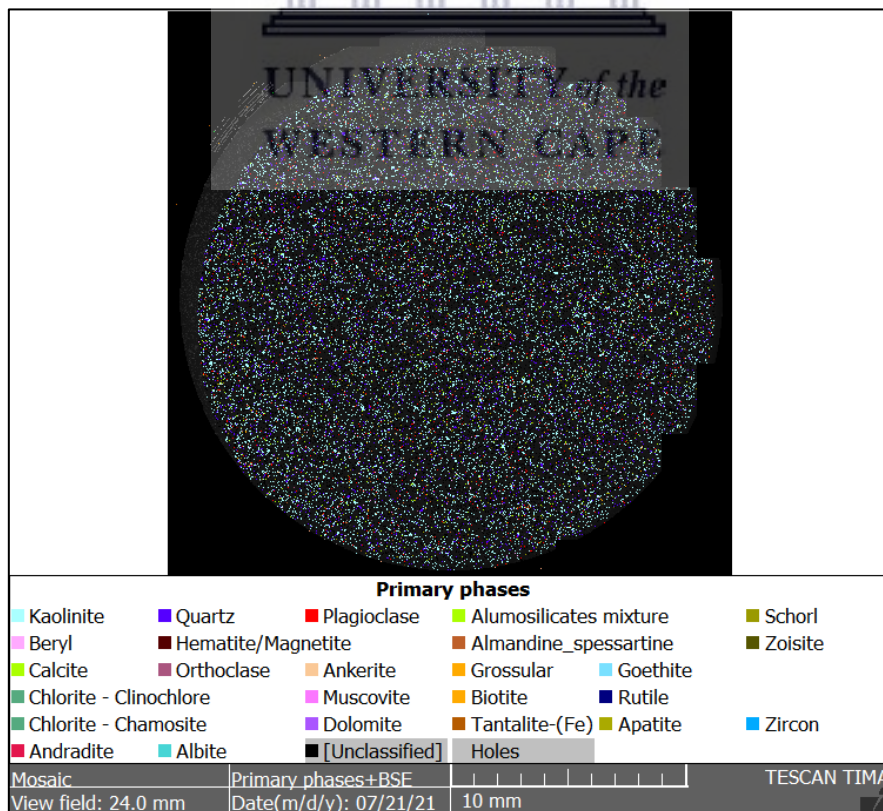
Figure 4.6: Primary mineral phases of Duvha CFA as determined by the TIMA analytical technique.
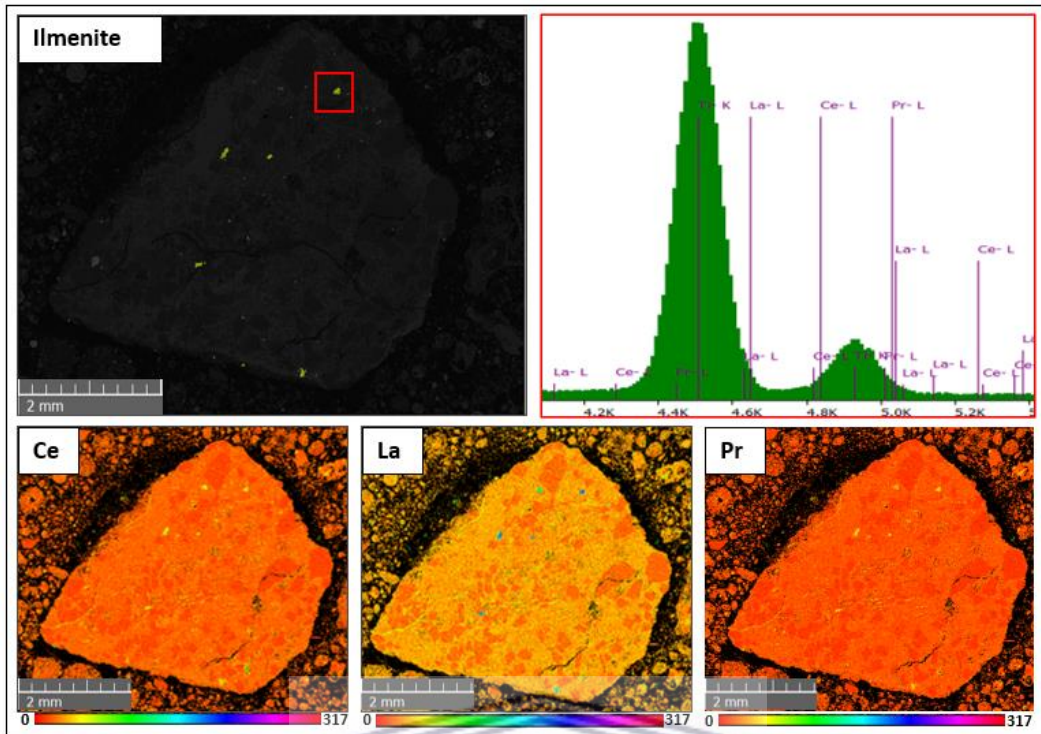
Figure 4.7: TIMA scan of ilmenite in an ilmenite bearing rock and corresponding EDX spectrum of ilmenite and elemental maps of Ce, La, and Pr
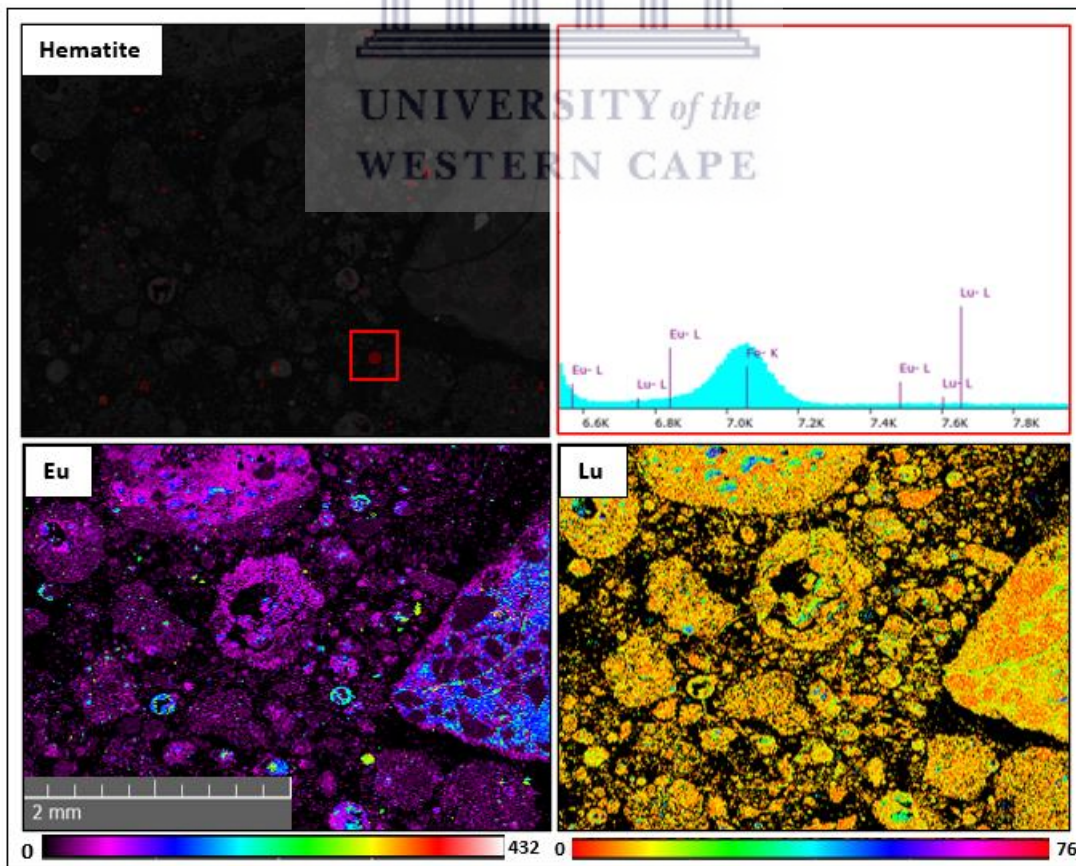
Figure 4.8: TIMA scan of hematite bearing particles and corresponding EDX spectrum of hematite and elemental maps of Eu and Lu.
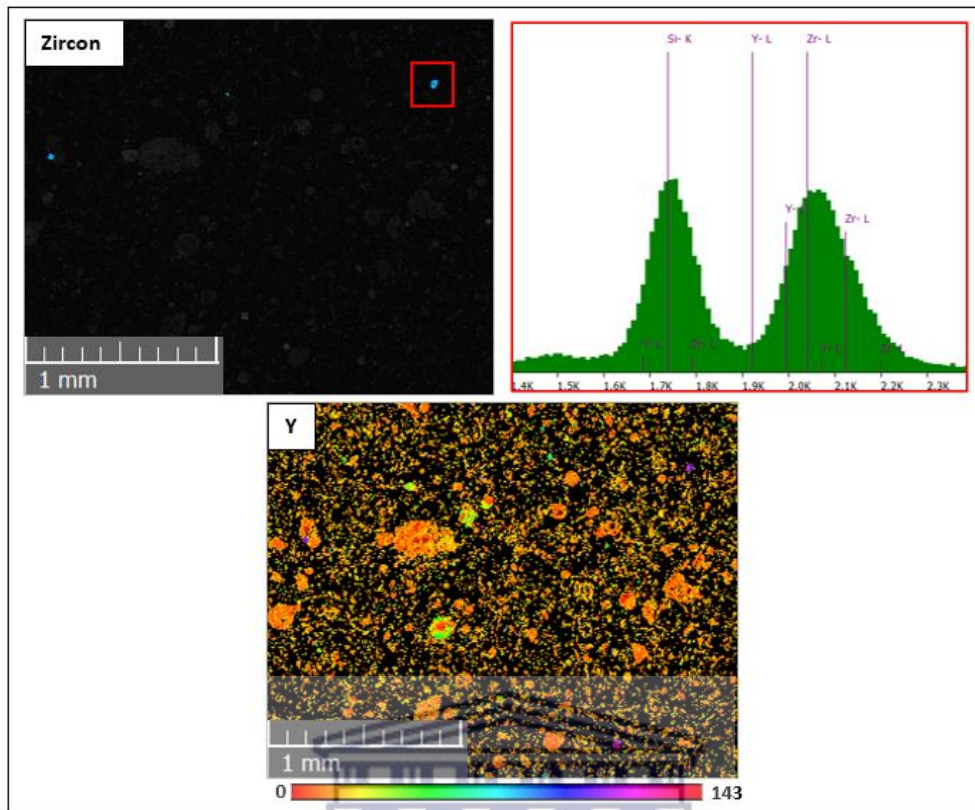
Figure 4.9: TIMA scan of zircon bearing particles and corresponding EDX spectrum of zircon and elemental map of Y.
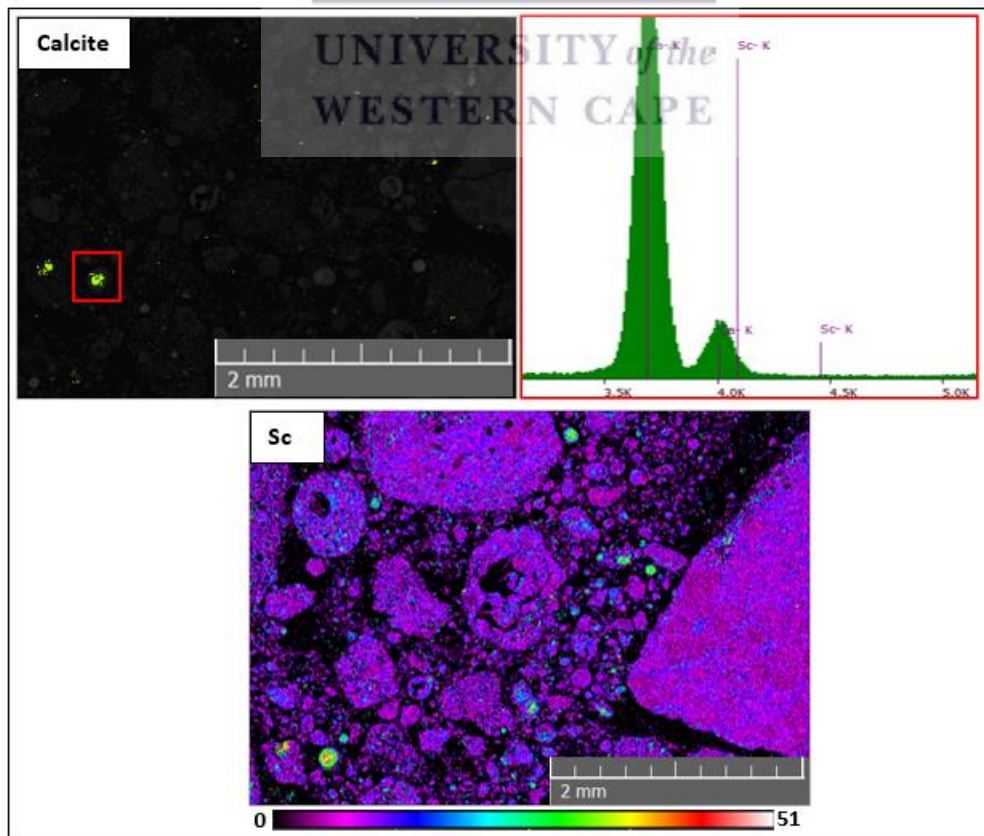
Figure 4.10: TIMA scan of calcite bearing particles and corresponding EDX spectrum of calcite and elemental map of Sc.

4.3   REE extraction from CFA using alkali fusion-acid leaching method

Tutuka, Duvha and Kendal CFA were subjected to alkali fusion with NaOH as an additive in preparation for acid leaching for the recovery of REEs using a 1:1 additive to CFA ratio at a temperature of 400°C for 2 hours. Then the fusion products were leached at 1:10 solid to liquid ratio, 90°C, 400 rpm (rotations per minute) rotation speed, 2 hr. leaching time and varying HCl concentrations of 1, 2 and 3 mol/L.

4.3.1   Individual REE extraction

The extraction of individual REEs as determined by the ICP-MS analytical technique is shown in Figure 4.11 (see Appendix C-Table C1).
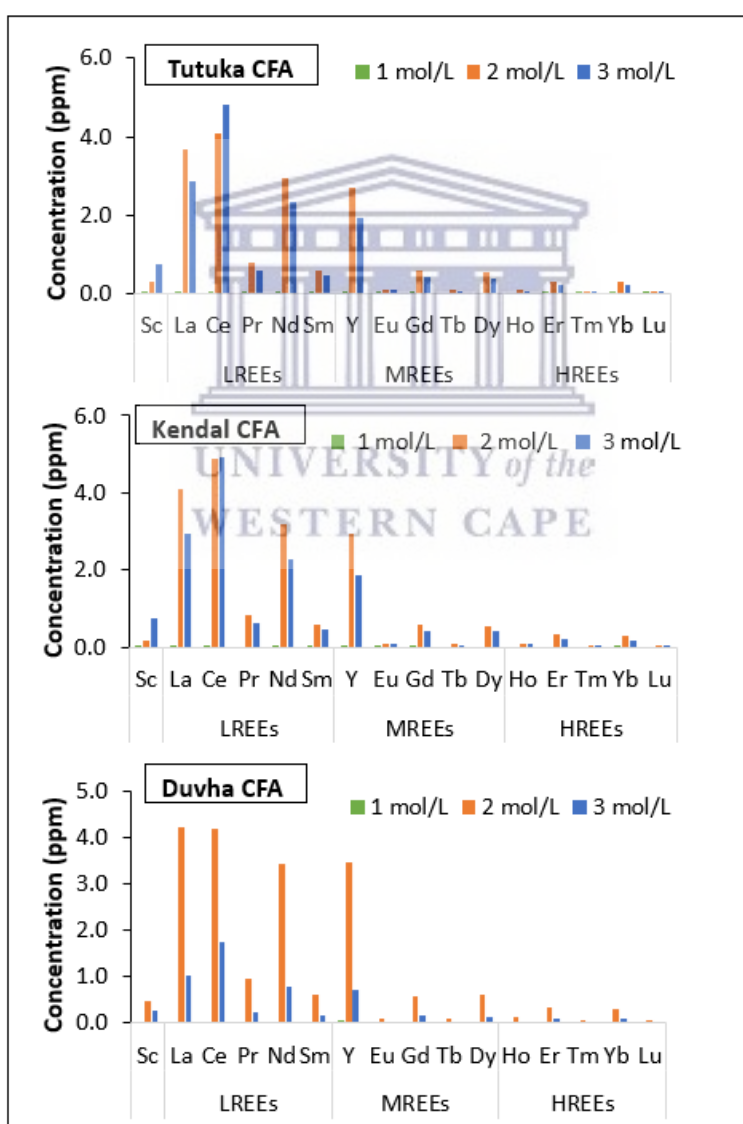
Figure 4.11: Effect of acid concentration (at 1, 2 and 3 mol/L HCl) on the extraction of REEs (in ppm) from Tutuka, Kendal and Duvha CFA as determined by ICP-MS.

Generally, The REE extraction from the Tutuka, Kendal and Duvha CFA followed a similar pattern. the extraction of individual REEs from the three CFAs increased when the acid concentration was increased from 1 mol/L to 2 mol/L then extraction decreased when acid concentration was increased to 3 mol/L.

In the Tutuka CFA, the REE that was extracted the most at 1 mol/L was Y (0.01 ppm), while Td, Dy and Ho were not extracted at all (0 ppm). At 2 mol/L the REE that was extracted the most Ce (4.07 ppm) and Lu was extracted the least (0.03 ppm). Similarly at 3 mol/L Ce was extracted the most (4.80 ppm) and Lu was extracted the least (0.03 ppm).

In Kendal CFA, the REE that was extracted the most at 1 mol/L was Y (0.002 ppm), while Tb, Dy, Ho, Tm and Lu were not extracted at all (0 ppm). At 2 mol/L Ce was extracted the most (4.89 ppm) while Lu was extracted the least (0.04). Similarly, at 3 mol/L Ce was extracted the most (4.92 ppm) and Lu was extracted the least (0.03 ppm).

In Duvha CFA, the REE that was extracted the most at 1 mol/L was Y (0.05 ppm), while Tb was not extracted at all (0 ppm). At 2 mol/L the REE that was extracted the most was La (4.21 ppm) while Lu was extracted the least (0.04 ppm). At 3 mol/L the REE that was extracted the most was Ce (1.73 ppm) and Lu was extracted the least (0.01 ppm).

Overall, REEs were extracted the most at an acid concentration of 2 mol/L. At 2 mol/L Ce was the REE that was extracted the most in Tutuka and Kendal CFA. However, in Duvha CFA La was extracted the most at 2 mol/L acid concentration. Ce and La are both LREEs and other neighbouring LREEs (Nd, Pr and Sm) were also generally extracted more than the MREEs (Y, Eu, Gd, Tb and Dy) and HREEs (Ho, Er, Tm, Yb and Lu).

4.3.2 Classified REE extraction

The effect of acid concentration on the extraction of LREEs, MREEs and HREEs from Tutuka, Kendal and Duvha CFA was evaluated and the findings are presented in Figure 4.12 (see Appendix C-Table C2). At a concentration of 1 mol/l, the MREEs extracted the most from Tutuka CFA (0.01 ppm) followed by LREEs (0.0003 ppm) then HREEs (0.0001 ppm). At 2 mol/L LREEs were extracted more (12 ppm) than MREE (4 ppm) and HREE (1 ppm). Similarly, at 3 mol/L LREEs were also extracted more (11 ppm) than MREEs (3 ppm) and HREEs (1 ppm).

In Kendal CFA at 1 mol/L MREEs were extracted the most (0.002 ppm) followed by LREEs (0.0001 ppm) then HREEs (0.000003 ppm). At 2 mol/L LREEs were extracted the most (14

ppm) followed by MREEs (4 ppm) then HREEs (1 ppm). At 3mol/L LREEs were extracted the most (11 ppm) followed by MREE (3 ppm) then HREEs (1 ppm).
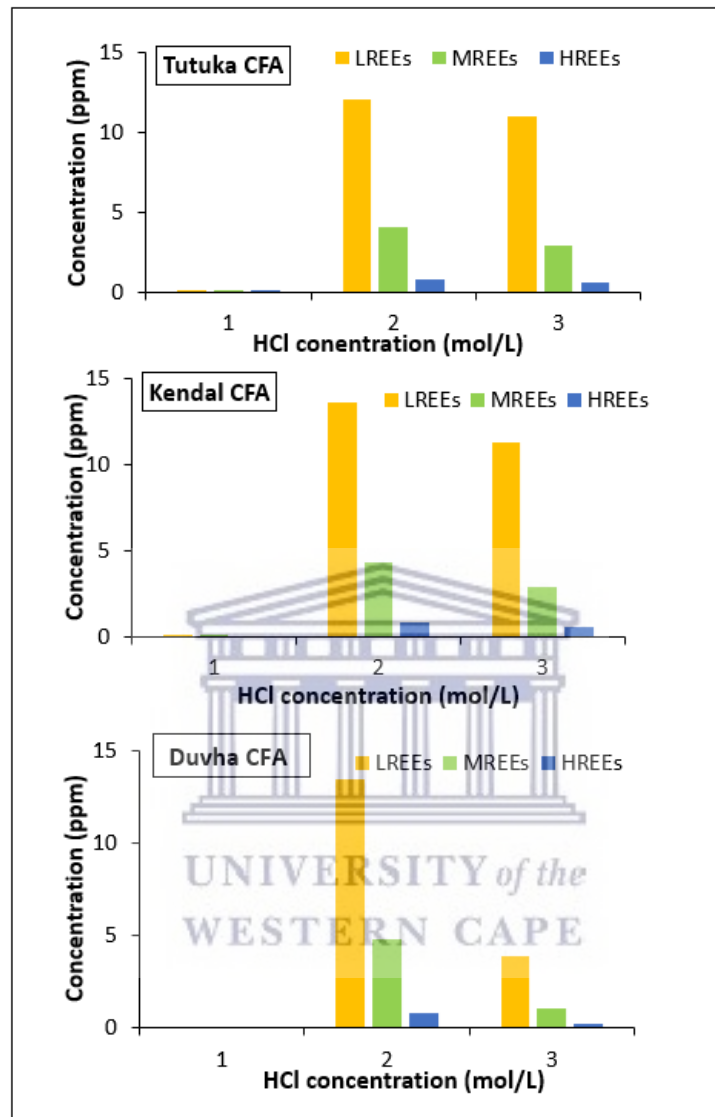
Figure 4.12: Effect of acid concentration on the extraction of LREEs, MREEs and HREEs from Tutuka, Kendal and Duvha CFA.

In the Duvha CFA at 1 mol/L acid concentration MREEs (0.06 ppm) were extracted the most followed by LREEs (0.001 ppm) then HREEs (0.0002 ppm). At 2 mol/L LREEs were extracted the most (13 ppm) followed by MREEs (5 ppm) then HREEs (1 ppm). At 3 mol/L LREEs were also extracted the most (4 ppm) followed by MREEs (1 ppm) then HREEs (0.2 ppm).

4.3.3   Total REE extraction

Figure 4.13 shows the effect of acid concentration on REE extraction. All three CFAs exhibited a similar REE extraction trend (see Appendix C-Table C3). In addition, the TREE extraction followed a similar trend to the individual REEs and classified REEs. REE extraction increased

68

as the acid concentration increased from 1 to 2 mol/L. Then REE extraction decreased when acid concentration increased to 3 mol/L.
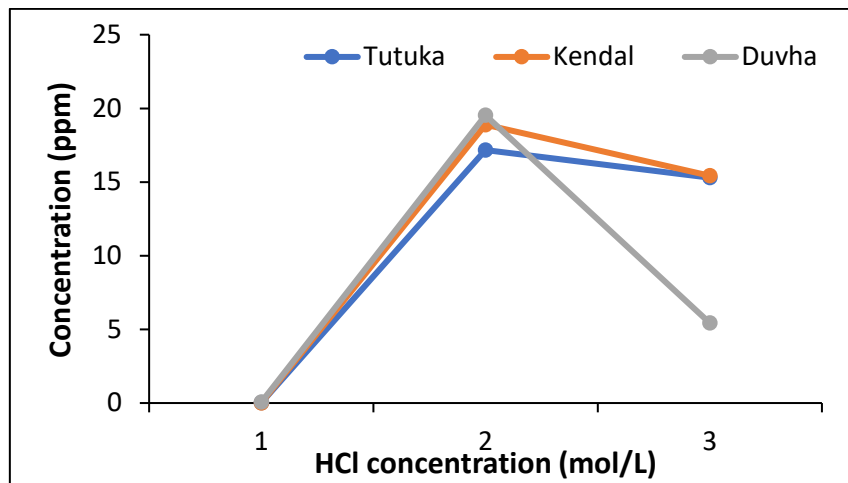
Figure 4.13: The effect of acid concentration on TREE extraction from Tutuka, Kendal and Duvha CFA.

The lowest REE extractions were achieved at 1 mol/L concentration with the greatest REEs being extracted in Duvha (0.058 ppm) followed by Tutuka (0.012 ppm) then Kendal CFA (0.002 ppm). At 2 mol/L TREE extraction was at its highest in all three CFAs, Duvha CFA had the most REEs extracted (19.528 ppm) followed by Kendal CFA (18.892 ppm) and then Tutuka CFA (17.172 ppm). At 3 mol/L the greatest REE extraction was from Kendal (15.434 ppm) followed by Tutuka (15.289 ppm) then Duvha CFA (5.428 ppm).

4.4 Effect of acid concentration on the recovery of REEs using alkali fusion -acid leaching method

The recovery of REEs from the CFA of the study was calculated using the following equation (Cao et al., 2018):

$$\propto = \frac{VC_2}{MC_1} \times 100 \ \%$$

(4.1)

$\propto$ = REE recovery %

V = volume of leachate in mL

M = the mass of CFA sample in g

C_1 = the element content in CFA sample in μg/g

C_2 = the element concentration in leachate in μg/ml.

4.4.1 Individual REE recovery

Figure 4.14 shows the effect of acid concentration on the recovery of individual REEs from Tutuka, Kendal and Duvha CFA (Appendix D-Table D1). Generally, the recovery of individual REEs from three CFAs improved when the acid concentration was increased from 1 mol/L to 2 mol/L then recovery decreased when acid concentration was increased to 3 mol/L.
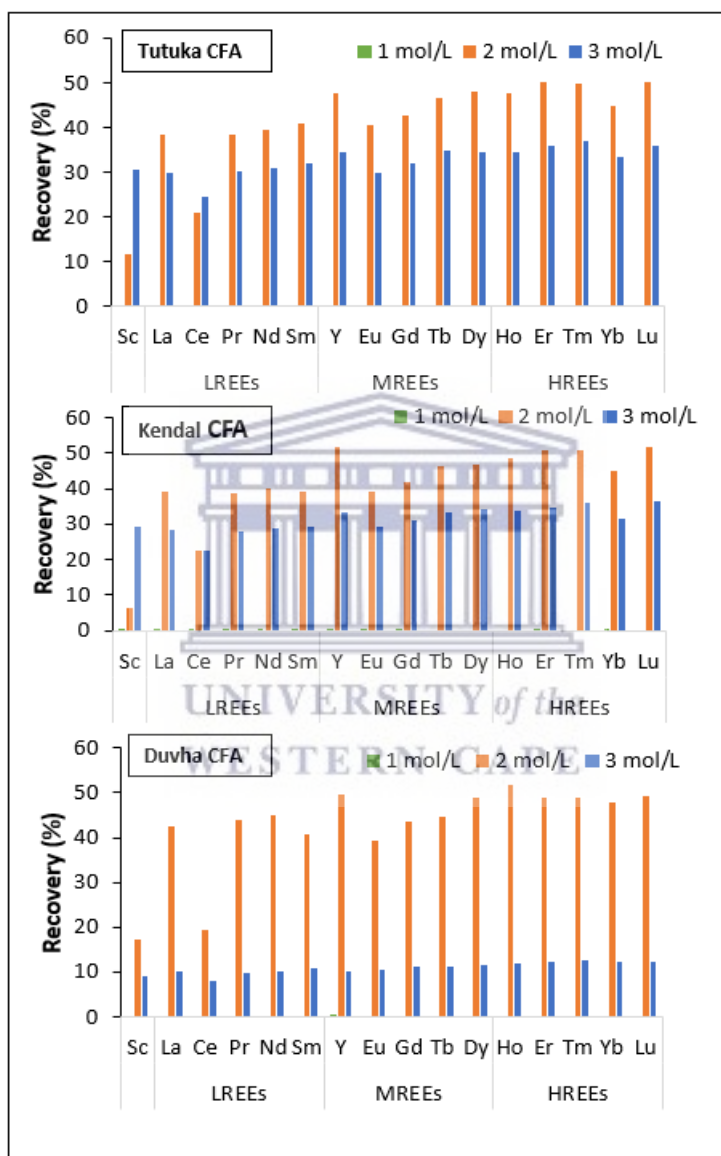
Figure 4.14: Effect of acid concentration (1, 2 and 3 mol/L) on recovery of individual REEs from Tutuka, Kendal and Duvha CFA.

In Tutuka CFA the REE that was recovered the most at 1 mol/L was Y with a recovery of 0.19%, while Ce, Tb, Dy and Ho were not recovered at all (0%). At 2 mol/L the REEs that were recovered the most were Er (50.36%). The REE that was recovered the least was Sc

(11.78%). At 3 mol/L the REE Tm was recovered the most (36.84%) and Ce was recovered the least (24.65%).

In the Kendal CFA, the REE that was recovered the most at 1 mol/L was Y (0.03%), while Lu, Tm, Ho, Dy and Tb were not recovered at all (0%). At 2 mol/L the REE that was recovered the most was Y (51.87%) and Sc was recovered the least (6.25%). At 3 mol/L the REE that was recovered the most was Lu (36.45%) and Ce was still recovered the least (22.70%).

In Duvha CFA the REE that was recovered the most at 1 mol/L was Y (0.78%) and Tb was not recovered at all (0%). At 2 mol/L the REE that was recovered the most was Ho (51.72%) and Sc was recovered the least (17.45%). At 3 mol/L the REEs that was recovered the most was Ho (11.99%) and Sc was recovered the least (9.31%).

4.4.2 Classified REE recovery

Figure 4.15 provides an overview of the effect of acid concentration on the recovery of LREEs, MREEs and HREEs from Tutuka, Kendal and Duvha CFA (Appendix D-Table D2). At 1 mol/l the MREEs recovered the most from Tutuka CFA (0.123%) followed by HREEs (0.005%) then LREEs (0.001%). At 2 mol/L HREEs were recovered slightly more (47.89%) than MREEs (46.78%) and LREEs were the least recovered (30.19%). Similarly, at 3 mol/L HREEs were recovered slightly more (34.80%) than MREEs (33.93%) and LREEs were the least recovered (27.65%).

In Kendal CFA, at 1 mol/L MREEs were recovered more (0.02%) than HREEs and LREEs which both had a recovery of 0%. At 2 mol/l MREEs were recovered the most (49.06%) however only slightly more than HREEs (48.33%) and LREEs were recovered the least (31.13%). At 3 mol/L HREEs were recovered the most (33.62%) however only slightly more than MREEs (33.01%) and LREEs were recovered the least (25.66%).

Similarly, for Duvha CFA, at 1 mol/L MREEs were recovered more (0.56%) than LREEs (0.01%) and HREEs (0.002%). At 2 mol/L HREEs were recovered (48.92%) slightly more than MREEs (48.29%), while LREEs were recovered the least (31.19%). At 3 mol/L HREEs were also recovered more (12.34%) than MREEs (10.46%) and LREEs (9.12%).
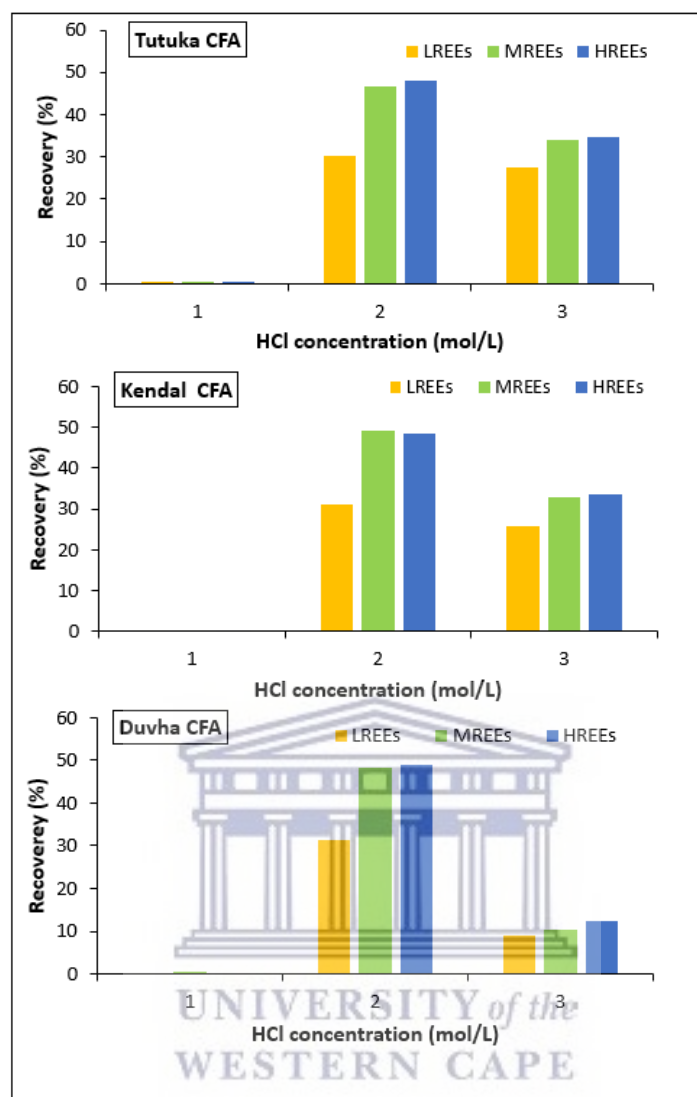
Figure 4.15: The effect of acid concentration on the recovery of LREEs, MREEs HREEs and TREEs from Tutuka, Kendal and Duvha CFA.

4.4.3 Total REE recovery

The recovery of individual and classified REEs generally followed a similar trend to the recovery of TREEs. Figure 4.16 shows the effect of the recovery of TREEs from the three CFAs (see Appendix D-Table D3). In general, the recovery of the TREEs from the Tutuka, Kendal and Duvha CFA, increase from a concentration of 1 to 2 mol/L and decreased when concentration was increased to 3 mol/L.

The TREE recovery from Tutuka CFA increased from 0 % to 33 % when the HCl concentration was increased from 1 to 2 mol/L and decreased to 29% when HCl concentration was increased to 3 mol/L. Similarly, the TREE recovery for Kendal CFA increased from 0 % to 33 % when HCl concentration was increased from 1 to 2 mol/L and decreased to 27 % when the HCl concentration was increased to 3 mol/L. The TREE recovery for Duvha CFA increased from 0

% to 34 % when the HCl concentration was increased from 1 to 2 mol/L and decreased to a very low 9 % when the HCl was increased to 3 mol/L. These results show that acid concentration affects REE recovery from CFA.
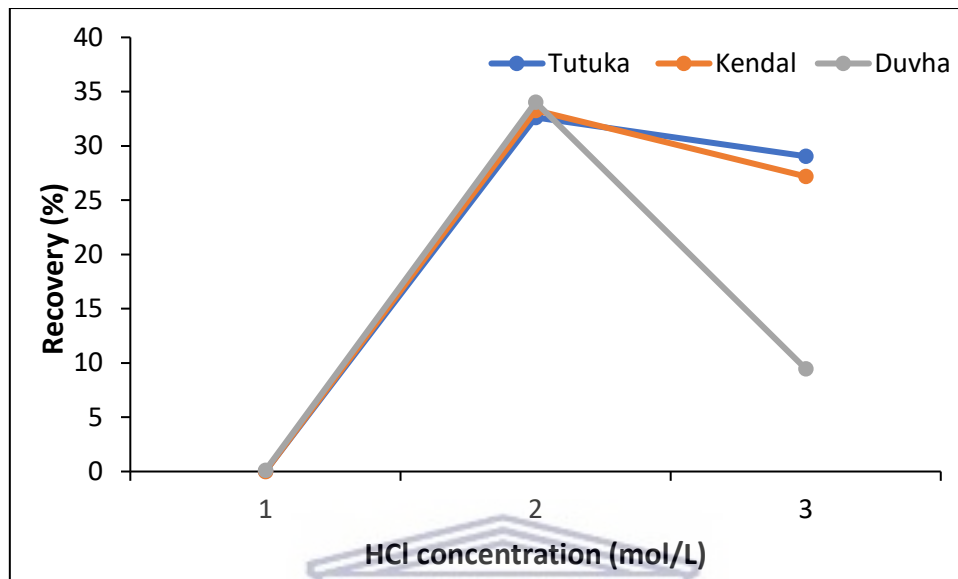
Figure 4.16: The effect of acid concentration on TREE recovery from Tutuka, Kendal and Duvha CFA.

Statistical analyses were used to determine if acid concentration had a significant effect on REE recovery from the three CFAs. Firstly, The Shapiro-Wilk test was used to determine the normality of REE recovery data. Secondly, The Kruskal-Wallis H test was used to determine if there were significant differences between REE recoveries at different acid concentrations. Lastly, The Mann-Whitney U test was used to determine which acid concentrations differed significantly in terms of REE recoveries.

The Shapiro-Wilk test showed that TREE recovery data was not normally distributed ($p < 0.05$) across different samples and acid concentrations except for the 3 mol/L concentration REE recovery data (Appendix E-Table E1). The same was observed with the skewness and kurtosis values of the REE recovery data were not between -1.96 to +1.96 except for 3 mol/L concentration REE recovery data. The skewness and kurtosis values of normally distributed data were between -1.96 to +1.96. Hence a non-parametric test instead of a parametric test was used to determine the significance of the effect of acid concentration of REE recovery.

The Kruskal-Wallis H test is a non-parametric statistical test that was used to determine if there were significant differences in TREE recovery at different acid concentrations (Appendix E Table E2). The Kruskal-Wallis H test showed that the TREE recoveries at 1, 2 and 3 mol/L

acid concentrations differed significantly ($p < 0.05$). The Kruskal Wallis H test showed that there was a statistically significant difference in REE recovery at different acid concentrations for Tutuka CFA, (Kruskal−Wallis test: H = 37.340, df = 2, p = <.001), with a mean rank REE recovery of 8.50 for 1 mol/L, 38.50 for 2 mol/L and 26.50 for 3 mol/L. The same was observed for Kendal CFA (Kruskal−Wallis test: H = 38.167, df = 2, p = <.001) with a mean rank REE recovery of 8.50 for 1 mol/L, 38.50 for 2 mol/L and 26.50 for 3 mol/L. The same was also observed for Duvha CFA (Kruskal−Wallis test: H =41.923, df = 2, p = <.001) with a mean rank REE recovery of 8.50 for 1 mol/L, 40.50 for 2 mol/L and 24.50 for 3 mol/L

Then the Mann-Whitney U test was used to determine which acid concentrations differed significantly in terms of REE recoveries (Appendix E Table E3). The Mann-Whitney U test indicated that REE recoveries at 2 mol/L acid concentration were significantly more than 1 mol/L and 3 mol/L for all CFA in the study. The TREE recoveries for Tutuka CFA at 2 mol/L (mean rank 24.50) were significantly higher than at 1 mol/L (mean rank 8.50) (Mann-Whitney U test: W = 0.00, P = < .001) and 3 mol/L (mean rank 10.50) (Mann-Whitney U test: W = 32.000, P = < .001). TREE recoveries for Kendal CFA at 2 mol/L (mean rank 24.50) were significantly greater than recoveries at 1 mol/L (mean rank 8.50) (Mann-Whitney U test: W = .000, P = < .001) and 3 mol/L (mean rank 10.50) (Mann-Whitney U test: W = 32.000, P = < .001) acid concentrations. The REE recoveries from Duvha CFA at 2 mol/L (mean rank 24.50) were significantly greater than recoveries at 1 mol/L (mean rank 8.50) (Mann-Whitney U test: W = .000, P = < .001) and 3 mol/L (mean rank 8.50) (Mann-Whitney U test: W = .000, P = < .001) acid concentrations.

4.4.4   REEs in the solid residue

The mineral phases that were retained in the solid residues of Tutuka, Kendal and Duvha CFA after alkali fusion-acid leaching were determined using XRD and TIMA analytical techniques. Figure 4.17 shows that the XRD peaks of mineral phases in the leached residues compared to the peaks of mineral phases in the original CFA.
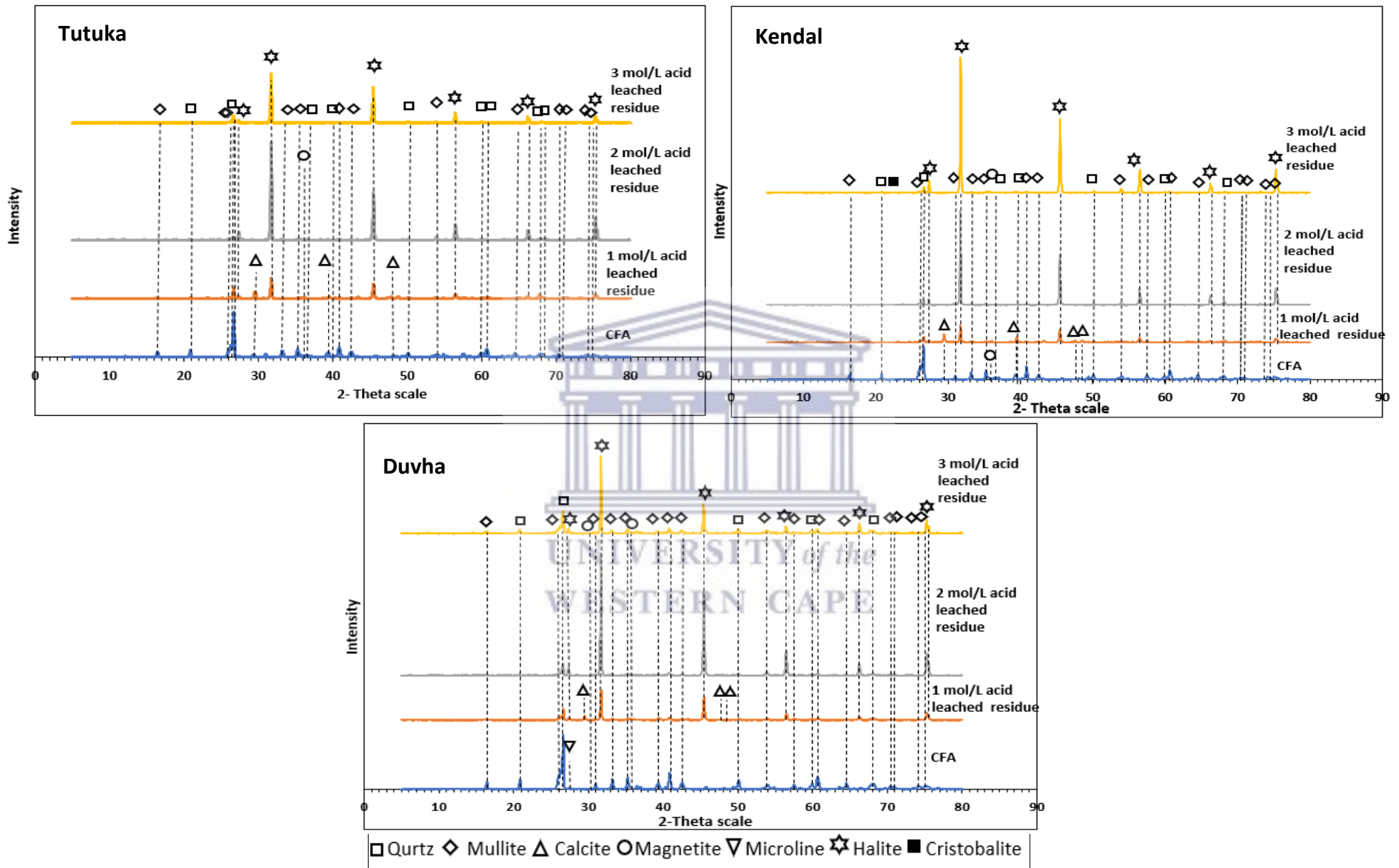
Figure 4.17 : XRD patterns of Tutuka, Kendal and Duvha CFA with their respective 1, 2 and 3 mol/L acid leaching residues.

The major phases of quartz and mullite that were present in the CFA were still present in the solid residues however to a lesser degree. The minor phases of calcite, magnetite and microcline that were present in the CFA were still present in the solid leached residues but also to a lesser degree. There was a slight presence of cristobalite in the 3 mol/L solid leached residue of the Kendal CFA. There were also large peaks of halite (NaCl) in all the leached residues however halite was not present in the CFA.

The TIMA analytical technique was used to determine primary phases that are associated with REEs in the solid leached residue. The TIMA scans of the primary phases in the 2 mol/L acid solid leached residue of Tutuka, Kendal and Duvha are shown in Figure 4.18, Figure 4.19 and Figure 4.20 respectively. The primary phases kaolinite, quartz and plagioclase which were in abundance in the original CFAs were present in small quantities in the solid leached residues. The aluminosilicate mixture is the dominant phase in the solid leached residues of Tutuka and Kendal CFA. The dominant phase in the Duvha residue was quartz. There was also evidence of nepheline, one of the alkali fusion products, in the TIMA scans of the solid leached residues of Tutuka and Kendal.

The phases that had an abundance of REEs in the original CFA, were still present in all the solid leached residues however in smaller quantities (see Figure 4.21, Figure 4.22 and Figure 4.23) (see Appendix F-Table F2-4). The LREE rich phases ilmenite, allanite and rutile were still present in the solid leached residues. However, ilmenite and allanite were present in small quantities, they were not easily detected in the TIMA images of the residues. On the other hand, rutile was still easily detected however it was seen in much smaller quantities than in the original CFA (see Figure 4.21). The MREE and HREE rich hematite were present in the solid leached residue (see Figure 4.22) as well as goethite and almandine. The Y rich zircon was also present in the solid leached residues (see Figure 4.23). Calcite was also present in the solid leached residues; it had an abundance of Sc. However, it was barely visible in the TIMA image and it was so small an EDX spectrum could not be generated for calcite.
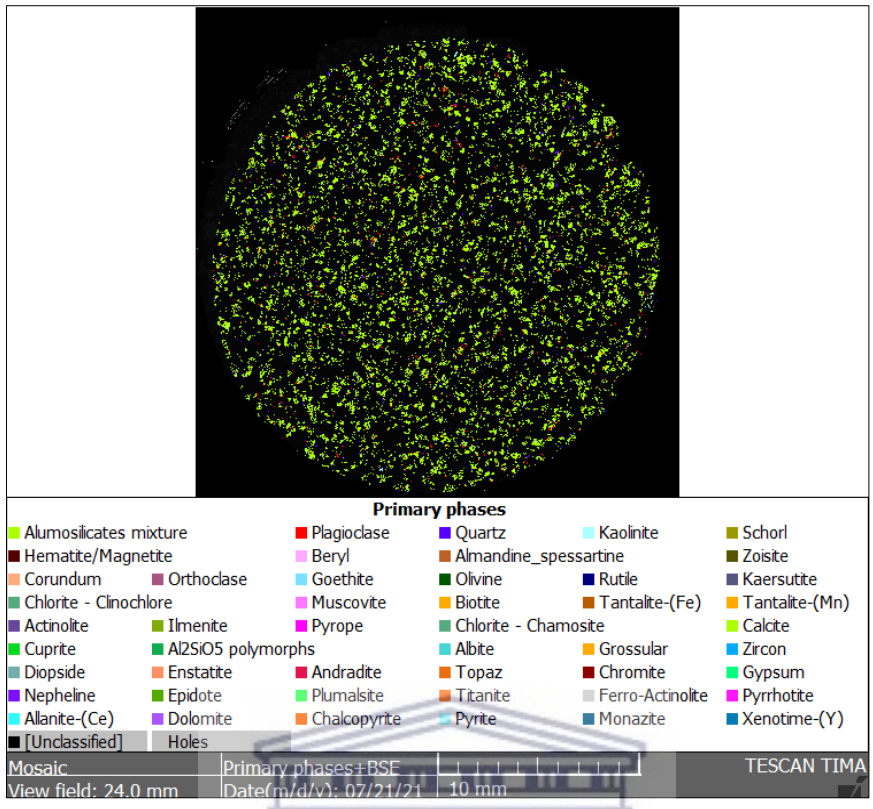
Figure 4.18: TIMA scan showing primary mineral phases of the 2 mol/L acid leached residue of Tutuka CFA as determined by the TIMA analytical technique.
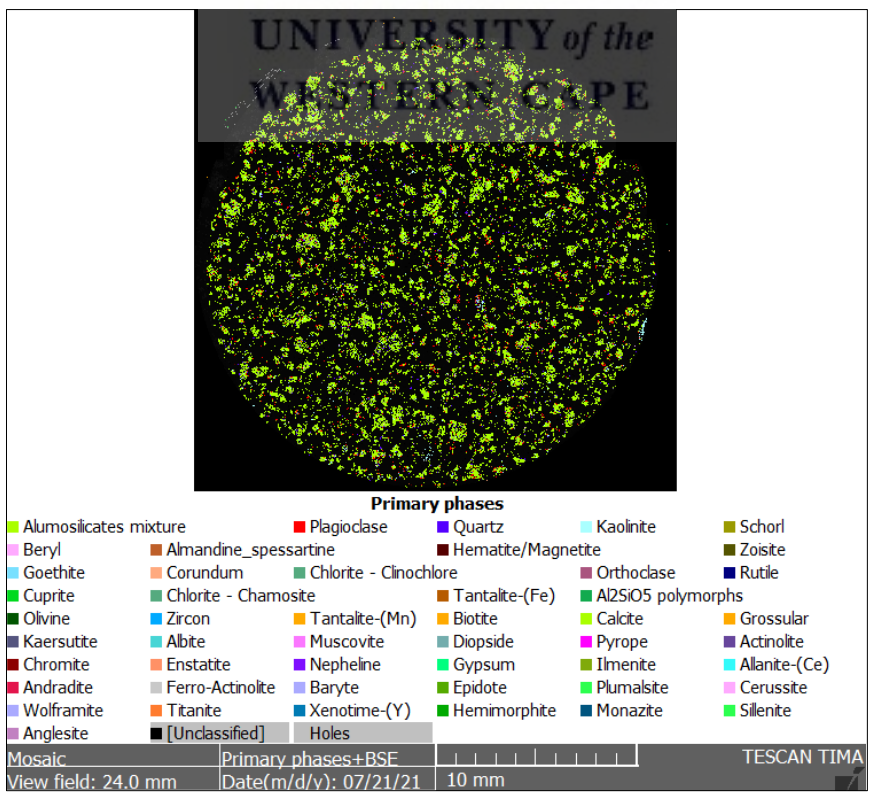
Figure 4.19: TIMA scan showing primary mineral phases of the 2 mol/L acid leached residue of Kendal CFA as determined by the TIMA analytical technique.
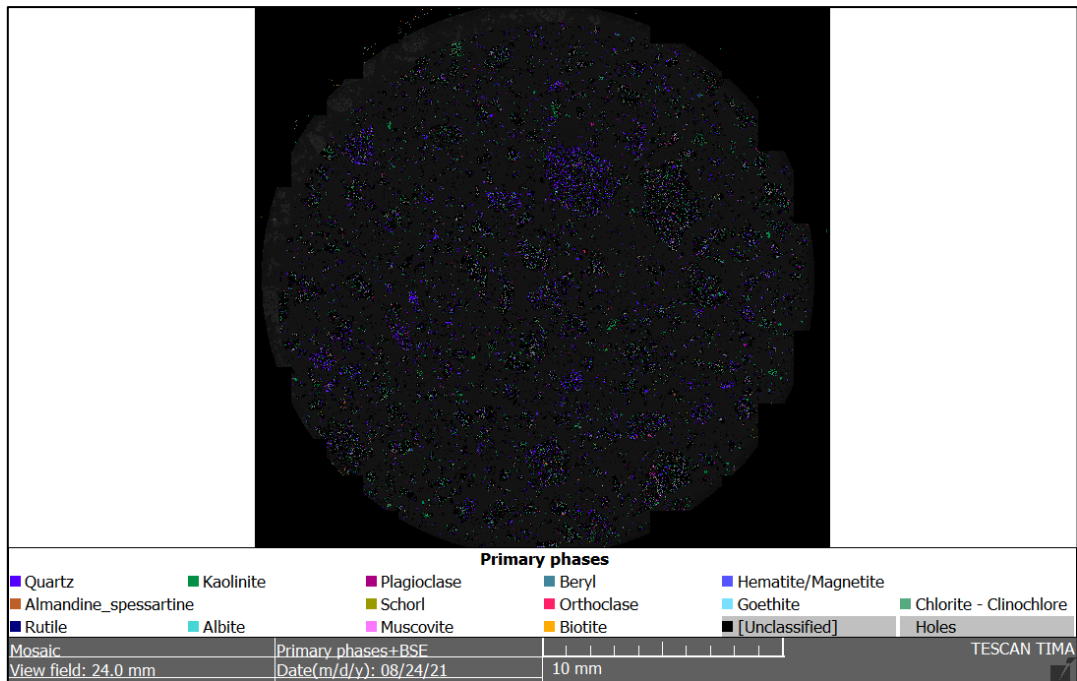
Figure 4.20: Primary mineral phases of the 2 mol/L acid leached residue of Duvha CFA as determined by the TIMA analytical technique.
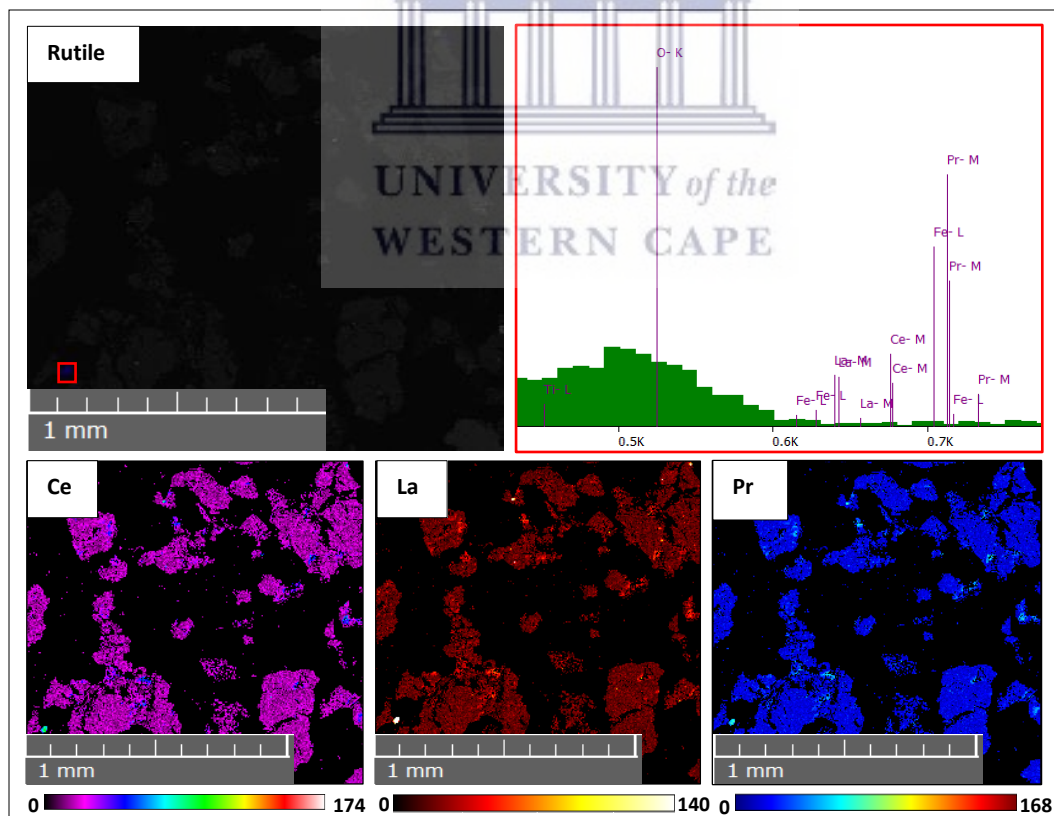
Figure 4.21: TIMA scan of rutile (blue) and corresponding EDX spectrum of rutile and elemental maps of Ce, La, and Pr for 2 mol/L acid leached residue
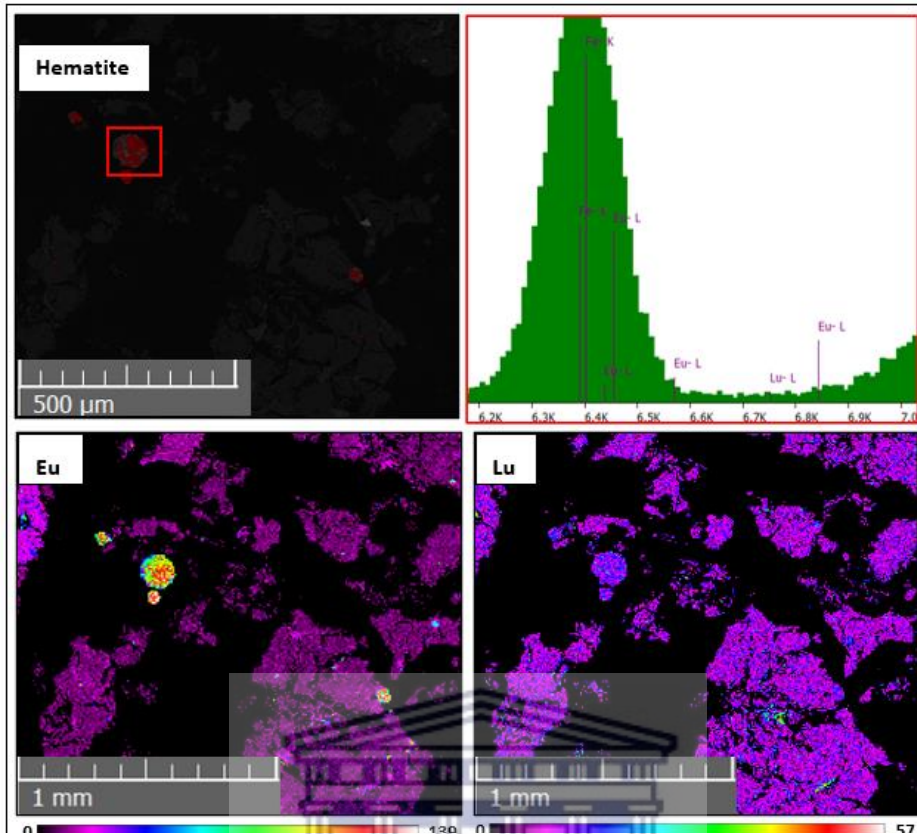
Figure 4.22: TIMA scan of hematite and corresponding EDX spectrum of hematite and elemental maps of Eu and Lu for 2 mol/L acid leached residue.
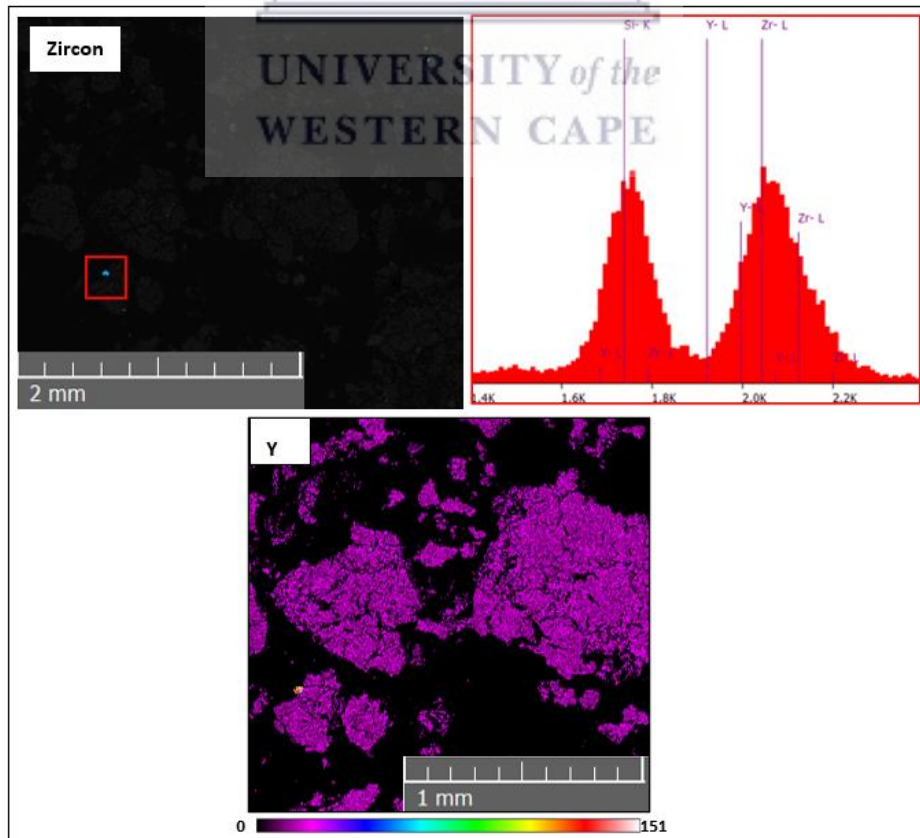
Figure 4.23: TIMA scan of zircon and corresponding EDX spectrum of hematite and elemental map of Y for 2 mol/L acid leached residue.

Figure 4.24 shows the concentration of REEs in Tutuka, Kendal and Duvha leached residues compared to their respective leachates and original CFA (see Appendix F-Table F5).
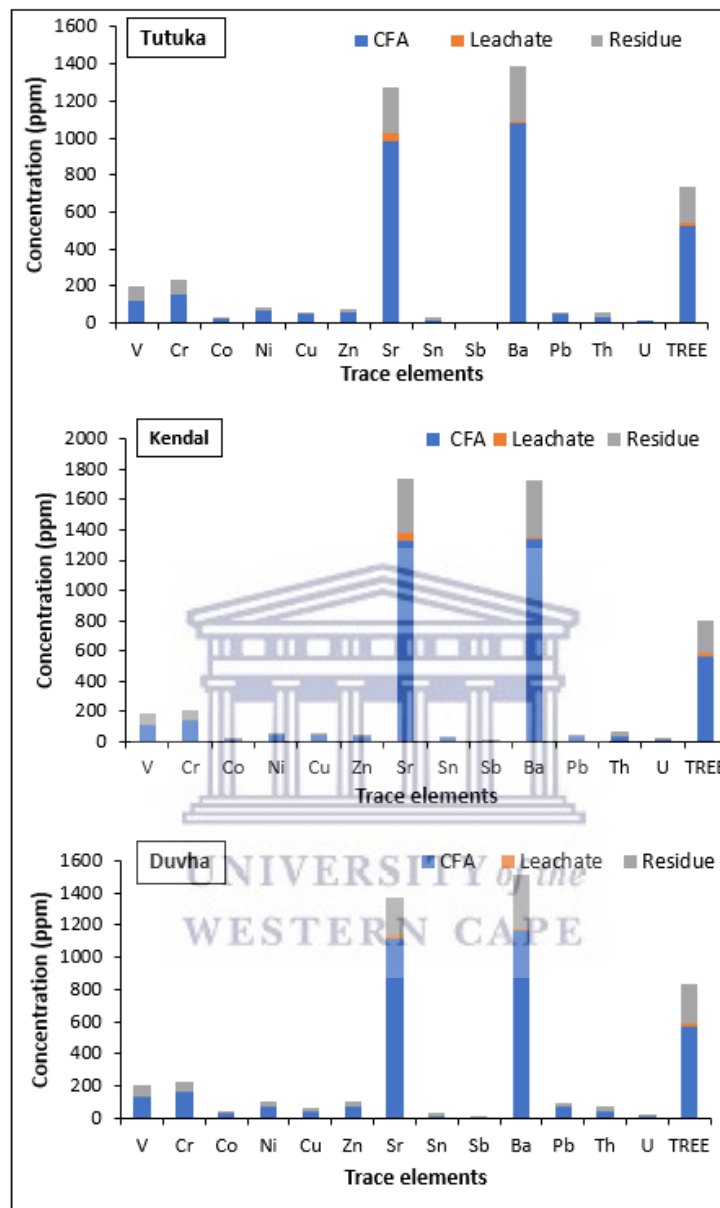
Figure 4.24: Concentration of REEs in solid residue, leachates and leached residue of Tutuka, Kendal and Duvha CFA.

In the solid leached residues of Tutuka, Kendal and Duvha CFA REEs were detected. The concentrations of REEs in the solid leached residues followed the same trend as the concentration of REEs in the original CFAs and leachate. LREEs were more abundant than MREEs and HREEs in the residues like in original CFA and leachates. The most abundant REE was Ce in the solid leached residues. The concentration of Ce was 90.58, 98.10 and 115.78 ppm for solid leached residues of Tutuka, Kendal and Duvha CFA. The least abundant REE was Lu in the solid leached residues. The concentration of Lu was 0.23, 0.25 and 0.28 for the

solid leached residue of Tutuka, Kendal and Duvha CFA respectively. The TREE concentration was 191.2, 211.4 and 241.6 ppm in the solid leached residues Tutuka, Kendal and Duvha CFA respectively. The solid leached residue of Duvha CFA had the highest TREE concentration and Tutuka had the lowest TREE concentration just like in the original CFA.

4.5 Environmental implications of REE recovery from South African CFA using the alkali fusion – acid leaching method.

4.5.1 Trace elements in the leachate

The presence and concentration of trace elements that were in the leachates extracted from Tutuka, Kendal and Duvha CFA during acid leaching at an HCl concentration of 2 mol/L were determined using the ICP-MS analytical technique. The concentration of trace elements, pH and EC values measured were compared to the Target Water Quality Range (TWQR) of South Africa for domestic water use (DWAF, 1996) as depicted in Table 4.2. DWAF (1996) defines TWQR as "The TWQR for a particular constituent and water use is defined as the range of concentrations or levels at which the presence of the constituent would have no known adverse or anticipated effects on the fitness of the water assuming long-term continuous use, and for safeguarding the health of aquatic ecosystems." The results shows that all the leachates had trace elements including toxic elements Pb, As, Cr and Hg and radionuclides such as Th and U. All the trace elements that had their TWQR documented by DWAF (1996) had concentrations higher than their respective TWQR for all three leachates except for V, Hg, Zn and Cu. The concentration of V was only within the TWQR quality range (0-0.1 ppm) for the Tutuka (0.0164 ppm) and Kendal leachates (0.0632 ppm). The concentration of Hg was within the TWQR quality range (1-0.006 ppm) for all leachate (0.0002-0.0004 ppm). The concentration of Zn was also within the TWQR quality range (0-3 ppm) for all leachates (1.0244-1.9399 ppm). The concentration of Cu was only within the TWQR quality range (0-1 ppm) for the Duvha leachate (0.9717 ppm).

The concentrations of highly toxic elements Pb, As and Cr were also higher than their respective TWQR values which were between 1.3342 - 2.1362 ppm, 0.0486 - 0.0903 ppm and 2.0293 - 3.0019 respectively. The concentration of the radionuclide U ranged from 0.39-0.468 ppm which was also higher than its respective TWQR value as well. The concentrations of Mn (4.1145 - 9.9533 ppm), Se (0.0334 - 0.0573 ppm), Cd (0.0070 - 0.0183 ppm) were also higher than their respective TWQRs. The pH values of the leachates were also very low (2.45 -2.71)

compared to the TWQR (6-9) unlike the electrical conductivity (EC) values (103.4 - 113.3 mS/cm) which were within the TWQR (0- 703.125 mS/cm).

Table 4.2: The concentration of trace elements (ppm) in the leachate extracted from Tutuka, Duvha and Kendal CFA as determined by ICP-MS with their respective TWQR, EC and pH values.

Trace element	Tutuka CFA	Kendal CFA	Duvha CFA	TWQR
V	0.0164	0.0632	0.2144	0 - 0.1
Cr	2.6816	3.0019	2.0293	0 - 0.05
Mn	9.9533	7.3437	4.1145	0 - 0.05
Co	0.6181	0.2866	0.4425	NA
Ni	1.5473	0.8965	0.9209	NA
Cu	1.6643	1.6489	0.9717	0 - 1
Zn	1.9399	1.0244	1.3143	0 - 3
As	0.0488	0.0486	0.0903	0 - 0.01
Se	0.0436	0.0573	0.0334	0 - 0.02
Mo	0.0025	0.0129	0.0335	NA
Cd	0.0183	0.0070	0.0121	0 - 0.003
Sn	0.0006	0.0015	0.0158	NA
Sb	0.0004	0.0005	0.0027	NA
Ba	2.9379	10.8718	2.4261	NA
Hg	0.0004	0.0002	0.0003	0.006-1
Pb	2.1362	1.3342	1.5313	0 - 0.01
B	5.3560	4.4940	0.0000	NA
Sr	48.5500	53.6200	24.9500	NA
Th	0.01	0.035	0.160	NA
U	0.40	0.468	0.39	0 - 0.070
pH	2.59	2.71	2.45	6-9
EC (mS/cm)	103.4	104.6	113.3	0- 703.125
NA = Not available				

The recovery of trace elements was also compared to the recovery of TREEs, see Figure 4.25 (see Appendix G-Table G1). Only the trace elements that were detected by ICP-MS in both the leachate and original CFA were compared to the recovery of TREEs. The recovery of most trace elements was lower than the recovery of TREEs from Tutuka and Kendal leachates. However, in the Duvha leachate, the recovery of all the trace elements was lower than the recovery of REEs. The recovery of Pb, Cu and Sr was higher than the recovery of TREEs in the Tutuka and Kendal CFA. TREEs were recovered at 33% for both Tutuka and Kendal CFA.

82

Pb, Cu an Sr was recovered at 45, 49 and 36% respectively in Tutuka CFA. Pb, Cu and Sr were recovered at 37, 40 and 38% respectively in the Kendal CFA.
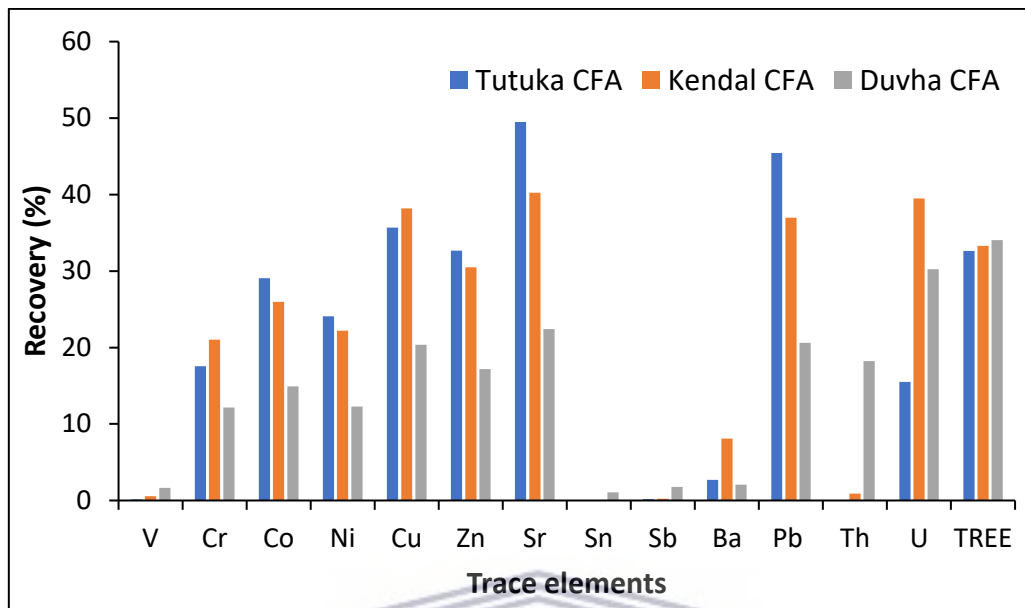
Figure 4.25: Recovery of trace elements compared to the recovery of TREEs from Tutuka, Kendal and Duvha CFA using the alkali fusion-acid leaching method.

4.5.1   Trace elements in the leached residue

All the trace elements that were present in the original CFA were present in the solid leached residues of all three CFAs however, in lower concentrations (see Table 4.3). The trace element concentration followed a similar for the solid leached residues of Tutuka, Kendal and Duvha CFA. Ti had the highest concentrations for Tutuka, Kendal and Duvha CFA (4671, 5050 and 5433 ppm respectively). Tl concentrations were the lowest for Tutuka, Kendal and Duvha CFA (0.35, 0.25 and 0.89 ppm respectively). The toxic elements Pb, Cr including radioactive trace elements Th and U were also present in all the solid residue. Duvha residue had higher concentrations of these toxic elements than both Kendal and Tutuka residue like the original CFA except for Cr. In the Tutuka residue Pb, Cr, Th and U had concentrations of 11.02, 75.96, 23.58 and 3.90 ppm respectively. In the Kendal residue, Pb, Cr, Th and U had concentrations of 9.53, 60.96, 28.15, 4.21 ppm respectively. In the Duvha residue Pb, Cr, Th and U had concentrations of 19.19, 56.55, 30.63, 4.68 ppm respectively.

Table 4.3: Concentration of trace elements in Tutuka, Kendal and Duvha acid leached solid residues determined by ICP-MS analytical technique.

Trace elements	Tutuka	Kendal	Duvha
Li	26.56	34.75	33.28
P	969.26	1089.63	1256.00
Ti	4671.11	5050.33	5433.11
V	77.71	71.23	76.34
Cr	74.96	60.96	56.55
Co	7.13	3.65	9.15
Ni	23.00	13.68	24.93
Cu	13.65	12.95	15.33
Zn	18.69	14.61	28.40
Ga	24.98	23.77	27.42
Rb	12.80	14.26	13.57
Sr	245.18	349.93	228.19
Zr	177.51	205.50	205.92
Nb	22.81	26.47	25.30
Sn	11.43	12.99	17.15
Sb	1.52	1.69	2.38
Cs	3.41	4.73	4.41
Ba	298.92	370.16	336.55
Hf	5.11	6.09	6.37
Ta	1.57	1.84	2.03
W	2.57	2.19	2.92
Tl	0.35	0.25	0.89
Pb	11.02	9.53	19.19
Th	23.58	28.15	30.63
U	3.90	4.21	4.68

4.5.2 Chapter Summary

The South African CFA in this study was characterized to determine if it is viable for REE recovery. The characteristics of Tutuka, Kendal and Duvha CFA were determined through the use of different analytical techniques to determine the major, trace (including REEs) and mineral composition of the CFA. The XRF analytical technique determined that the major elements that reside in the CFA of the study were silicon, aluminium, iron and calcium. The CFA was classified as Class F according to the ASTM C 618 (1993).

The concentration of the trace elements of the CFA in the study followed a similar trend. Highly toxic trace elements that were detected in the CFA were lead, chromium including the radionuclides thorium and uranium. The CFA in the study also had a substantial amount of REEs. The REE concentration in Tutuka (526.35 ppm), Kendal (567.68 ppm) and Duvha (573.77 ppm) CFA.

84

The major crystalline phases of Tutuka, Kendal and Duvha CFA as detected by the XRD analytical technique were quartz and mullite. Magnetite appeared to a lesser extent in all the CFA. Low amounts of calcite appeared in the Tutuka and Kendal CFA alone and even lower amounts of microcline appears in the Duvha CFA alone. The other crystallin phases that are known to contain REEs such as mullite and quartz were detected by the XRD. The TESCAN TIMA analytical technique was used to find other mineral phases that were associated with REEs in the CFA. The TIMA scans of the CFA in the study showed that REE-bearing phases were present. REEs were found in abundance in different phases in the CFA. Ilmenite, allanite and rutile had an abundance of LREEs. MREEs and HREEs were more abundant in minerals such as goethite, hematite and almandine. Zircon had an abundance of Y and calcite had an abundance of Sc.

The REE extraction results show that the REE that was generally extracted the most at each acid concentration was Ce which is an LREE. The LREEs were generally extracted more than MREEs and HREEs. The acid concentration that extracted the most REEs was the 2 mol/L acid concentration. At 2 mol/L acid concentration, the Duvha CFA extracted the most REEs followed by Kendal then Tutuka CFA. The extraction of REEs from the CFA in this study using the alkali fusion-acid leaching method was very low even at the acid concentration of 2 mol/L (17.72-19.53 ppm).

The relationship between acid concentration and REE recovery was investigated in the present study. Acid concentration had a significant effect on the recovery of REEs. These recovery results show that generally when using the alkali fusion-acid leaching method REE recovery follows the same trend as REE extraction from the CFA of this study. At a low acid concentration of l mol/L low REE recovery and extraction is achieved. As acid concentration increases 2 mol/L REE recovery and extraction increases. When acid concentration is further increased to 3 mol/L REE extraction and recovery decreased.

LREEs were generally extracted more than MREEs and HREEs. On the other hand, HREEs and MREEs were recovered similarly and were also recovered more than LREEs. MREEs and HREEs were more abundant in the same minerals such as goethite, hematite and almandine. LREEs were more abundant in different minerals, such as allanite, ilmenite and rutile.

XRD and TIMA results showed that although the alkali fusion-acid leaching method was able to dissolve REE-bearing minerals (mullite, quartz, allanite zircon etc) these minerals were not dissolved completely.

REE recovery using the alkali fusion-acid leaching method has environmental implications. The leachates of all the CFA have low pH with the presence of trace elements of major concern lead (Pb), arsenic (As) chromium (Cr) and mercury (Hg) including the radionuclides thorium (Th) and uranium (U). All the trace elements in the leachate that were documented by DWAF (1996) had concentrations higher than their respective Target Water Quality Range (TWQR) for all three CFA in the study except for Hg. The recovery of most trace elements was lower than the recovery of TREEs from Tutuka and Kendal CFA. However, in the Duvha CFA, the recovery of all the trace elements was lower than the recovery of REEs. The recovery of Pb, Cu and Sr was higher than the recovery of TREEs in the Tutuka and Kendal CFA

The solid residue had all the trace elements found in the original CFA however at much lower concentrations. Trace elements of major concern like Pb and Cr and radionuclides Th and U were removed to a significant degree.

5 Discussion

5.1 Introduction

There has been extensive research going into characterizing REEs in CFA (Ripfumelo, 2012; Franus et al., 2015; Taggart et al., 2016; Wagner & Matiane, 2018) but, little has been done to determine efficient extraction methods to recover REEs from CFA (King et al., 2018). Therefore, this study aimed to investigate the effectiveness of alkali fusion-acid leaching for the recovery of REEs from South African CFA and determine the optimal acid concentration for REE recovery in South African CFA.

5.2 Characteristics of African CFA South

5.2.1 Major and trace elements

The elemental composition of CFA plays a major role in the recovery of REEs (Taggart et al., 2018). This study has shown the major and trace elements found in three South African CFA (i.e., Tutuka, Kendal and Duvha CFA). The predominant major elements of Tutuka, Kendal and Duvha CFA were silicon dioxide (SiO_2), aluminium oxide (Al_2O_3), ferric oxide (Fe_2O_3) and calcium oxide (CaO) as determined by XRF analytical technique (as shown in Figure 4.1, Appendix A- Table A1). SiO_2 is the most abundant in all three CFA this is expected because South Africa only produces siliceous (pozzolanic) CFA (SACAA, 2020; Wagner & Matiane, 2018). The CaO content of the CFA from all three power stations ranges from 3.57 to 5.59 % and their sum of aluminium, silicon, and iron oxides is greater than 70% and the loss of ignition (LOI) is less than 6% making all the CFA Class F, according to (ASTM C 618, 1993). These results align with those reported by Methode Kalombe et al. (2020) when determining major elements of CFA from two South African power stations. Since South Africa CFA has low CaO content it is recommended to pre-treat the CFA to improve REE recovery during acid leaching. When using the direct acid leaching method on CFA with low CaO content there is lower REE recovery compared to using the method on CFA with high CaO content. Preconditioning of the CFA before acid extraction improves the REE recoveries (Taggart et al., 2016). Thus, in this study, the alkali fusion-acid leaching method was used to recover REEs from South African CFA.

The ICP-MS analytical technique detected a range of trace elements in the CFA of the study as presented in Table 4.1. Highly toxic elements that were detected from the CFA were Pb, Cr including radioactive trace elements Th and U. These highly toxic elements were in high concentrations in all the CFA with Duvha CFA having higher concentrations of these elements

than both Kendal and Tutuka CFA. Studies by Gitari et al. (2009), Fatoba (2010) and Eze (2014) also found that South African CFA has a range of trace elements including Pb, Cr, Th and U. Thus, the recovery of REEs from the CFA in this study had the potential to remove highly toxic trace elements which could make the residual CFA safer to dispose of.

5.2.2   Rare Earth Element Analysis on South African CFA

CFA potentially contains the full range of REEs; most conventional REE mines extract only a few of these elements. However, limited research appears in the literature on REE occurrence in South African CFA (Wagner & Matiane, 2018). This study has shown that indeed South African CFA contains the full range of REEs (see Figure 4.2, Appendix A-Table A3). The concentrations of REEs in Tutuka, Kendal and Duvha raw CFA had a similar trend. The REE with the highest concentration was Ce and Lu had the lowest concentration in all the CFA of this study. In addition, LREEs were generally in higher concentration than MREEs and the HREEs. Sc was also in high concentration. LREEs are generally more abundant than MREEs and or HREEs (Ripfumelo, 2012; Franus et al., 2015; US Department of Energy, 2017; Huang et al., 2019; Pan et al., 2020). The larger ionic radii of LREEs keep them separate from other elements this is why they can be found in greater contents (An, 2014). The Oddo -Harkin's effect, where REEs with even atomic numbers are generally in greater abundance than odd-numbered elements adjacent to them on the periodic table (Kashiwakura et al., 2013; An, 2014; Taggart et al., 2018), can also be observed in the REE concentrations in all CFA of this study. For example, Ce with an even atomic number of 58 is in greater abundance than the La and Pr which have odd atomic numbers of 57 and 59 respectively. Ce is also the most abundant REE throughout all three CFA in the study.

The excessive REEs were more abundant than the critical and uncritical (La, Pr, Sm and Gd) REEs in the CFA of the study. The critical REE concentration (154.22 to 170.29 ppm) of the three CFAs was more abundant than the critical REE concentration (70.2 ppm) of the Upper Continental Crust (UCC) by Taylor & McLennan (1985).

The Total Rare Earth Element (TREE) concentration Tutuka, Kendal and Duvha CFA were measured to be 526.35, 567.68 and 573.77 ppm respectively. Duvha CFA had the highest TREE content of all the three power stations and Tutuka had the lowest. The TREE concentrations were comparable to TREE concentrations found in studies by Akinyemi et al. (2012) (517.8 ppm), (Eze et al., 2014) (480.42 ppm) and (Ripfumelo, 2012) (559.20 ppm) which studied South African CFA. Furthermore, in a global context, the TREE content of the

Tutuka, Duvha and Kendal CFA was comparable to the TREE content found in CFA from China and the U.S.A. Studies by Cao et al. (2018) and Tang et al. (2019) showed that the TREE concentration of the CFA from the Panbei power station in Guizhou, China was 489 ppm and 494.77 ppm respectively. While Taggart et al. (2018) found TREE content of 524 ppm from Illinois Basin CFA in the U.S.A. The TREE concentration of Tutuka, Duvha and Kendal CFA was more abundant than the TREE concentration (168.4 ppm) of the Upper Continental Crust (UCC) by Taylor & McLennan (1985). The Tutuka, Duvha and Kendal CFA also had a higher TREE concentration than the TREE concentration of the average world coals (68.5 ppm) and the average CFA globally (445ppm) by Ketris & Yudovich (2009). Thus, Tutuka, Kendal and Duvha CFA can be considered as viable options for REE recovery.

5.2.2.1 Mineralogical analysis

In Tutuka, Kendal and Duvha CFA, the major crystalline phases were quartz (SiO_2) and mullite ($Al_44Si.2O_9.6$) according to the XRD pattern (see Figure 4.4). Magnetite ($FeFe_2O_4$) appears to a lesser extent in all the CFA. Low amounts of calcite ($CaCO_3$) appear in the Tutuka and Kendal CFA alone and even lower amounts of microcline ($KAlSi_3O_8$) appears in the Duvha CFA alone. These results were expected since CFA from bituminous coals generally has a presence of mullite and a lesser amount of quartz, unburned carbon, iron oxides (hematite and magnetite), spinel, goethite and pyrrhotite (Franus et al., 2015).

Quartz in CFA is a major crystalline phase that exists as a hard mineral commonly found as cell and pore infillings in the organic matter of coal and is usually a primary mineral because it is mostly unaltered by the combustion process due to its high fusion temperature (Ward et al., 2009; Akinyemi, 2011; Eze, 2014). Another primary mineral is microcline, which occurs in coal and may pass through the combustion process and accumulate in ashes (Hower et al., 2017). Mullite is a secondary mineral as it does not exist in coal however it is formed from the decomposition of kaolinite, an aluminosilicate mineral in the coal (Koukouzas et al., 2009; Eze, 2014). Magnetite is also a secondary mineral that is formed from the oxidation of pyrite and other iron-bearing minerals in coal (Eze, 2014). Calcite is another secondary mineral that was likely formed in the Tutuka and Kendal CFA through the reaction of lime (CaO) contained in the CFA with ingressed carbon dioxide (CO_2) (Eze et al., 2013). When CFA is exposed to CO_2 in the air after coal combustion and there is an adequate amount of lime (CaO) in the CFA, CaO can react with CO_2 which leads to the crystallization of $CaCO_3$.

Studies have indicated that REEs reside in the dominant amorphous glass phase of CFA (Taggart et al., 2016; Hower et al., 2019; Guo-qiang et al., 2020). However, the XRD analytical technique was unable to differentiate the amorphous glass phase in all the CFAs. Crystalline phases that are known to contain REEs which were detected by XRD were mullite and quartz. Mullite contains aluminium (Al) where REEs reside (Taggart et al., 2018) and to a lesser degree, the mineral quartz contains REEs as well (Kolker et al., 2017).

The primary phases associated with REEs in the CFA in this study as detected by the TIMA analytical technique are shown in Table 5.1. These phases are known to be associated with REEs from literature (Madison et al., 2017; Maledi, 2017; Balaram, 2019; Hower et al., 2019).

Table 5.1: Primary phases associated with REEs in Tutuka, Kendal and Duvha CFA detected by TIMA analysis.

REE-bearing phases	Tutuka CFA	Kendal CFA	Duvha CFA
Plagioclase	x	x	x
Kaolinite	x	x	x
Rutile	x	x	x
Allanite	x		
Quartz	x	x	x
Aluminosilicate mixture	x	x	x
Zircon	x		x
Apatite			x
Ilmenite	x		
Actinolite	x		
Zoisite	x	x	x
Hematite	x	x	x
Goethite	x	x	x
Almandine	x	x	x
Calcite	x	x	x
Chlorite-Chamosite		x	x
Chlorite-Clinochlore	x	x	x
Ankerite	x	x	x
Grossular	x	x	x
Tantalite		x	x

The majority of the phases associated with REEs were found in all the CFA samples that were investigated. However, the minerals apatite, chlorite-chamosite and tantalite were not detected as primary phases in Tutuka CFA. In Kendal CFA, allanite, zircon, apatite, ilmenite and actinolite were not detected as primary phases. While in the Duvha CFA allanite, ilmenite and actinolite were not detected as primary phases.

The TIMA results also showed that different minerals are enriched with different classes of REEs. Ilmenite, allanite and rutile had an abundance of LREEs (see Figure 4.7). MREEs and HREEs were more abundant in minerals such as goethite, hematite and almandine (see Figure 4.8). Zircon had an abundance of Y (see Figure 4.9) and calcite had an abundance of Sc (see Figure 4.10) (see Appendix A-Table 4-6). Liu et al. (2019) showed that different mineral phases preferentially accommodate LREEs or HREEs in Class F and Class C CFA from major coal basins in the U.S. LREEs were more enriched in monazite/rhabdophane and HREEs in xenotime/churchite, lime, and zircon. The authors explained that this might be due to the gradually decreasing cation radii of REEs with increasing atomic number (i.e., lanthanum contraction), which changes the compatibility of individual REE elements for a specific mineral phase. These REE-bearing minerals are difficult to dissolve during leaching. Thus a pre-treatment of the CFA is required to decomposed these REE-bearing minerals into more acid soluble forms (Zhang & Honaker, 2020). Furthermore, strong acids and high temperatures are required to dissolve the amorphous phases in CFA and decompose acid-resistant minerals such as mullite into soluble forms of Al to effectively recover REEs (Taggart et al., 2016). Preconditioning of CFA by fusion with alkaline additives such as sodium hydroxide (NaOH) and sodium carbonate (Na_2CO_3) before acid leaching has been shown to improve REE recoveries (Taggart et al., 2018; Tang et al., 2019). Fusion activates the inert material from CFA based on the reaction with a sodium or calcium compound at high temperature, in which the phases such as quartz and mullite can be transferred into a series of soluble silicates such as nepheline, and noselite, to provide good materials for subsequent acid leaching (Yao et al., 2014; Taggart et al., 2018). Therefore, in this study, the alkali fusion-acid leaching method was used to recover REEs from Tutuka, Kendal and Duvha CFA.

5.3 Effect of acid concentration on the recovery of REEs using alkali fusion -acid leaching method.

Acid concentration has been proven to be one of the most influential factors in REE acid leaching experiments (Taggart et al., 2018; Tang et al., 2019; Pan et al., 2020). However, the optimal acid concentration for the recovery of REEs from CFA differs for different studies (Cao et al., 2018; Tang et al., 2019; Rybak & Rybak, 2021). In this study acid concentration also had a significant effect on REE extraction and recovery from Tutuka, Kendal and Duvha CFA.

5.3.1 REE extraction

Acid concentration had a significant effect on REE extraction from Tutuka, Kendal and Duvha CFA. The REE extraction from the three CFAs followed a similar pattern. Generally, the extraction of individual REEs from the CFA increased when acid concentration was increased from 1 mol/L to 2 mol/L then extraction decreased when acid concentration was increased to 3 mol/L (Figure 4.11, Appendix C-Table C1).

The REE that was generally extracted the most at each acid concentration was Ce which is an LREE. The LREEs were generally extracted more than MREEs and HREEs (see Figure 4.12, Appendix C-Table C2). This was expected because Ce was the most abundant REE in the original CFA and LREEs were generally more abundant than MREEs and HREEs in the original CFA.

At 2 mol/L TREE extraction was at its highest, Duvha CFA had the most REEs extracted (19.528 ppm) followed by Kendal CFA (18.892 ppm) and then Tutuka CFA (17.172 ppm) (see Figure 4.13, Appendix C-Table C3). Thus the extraction of REEs from the CFA in this study using the alkali fusion-acid leaching method was very low even at the acid concentration of 2 mol/L. A study by Eze (2014) showed higher TREE extraction (283.85 ppm) from CFA from the Matla power station in South Africa using HCl as a lixiviant. However, the trend in the REE extraction of individual and classified REEs was similar to this study. LREEs were generally extracted more than MREEs and HREEs, Ce was also the most extracted REE. The difference in REE extraction values from this study and the study by Eze (2014) was probably due to different leaching methods and CFA from different power stations.

5.3.2 Individual and classified REE recovery

Generally, the recovery of individual REEs from the CFA in this study improved when acid concentration was increased from 1 mol/L to 2 mol/L then recovery decreased when acid concentration was increased to 3 mol/L (Figure 4.14, Appendix D-Table D1). This trend was similar to the extraction of REEs from the three CFAs.

The MREE Y and the MREE and Er, Ho, Tm and Lu were generally recovered the most. It is worth noting that Ce was the most abundant REE in all the CFA of this study (see section 4.2.3) and it was also generally extracted the most (see section 4.3.1). However, Ce was one of the REEs with lower recoveries from the CFA in this study at each acid concentration. The other LREEs (La, Pr, Nd and Sm) neighbouring Ce also generally had lower recoveries than the MREEs and HREEs even though they were more abundant in the original CFA. Generally,

MREEs and HREEs were recovered similarly and they were also recovered more than LREEs in all the CFA of this study (see Figure 4.15, Appendix D-Table D2). Lin et al. (2021) found similar results when recovering REEs from coal ash from Kentucky, USA with 1 mol/L of HCl. MREEs were recovered slightly more (28%) than HREEs (27%) and LREEs were recovered the least (17%). The authors explained that the increased leachability of MREEs and HREEs in the ash can be explained by their organic association in the parent coal. During coal combustion organic matrix is broken down, these MREEs and HREEs either transformed from the insoluble to the soluble state or became more accessible to the leaching agent or both. In contrast, LREEs are mainly associated with inorganic minerals in coal. Coal combustion might transform soluble LREE-bearing minerals into insoluble ones. In addition, Taggart (2017) found similar results when recovering REEs from CFA from Illinois, Powder River and Appalachian Basins. The recovery of HREEs (Tb to Lu, including Y due to its atomic radius) was higher than for LREEs (La through Gd). This difference was most evident in Powder River Basin CFA ($57.1 \pm 4.7\%$ LREE recovery vs. $65.5 \pm 2.1\%$ HREE recovery). However, the abundance of HREEs was lower than that of LREEs in the original CFA.

In this study, MREEs and HREEs were abundant in the same minerals in the original CFA and LREEs were abundant in other minerals. In the TIMA scans of the original CFA LREEs were found in abundance in ilmenite, allanite and rutile phases. MREEs and HREEs were found mainly in hematite, goethite and almandine. This could explain why the recoveries of MREEs and HREEs recovery was similar.

These results show that that the alkali-fusion-acid leaching method favours the recovery of MREEs and HREEs more than LREEs. This indicates that the more valuable HREEs can be preferentially recovered. HREEs are more valuable than LREEs and MREEs because HREEs are found at a lower concentration on the Earth's crust (An, 2014). However, HREEs have much lower abundances than MREEs and LREEs, so even increased HREE recovery may not result in meaningfully higher recoveries by mass.

5.3.3 Total REE recovery

The recovery of individual and classified REEs generally followed a similar trend to the recovery of TREEs. In general, the recovery of the TREEs from Tutuka, Kendal and Duvha CFA tended to increase from a concentration of 1 to 2 mol/L and decreased when concentration was increased to 3 mol/L (see Figure 4.16, Appendix D-Table D3).

Tang et al. (2019) and Cao et al. (2018) also investigated the effect of acid concentration on the recovery of REEs from Panbei power station CFA in China. In the study by Tang et al. (2019) the alkali fusion-acid leaching method was used like in this study. While in the study by Cao et al. (2018) direct acid leaching was used. At 1 mol/L HCl concentration, the amount of HCl was insufficient for the requirements of the leaching process in both studies. Cao et al. (2018) further explained that at low acid concentrations most of the acid was depleted by the major elemental oxides (Al_2O_3, Fe_2 and CaO) and only a small amount of acid was involved in the reaction with the rare earth compounds.

The reactions between HCl and CFA during acid leaching for the recovery of REEs can be explained by the following equations (Cao et al., 2018):

$$Al_2O_3 + 6HCl = 2AlCl_3 + 3H_2O \qquad (5.1)$$

$$Fe_2O_3 + 6HCl = 2FeCl_3 + 3H_2O \qquad (5.2)$$

$$CaO + 2HCl = CaCl_2 + H_2O \qquad (5.3)$$

$$RE_2O_3 + 6HCl = 2RECl_3 + 3H_2O \qquad (5.4)$$
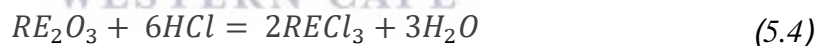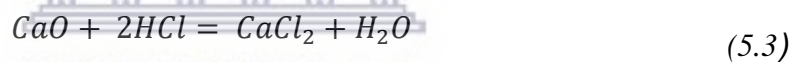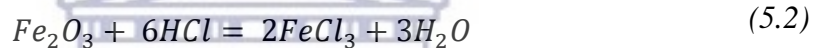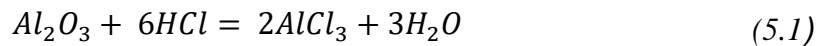
HCl is often preferentially reacted with the oxides of the major metal such as Al_2O_3, Fe_2O_3 and CaO in CFA as shown in Equations (5.1), (5.3) and (5.3) and then the reactions between HCl and oxides of REEs (RE_2O_3) proceed as indicated in equation (5.4). This is because REEs tend to be encased within the Fe, Ca-rich aluminosilicate glass thus HCl first reacts with the major elements then reacts with REEs. The REEs are encapsulated in the body of CFA and they are dissolved and released layer by layer during the leaching process. The leaching kinetics can also be explained using the shrinking core model (SCM) (Levenspiel, 1999). With the use of SCM, CFA particles can be seen as spherical particles which contain REEs. If the migration of H^+ in the solution is not limited by solution concentration and the solid−liquid ratio, H^+ reacts with the REEs at the surface of the CFA particle, and rare earth ions are dissolved out from the particle surface and diffuse into the solution. As a result, low acid concentration (1 mol/L) produces lower REE recovery (Cao et al., 2018). In the study by Tang et al. (2019) the optimal

acid concentration for REE recovery was 2 mol/L because as acid concentration increased to 3 mol/L the increase in acid concentration led to increased dissolution of silicon and iron. Thus, a small amount of flocculation was formed on the surface of leach residue in suspension. This hindered the contact between hydrogen ions (H$^+$) and solid particles which led to a decrease in the REE recovery. On the other hand, the study by Cao et al. (2018) showed that REE recovery continued to increase as acid concentration increased until acid concentration reached 3 mol/L. The REE recovery no longer increased at concentrations higher than 3 mol/L because partially encapsulated REEs have no opportunity to contact the acid even though the REE recovery is no longer limited by the lack of H$^+$. Therefore, it was concluded that 3 mol/L was the optimal acid concentration to leach REEs from CFA.

The trend of REE recovery in Tutuka, Duvha and Kendal was similar to the study by Tang et al. (2019). When the acid concentration was at 1 mol/L the amount of HCl was not enough to meet the requirements of the leaching process. As acid concentration increased to 2 mol/L there are more H$^+$ to react with the alkali fusion products, which in turn increased REE recovery. At 3 mol/L there is even more H$^+$ to react with the fusion products, however, the increase in H$^+$ increases the formation of silicic acid which forms a gel layer that inhibits contact of hydrogen ions (H$^+$) and with the solid particles Thus, decreasing REE recovery.

The formation of silicic acid during leaching can be explained from the reactions that occur between the fusion product and HCl can be explained using the following equations (Pan et al., 2020):

$$NaAlSiO_4 + 4HCl = NaCl + AlCl_3 + H_4SiO_4$$
<div align="right">(5.5)</div>

$$Na_2SiO_3 + 2HCl = 2NaCl + H_2SiO_3$$
<div align="right">(5.6)</div>
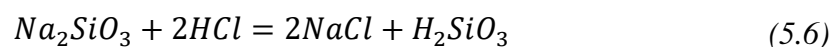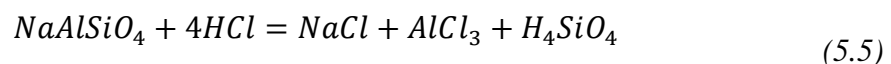
NaAlSiO$_4$ (nepheline) and Na$_2$SiO$_3$ (sodium silicate) are products of alkali fusion of CFA with NaOH. When NaAlSiO$_4$ reacts with HCl, the reaction produces NaCl (sodium chloride), AlCl$_3$ (aluminium chloride) and H$_4$SiO$_4$ (silicic acid). When Na$_2$SiO$_3$ reacts with HCl the reaction produces NaCl and H$_2$SiO$_3$ (metasilicic acid). The silicic acid gel layer was observed when leaching CFA at 2 mol/L and an even thicker gel layer was observed after leaching at 3 mol/L (see Figure 5.1). The gel layer made it very difficult to filter the acid leaching residue because the gel blocked the pores of the filtration paper especially when acid concentration was 3 mol/L.

The silicic acid gel has a very low solubility which can limit the leaching of REEs (Pan et al., 2020). This could be the reason why at 3 mol/L REE recovery was reduced.

According to King et al. (2018), the formation of a silicon-rich gel layer can form over ash during the acid leaching process, which could limit subsequent diffusion of other ions from the ash under alkaline conditions. The study explored different methods for recovery of REEs from Illinois, Powder River and Appalachian basin ash. The methods included alkaline leaching using aqueous NaOH followed by dilute acid (HCl) leaching which was found to improve the recovery of REEs when compared to direct acid leaching. However, the formation of a silica gel layer was a limiting factor for the leaching of REEs under alkaline conditions.
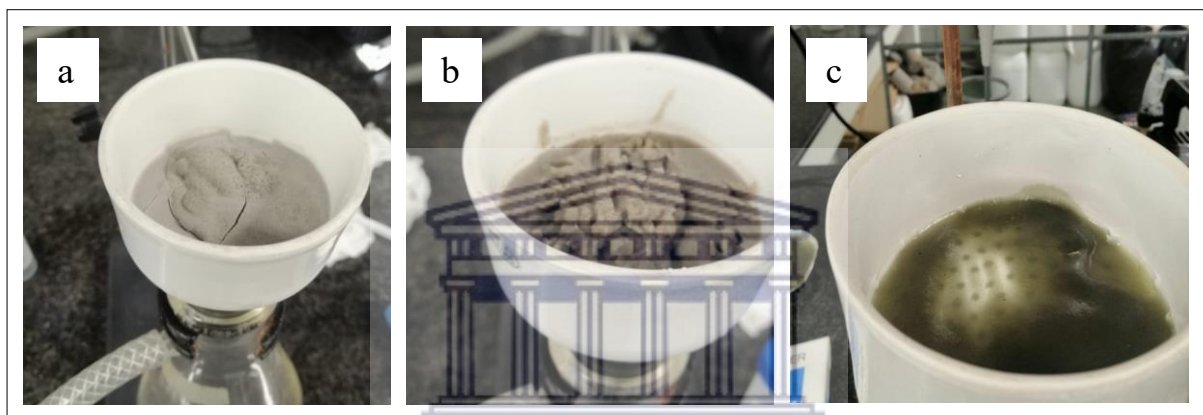
Figure 5.1: Appearance of Silicic gel layer in a) 1 mol/L solid residue b) 2 mol/L solid residue and c) 3 mol/L solid residue of Tutuka CFA.

The study showed that Ca content in the CFA could have played a part in the formation of the silica gel during leaching. The abundance of Ca can result in the formation of silicates that can destabilize the gel layer and reduce the amount of SiO_2. The study by King et al. (2018) and another study by Taggart et al. (2016) showed that when CFA has higher amounts of Ca (22.9-33.6%), REEs are extracted to a larger extent. In this study the CFA has relatively low Ca ranging from 3.57-5.59% (see Figure 4.1) this explains the production of silicic acid gel in the CFA during acid leaching.

These recovery results show that generally when using the alkali fusion-acid leaching method REE recovery follows the same trend as REE extraction from Tutuka, Duvha and Kendal CFA of this study. At a low acid concentration of 1 mol/L low REE recovery and extraction is achieved. As acid concentration increases 2 mol/L REE recovery and extraction increases. When acid concentration is further increased to 3 mol/L REE extraction and recovery decreased. Therefore, acid concentration of 2 mol/L was the optimal concentration for REE recovery and extraction using alkali fusion acid leaching for the CFA in this study.

The REE-bearing mineral phases that were present in the original CFA were still present in the acid leached residues. The major phases of quartz and mullite that were present in the XRD patterns of the CFA were still present in the XRD patterns of the solid residues however to a lesser degree (Figure 4.17). These major phases were dissolved as a result of the alkali fusion-acid leaching however they were not dissolved completely. This is the reason why there was low extraction and recovery of REEs from the CFA in the study because mullite and quartz which normally contain REEs were still retained in the residue. There were also large peaks of halite in all the leached residues however halite was not present in the original CFA. Halite was not present in the original CFA this was probably because halite was a product of alkali fusion-acid leaching. Sodium (Na^+) was introduced to the CFA during fusion from the reaction between NaOH with mullite ($3Al_2O_3 \cdot 2SiO_2$) and quartz (SiO_2) (Pan, Hassas, et al., 2020):

$$6NaOH(s) + 3Al_2O_3 \cdot 2SiO_2(s) = 2NaAlSiO_4(s) + 4NaAlO_2(s) + 3H_2O(g) \qquad (5.7)$$

$$2NaOH(s) + SiO_2(s) = Na_2SiO_3(s) + H_2O \; (g) \qquad (5.8)$$
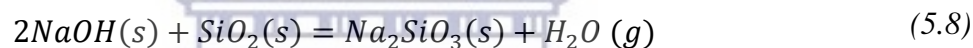
NaOH was reacted with mullite and quartz in CFA to produce nepheline ($NaAlSiO_4$) and sodium silicate (Na_2SiO_3). The reaction of nepheline and sodium silicate with HCl during leaching produced NaCl (halite) (as seen in equations 5.5 and 5.6).

The TIMA scans also show that the primary phases kaolinite, quartz and plagioclase which were in abundance in the original CFA were barely visible in the solid leached residues (Figure 4.18, Figure 4.19 and Figure 4.20). The aluminosilicate mixture was the dominant phase in the solid leached residues of Tutuka and Kendal CFA. The dominant phase in the solid leached residue of Duvha CFA was quartz. There was also evidence of nepheline in the TIMA scans of the solid leached residues of Tutuka and Kendal CFA. Nepheline was not present in the original CFA; this was because nepheline was a product of alkali fusion (see equation 5.7).

The phases that had an abundance of REEs in the original CFA, were still present in all the solid leached residues however in smaller quantities (see Figure 4.21, Figure 4.22 and Figure 4.23) (see Appendix F-Table F1-3). The alkali fusion-acid leaching method was able to remove LREE rich ilmenite and allanite to the point that they were not visible in the TIMA images of the residues. However, LREE-bearing rutile was less susceptible to the alkali fusion-acid leaching method as it was still very visible in the residue images. The MREE and HREE rich hematite was still visible in the residue as well as goethite and almandine. The Y rich zircon

was also present in the solid residues. Calcite was also present in the residue; which had an abundance of Sc. However, it was barely visible in the TIMA images.

The residues of Tutuka, Kendal and Duvha CFA still retained a substantial amount of REEs (Figure 4.24, Appendix F-Table F4). The solid leached residue of Duvha CFA (241.6 ppm) had the highest TREE concentration followed by that of Kendal CFA (211.4 ppm) then Tutuka CFA (191.2 ppm). LREEs were more abundant than MREEs and HREEs in the solid leached residues like in the original CFA and the leachates. The most abundant REE was still Ce in the residues, like in the original CFA and the leachates.

The results showed that although the alkali fusion-acid leaching method was able to dissolve REE-bearing minerals, these minerals were not dissolved completely. This is one of the reasons why there were low REE recoveries and extractions from the Tutuka, Duvha and Kendal CFA using the alkali fusion-acid leaching method. Changing alkali fusion conditions by increasing fusion temperature or time to further break down the acid-resistant REE-bearing phases could make REEs more accessible during acid leaching and improve REE recoveries. The solid leached residue of the study can also be leached again to recover the REEs that were retained.

5.4 Environmental implications of REE recovery from South African CFA using the alkali fusion – acid leaching method.

Acid concentration has a significant effect on the leaching of REEs however it also affects the leaching of other trace elements including elements of potential environmental concern from CFA (Be, Cd, Co, Cu, Fe, Mg, Mn, Ni, Pb, Si, Sn, Th, Tl, U) (Izquierdo & Querol, 2012). More investigations are needed to understand the environmental trade-offs of recovering metals from CFA (Taggart et al., 2018). The elemental composition leachates after acid leaching will be critical for downstream processing that further concentrates the REEs and the disposal of the lixiviant (King et al., 2018).

This study showed that there was a range of trace elements that were coextracted with REEs in the leachates. When the concentration of trace elements was compared to the Target Water Quality Range (TWQR), most of the trace elements had concentrations higher than their respective TWQR for all three lixiviants (Table 4.2). Hg, Zn and Cu were the only trace elements that were within their TWQR ranges. The concentrations of highly toxic elements Pb, As and Cr were also higher than their respective TWQR values. The pH values of the lixiviants were also very low compared to the TWQR however, the electrical conductivity (EC) values were within the TWQR.

Gitari et al. (2009) investigated the effect of pH on the release of major and trace species in selected South African CFA and found that the concentration of most major and minor species found in the leachates of the CFA was observed to be higher than their respective TWQRs at lower pH values. The study showed that the concentration of trace elements such as Ni, Pb, Cu and Fe increased when pH was <9. The pH values in this study were between 2.45 -2.71.

The recovery of most trace elements was also lower than the recovery of TREEs in the Tutuka and Kendal leachates (see Figure 4.25, Appendix G-Table G1). However, in the Duvha leachates, the recovery of all the trace elements was lower than the recovery of REEs. This shows that the alkali fusion-acid leaching method favours the leaching of REEs more than other trace elements, especially from the Duvha CFA.

King et al. (2018) also showed that trace elements of potential concern were recovered with REEs. The trace elements Cr, V, Pb, Se, As, U and Mo were present with REEs in the leachates after leaching CFA. The recovery of the trace elements was due to acid leaching with a strong acid like HCl at low pH values. HCl is very effective in leaching heavy metals especially at low pH values (Huang et al., 2011)

These results show that the alkali fusion acid leaching method is non-selective, REEs were coextracted with other trace elements at high concentrations. Thus, disposing of the leachates could be environmentally harmful. Further treatment of lixiviant is required after REE recovery to increase pH and remove the trace elements with special regard given to the removal of Pb, As, Cr and U. The addition of an alkali to the leachates after acid leaching can improve the pH and aid in the downstream separation of REEs from leachates. The leachates were not the only product of alkali fusion - acid leaching of environmental importance, the acid leached solid residue also needs to be safely disposed of.

All trace elements that were present in the original CFA were present in the solid leached residues of all three CFAs however, in lower concentrations see (Table 4.3) . The toxic elements Pb, Cr including radioactive trace elements Th and U that were present in the CFA were also present in all three solid leached residues. Duvha solid leached residue had higher concentrations of these toxic elements than both Kendal and Tutuka solid leached residues like the original CFA except for Cr. Although the solid leached residues have retained all trace elements, the trace elements were less concentrated in the solid leached residues than the original CFAs. Thus, making the residue safer to dispose of than the original CFA.

5.5 Chapter summary

The major elements of Tutuka, Kendal and Duvha CFA are silicon dioxide (SiO_2), aluminium oxide, ferric oxide and calcium oxide. All the CFA in this study is Class F, according to (ASTM C 618, 1993). South Africa CFA has low CaO content it is recommended to pre-treat the CFA to improve REE recovery during acid leaching. The recovery of REEs from the CFA in this study had the potential to remove highly toxic trace elements which could make the residual CFA safer to dispose of. However, concentrating these highly toxic trace elements in the lixiviant after alkali fusion-acid leaching could be environmentally damaging. South African CFA contains the full range of REEs. LREEs were generally in higher concentration than MREEs, and HREEs. Sc which is neither light, medium nor heavy was also in high concentration. Duvha CFA had the highest TREE content of all the three power stations and Tutuka had the lowest. The REE contents found in this study were also comparable with that found in other South African CFA. Furthermore, in a global context, the TREE content of the CFA in this study was comparable to the TREE content found in CFA from China and the U.S.A. The primary phases associated with REEs were detected in the CFA of this study. Crystalline phases that are known to contain REEs were detected in the CFA. The results also showed that different minerals are enriched with different classes of REEs. Ilmenite, allanite and rutile had an abundance of LREEs. MREEs and HREEs were more abundant in minerals such as goethite, hematite and almandine. Zircon had an abundance of Y and calcite had an abundance of Sc. These REE-bearing minerals are difficult to dissolve during leaching. Thus, a pre-treatment of the CFA is required to decomposed these REE-bearing minerals into more acid soluble forms.

The REE extraction results show that the REE that was generally extracted the most at each acid concentration was Ce which is an LREE. The LREEs were generally extracted more than MREEs and HREEs. This is expected because Ce was the most abundant REE in the original CFA and LREEs were generally more abundant than MREEs and HREEs in the original CFA. The acid concentration that extracted the most REEs was the 2 mol/L acid concentration. At 2 mol/L acid concentration, the Duvha CFA extracted the most REEs followed by Kendal then Tutuka CFA. The extraction of REEs from the CFA in this study using the alkali fusion-acid leaching method was very low even at the acid concentration of 2 mol/L (17.72-19.53 ppm).

Acid concentration had a significant effect on the recovery of REEs. These recovery results show that generally when using the alkali fusion-acid leaching method REE recovery follows the same trend as REE extraction from the CFA of this study. At a low acid concentration of l

mol/L low REE recovery and extraction is achieved. As acid concentration increases 2 mol/L REE recovery and extraction increases. When acid concentration is further increased to 3 mol/L REE extraction and recovery decreased. At 1 mol/L HCl concentration, the amount of HCl was insufficient for the requirements of the leaching process thus low REE recovery is achieved. As acid concentration increased from 1 to 2 mol/L there are more H^+ to react with the alkali fusion products, which in turn increased REE recovery. At 3 mol/L there is even more H+ to react with the fusion products, however, the increase in H+ increases the formation of silicic acid which forms a gel layer that inhibits contact of hydrogen ions (H^+) and with the solid particles. Thus, decreasing REE recovery. Therefore, an acid concentration of 2 mol/L was the optimal concentration for REE recovery and extraction using alkali fusion acid leaching for the CFA in this study. However, REEs that were extracted the most were not necessarily recovered the most. LREEs were generally extracted more than MREEs and HREEs. On the other hand, HREEs and MREEs were recovered similarly and were also recovered more than LREEs. This was due to the difference in mineral associations of the LREE compared to MREEs and HREEs. MREEs and HREEs were more abundant in the same minerals such as goethite, hematite and almandine. LREEs were more abundant in different minerals, such as allanite, ilmenite and rutile.

The alkali fusion-acid leaching method was able to recover REEs from the CFA in this study however the low recovery (33-34%) even at the optimal concentration of 2 mol/L showed that there is still a substantial amount of REEs retained in the acid leached residues. XRD and TIMA results showed that although the alkali fusion-acid leaching method was able to dissolve REE-bearing minerals (mullite, quartz, allanite zircon etc) these minerals were not dissolved completely. This could be one of the reasons why there were low REE recoveries and extractions from the CFA in the study using the alkali fusion-acid leaching method. Changing alkali fusion conditions by increasing fusion temperature or time to further break down the acid-resistant REE-bearing phases could improve REE recoveries.

REE recovery using the alkali fusion-acid leaching method has environmental implications. The concentration of trace elements was determined using the ICP-Ms analytical technique. The lixiviant and solid residue that was separated after the leaching process both had trace elements that were environmentally concerning. The lixiviant of all the CFA has low pH with the presence of trace elements of major concern Pb, As, Cr and Hg including the radionuclides Th and U. All the trace elements in the lixiviant that were documented by DWAF (1996) had concentrations higher than their respective TWQR for all three CFA in the study except for

101

Hg. The recovery of most trace elements was lower than the recovery of TREEs from Tutuka and Kendal CFA. However, in the Duvha CFA, the recovery of all the trace elements was lower than the recovery of REEs. The recovery of Pb, Cu and Sr was higher than the recovery of TREEs in the Tutuka and Kendal CFA

The lixiviant requires further treatment to reduce pH and remove the trace elements V, Mn, Cu and Zn and with special regard given to the removal of Pb, As, Cr and U before disposal. The solid residue had all the trace elements found in the original CFA however at much lower concentrations. Trace elements of major concern like Pb and Cr and radionuclides Th and U were removed to a significant degree. The alkali fusion-acid leaching method results in a lixiviant with low pH and a high concentration of trace elements of major environmental concern. However, the solid residue has these trace elements in much lower concentrations than the lixiviant and original CFA making the residue safer to dispose of in the environment.

6   Conclusion and recommendations

6.1   Introduction

REEs have been recognised as critical raw materials that are an important part of many emerging technologies (Franus et al., 2015). Their demand has been increasing in the past decades due to their unique electrochemical, magnetic, and luminescent properties (Taggart et al., 2018). As a result of the increasing demand for REEs, there has been an investigation of secondary sources, including coal deposits and coal combustion residues. The investigation of CFA as a potential source of REE is a new research area and it is attracting a fair amount of attention and investment globally (Taggart et al., 2016, 2018; King et al., 2018; Tang et al., 2019; Wang et al., 2019). Despite this, there is limited knowledge of REE occurrence in South African coals and CFA (Wagner & Matiane, 2018). There has also been extensive research going into characterizing REEs in CFA (Ripfumelo, 2012; Franus et al., 2015; Taggart et al., 2016; Wagner & Matiane, 2018) but, little has been done to determine efficient extraction methods to recover REEs from CFA (King et al., 2018). Acid concentration has been proven to be one of the most influential factors in REE acid leaching experiments (Taggart et al., 2018; Tang et al., 2019; Pan et al., 2020). However, the optimal acid concentration for the recovery of REEs from CFA differs for different studies (Cao et al., 2018; Tang et al., 2019; Rybak & Rybak, 2021).

The study aimed to investigate the effectiveness of alkali fusion-acid leaching for the recovery of REEs from South African CFA and determine the optimal acid concentration for REE recovery in South African CFA. To achieve the aim South African CFA was characterized according to major and trace elements and mineral phases. Then the alkali fusion acid leaching method was used to examine the relationship between REE recovery and acid leaching concentration to determine the optimal acid concentration for the recovery of REEs from the CFA. Finally, the presence and concentration of trace elements that were co-extracted with REEs from CFA in acid leached lixiviant and those present in the solid residue were examined to determine whether these elements are of environmental concern.

6.2   Characteristics of South African CFA

The Tutuka, Kendal and Duvha CFA exhibit Class F characteristics. The pozzolanic characteristic of Class CFA makes it excellent in enhancing concrete performance and as a result, the building and construction industries have widely investigated CFA utilisation within these industries. Therefore it can be utilized as a replacement or addition to portland cement

concrete (PCC) (ASTM C 618, 1993). The CFAs also had a substantial amount of REEs and a range of other trace elements. Duvha CFA (573.77 ppm) had more REEs than Tutuka (526.35 ppm) and Kendal CFA (567.68 ppm). The study confirmed that REEs occur in acid-resistant REE-bearing phases such as mullite, quartz, rutile zircon found in the CFA. Thus, preconditioning of the CFA using alkali fusion was needed to break acid-resistant REE-bearing phases before being leached with a strong acid to recover REEs. Overall, this study showed that the Tutuka, Kendal and Duvha CFA could provide a substantial amount of REEs in South Africa. However, the feasibility of recovery depends on the development of extraction technologies that could be tailored to REE-bearing phases like aluminosilicate glass, mullite, quartz and ilmenite and hematite.

6.3   Effect of acid concentration on the extraction and recovery REEs using alkali fusion-acid leaching method

This study has shown that acid concentration has a significant effect on REE extraction and recovery from CFA using the alkali fusion-acid leaching method. The acid concentration of 2 mol/L was the optimal concentration for REE recovery using alkali fusion acid leaching for the CFA in this study. REE extraction and recovery increased as HCl concentration increased from 1 to 2 mol/L and decreased as acid concentration increased to 3 mol/L. A silicic acid gel layer formed when leaching CFA at 2 mol/L and became thicker with an increase in acid leaching concentration to 3 mol/L. The formation of a silicon-rich gel layer over the CFA was possibly the main factor that limited the subsequent diffusion of REEs. In addition, the study showed that the alkali fusion-acid leaching favoured the recovery of medium rare earth elements (MREEs) and heavy rare earth elements (HREEs) over light rare earth elements (LREEs) because of their mineral associations. Duvha CFA recovered more (34%) REEs than both Kendal and Tutuka CFA (33%). Furthermore, Duvha CFA had a greater abundance of REEs than both Kendal and Tutuka CFA. Therefore, Duvha CFA is more viable than Kendal and Tutuka CFA for REE recovery using the alkali fusion acid leaching method. The study also showed that although the alkali fusion-acid leaching method was able to dissolve REE-bearing minerals (mullite, quartz, allanite zircon etc) these minerals were not dissolved completely. This could be one of the reasons why there were low REE recoveries and extractions from the CFA in the study using the alkali fusion-acid leaching method. The alkali fusion conditions might not have been ideal to break acid-resistant phases.

6.4 Environmental implications of REE recovery from South African CFA using the alkali fusion – acid leaching method.

The disposal of the leachate and solid residue after REE recovery using the alkali fusion-acid leaching method has environmental implications. The study showed that leachate of all the CFA has low pH with the presence of trace elements of major concern lead (Pb), arsenic (As) chromium (Cr) and mercury (Hg) including the radionuclides thorium (Th) and uranium (U). All the trace elements in the leachate that were documented by DWAF (1996) had concentrations higher than their respective Target Water Quality Range (TWQR) for all three CFA in the study except for Hg, Zn and Cu. Thus, the disposal of leachate without further treatment can be environmentally harmful. The solid leached residue still had all the trace elements found in the original CFA including Pb and Cr and radionuclides Th and U. However, the trace elements were less concentrated in the residue, making it safer to dispose of than the original CFA.

6.5 Recommendations

- The REE-bearing phases were still present in the solid leached residues after alkali fusion-acid leaching increasing the alkali fusion temperature or time to break these phases could improve the REE recovery from CFA by making them more accessible during leaching.

- The formation of silicic acid gel was a limiting factor for the recovery of REEs in South African CFA. To improve REE recoveries from low CaO content CFA alkali fused CFA can be leached with water before being leached with acid to remove the majority of silica before acid leaching. A study by Pan et al. (2020) examined the recovery of REEs from CFA through sequential chemical roasting, water leaching, and acid leaching processes and found promising results.

- The solid leached residues in the study still had REEs present. Therefore, the CFA can be leached again to recover the REEs.

- The alkali fusion-acid leaching lixiviants have high concentrations of environmentally harmful trace elements. Therefore, trace element removal from the leachate is recommended before disposal. The addition of an alkali to the leachate after acid leaching is also recommended to improve the pH and aid in the downstream separation of REEs from leachate.

- There is limited research on REE separation from the leachate produced from acid leaching. REE separation methods will need to be developed to selectively recover

105

REEs from the leachate. REE recovery generates highly acidic lixiviants that will require highly selective separation methods to recover the REEs from other major soluble ions.

- Valuable trace elements such as Zn, Pb and Cu where selectively recovered with REEs using the alkali fusion-acid leaching method, thus the alkali fusion-acid leaching method can also be used to recover these valuable elements as well.

106

7   References

Akinyemi, S. A. (2011). *Geochemical and mineralogical evaluation of toxic contaminants mobility in weathered coal fly ash : as a case study , Tutuka dump site , South Africa* (Issue May). University of the Western Cape.

Akinyemi, S. A., Gitari, W. M., Akinlua, A., & Petrik, L. F. (2012). Mineralogy and Geochemistry of Sub-Bituminous Coal and Its Combustion Products from Mpumalanga Province, South Africa. *Analytical Chemistry*, *October*. https://doi.org/10.5772/50692

Alonso, E., Sherman, A. M., Wallington, T. J., Everson, M. P., Field, F. R., Roth, R., & Kirchain, R. E. (2012). Evaluating rare earth element availability: A case with revolutionary demand from clean technologies. *Environmental Science and Technology*, *46*(6), 3406–3414. https://doi.org/10.1021/es203518d

An, D. L. (2014). *Critical Rare Earths, National Security, and U.S.-China Interactions: A Portfolio Approach to Dysprosium Policy Design*. www.rand.org

ASTM C 618. (1993). *Annual Book of ASTM Standards. ASTM, Philadelphia, PA*.

Balaram, V. (2019). Rare earth elements: A review of applications, occurrence, exploration, analysis, recycling, and environmental impact. *Geoscience Frontiers*, *10*(4), 1285–1303. https://doi.org/10.1016/j.gsf.2018.12.005

Bisaka, K., Thobadi, I. C., & Pawlik, C. (2017). Extraction of rare earths from iron-rich rare earth deposits. *Journal of the Southern African Institute of Mining and Metallurgy*, *117*(8), 731–739. https://doi.org/10.17159/2411-9717/2017/v117n8a2

Bohlmann, H. R., Horridge, J. M., Inglesi-Lotz, R., Roos, E. L., & Stander, L. (2019). Regional employment and economic growth effects of South Africa's transition to low-carbon energy supply mix. *Energy Policy*, *128*(July 2018), 830–837. https://doi.org/10.1016/j.enpol.2019.01.065

Bunaciu, A. A., Udriştioiu, E. gabriela, & Aboul-Enein, H. Y. (2015). X-Ray Diffraction: Instrumentation and Applications. *Critical Reviews in Analytical Chemistry*, *45*(4), 289–299. https://doi.org/10.1080/10408347.2014.949616

Cao, S., Zhou, C., Pan, J., Liu, C., Tang, M., Ji, W., Hu, T., & Zhang, N. (2018). Study on Influence Factors of Leaching of Rare Earth Elements from Coal Fly Ash. *Energy and Fuels*, *32*(7), 8000–8005. https://doi.org/10.1021/acs.energyfuels.8b01316

Chen, Z. (2011). Global rare earth resources and scenarios of future rare earth industry. *Journal of Rare Earths*, *29*(1), 1–6. https://doi.org/10.1016/S1002-0721(10)60401-2

Dai, S., Zhao, L., Peng, S., Chou, C. L., Wang, X., Zhang, Y., Li, D., & Sun, Y. (2010). Abundances and distribution of minerals and elements in high-alumina coal fly ash from the Jungar Power Plant, Inner Mongolia, China. *International Journal of Coal Geology*, *81*(4), 320–332. https://doi.org/10.1016/j.coal.2009.03.005

DWAF. (1996). *Department of Water Affairs and Forestry Water Quality Guidlines Field Guide* (C. E. S. S Holmes (ed.); 2nd ed.). Department of Water Affairs and Forestry.

Eskom Holdings SOC Ltd. (2020a). *Duvha Power Station*. Eskom Heritage. https://www.eskom.co.za/sites/heritage/Pages/Duvha.aspx

Eskom Holdings SOC Ltd. (2020b). *Kendal Power Station*. https://www.eskom.co.za/Whatweredoing/ElectricityGeneration/PowerStations/Pages/Kendal_Power_Station.aspx

Eskom Holdings SOC Ltd. (2020c). *Tutuka Power Station*. http://www.eskom.co.za/Whatweredoing/ElectricityGeneration/PowerStations/Pages/Tutuka_Power_Station.aspx

Eze, C. P. (2011). *Chemical, Physical and Morphological Changes in Weathered Coal Fly Ash: A Case Study of Brine Impacted Wet Ash Dump*. University of the Western Cape.

Eze, C. P. (2014). *Determination of toxic elements, rare earth elements and radionuclides in coal fly ash, products and waste* (Issue December). University of the Western Cape.

Eze, C. P., Fatoba, O., Madzivire, G., Ostrovnaya, T. M., Petrik, L. F., Frontasyeva, M. V., & Nechaev, A. N. (2014). Elemental composition of fly ash: a comparative study using nuclear and related analytical techniques. *Chemistry-Didactics-Ecology-Metrology*, *18*(1–2), 19–29. https://doi.org/10.2478/cdem-2013-0014

Eze, C. P., Nyale, S. M., Akinyeye, R. O., Gitari, W. M., Akinyemi, S. A., Fatoba, O. O., & Petrik, L. F. (2013). Chemical, mineralogical and morphological changes in weathered coal fly ash: A case study of a brine impacted wet ash dump. *Journal of Environmental Management*, *129*, 479–492. https://doi.org/10.1016/j.jenvman.2013.07.024

Falcon, R. (1988). The Characteristics of Southern African Coals.pdf. *Journal- South African Institute of Mining and Metallurgy*, *88*(5), 145–161.

Fass, R., Geva, J., Shalita, Z. P., White, M. D., & Fleming, J. C. (1994). *Bioleaching Method for the Extraction of Metals from Coal Fly Ash using Thobacillus*.

Fatoba, O. O. (2010). *Chemical interactions and mobility of species in fly ash-brine co-disposal systems* (Issue November). University of the Western Cape.

Finkelman, R. B. (1999). Trace elements in coal. Environmental and health significance. *Biological Trace Element Research*, *67*(3), 197–204. https://doi.org/10.1007/BF02784420

Franus, W., Wiatros-Motyka, M. M., & Wdowin, M. (2015). Coal fly ash as a resource for rare earth elements. *Environmental Science and Pollution Research*, *22*(12), 9464–9474. https://doi.org/10.1007/s11356-015-4111-9

Gharabaghi, M., Noaparast, M., & Irannajad, M. (2009). Selective leaching kinetics of low-grade calcareous phosphate ore in acetic acid. *Hydrometallurgy*, *95*(3–4), 341–345.

Ghasemi, A., & Zahediasl, S. (2012). Normality Tests for Statistical Analysis: A Guide for Non-Statisticians. *Int J Endocrinol Metab*, *10*(2), 486–495. https://doi.org/10.5812/ijem.3505

Gitari, W. M., Fatoba, O. O., Petrik, L. F., & Vadapalli, V. R. K. (2009). Leaching characteristics of selected South African fly ashes: Effect of pH on the release of major and trace species. *Journal of Environmental Science and Health - Part A Toxic/Hazardous Substances and Environmental Engineering*, *44*(2), 206–220. https://doi.org/10.1080/10934520802539897

Gollakota, A. R. K., Volli, V., & Shu, C. M. (2019). Progressive utilisation prospects of coal fly ash: A review. *Science of the Total Environment*, *672*(April), 951–989. https://doi.org/10.1016/j.scitotenv.2019.03.337

Gottlieb, P., & Dosbaba, M. (2015). *The Use of the TIMA Automated Mineral Analyzer for the Characterisation of Ore Deposits and Optimization of Process Operations*. *September*.

Guo-qiang, W., Tao, W., Jia-wei, W., Yong-sheng, Z., & Wei-ping, P. (2020). Occurrence forms of rare earth elements in coal and coal gangue and their combustion products. In *Journal Of Fuel Chemistry And Technology* (Vol. 48, Issue 12).

Gupta, C. ., & Krishnamurthy, N. (2004). *Extractive Metallurgy of Rare Earths*. CRC Press, Boca Raton, FL.

Hagen, M. Van Der, & Järnberg, J. (2009). *Sulphuric, hydrochloric, nitric and phosphoric acids* (Vol. 43).

Hancox, P. J., & Götz, A. E. (2014). South Africa's coalfields - A 2014 perspective. In *International Journal of Coal Geology* (Vol. 132, pp. 170–254). Elsevier. https://doi.org/10.1016/j.coal.2014.06.019

Hart, R. J., Leahy, R., & Falcon, R. . (1982). Geochemical investigation of the Witbank coalfield using instrumental neutron activation analysis. *J. Radioanal. Chem.*, *71*(1–2), 285–297. https://doi.org/https://doi.org/10.1007/BF02516156

Hood, M. M., Taggart, R. K., Smith, R. C., Hsu-Kim, H., Henke, K. R., Graham, U., Groppo, J. G., Unrine, J. M., & Hower, J. C. (2017). Rare Earth Element Distribution in Fly Ash Derived from the Fire Clay Coal , Kentucky. *Coal Combustion and Gasification Products*. https://doi.org/10.4177/CCGP-D-1

Hower, J. C., Groppo, J. G., Henke, K. R., Graham, U. M., Hood, M. M., Joshi, P., & Preda, D. V. (2017). Ponded and Landfilled Fly Ash as a Source of Rare Earth Elements from a Kentucky Power Plant. *Coal Combustion and Gasification Products*, *9*(1), 1–21. https://doi.org/10.4177/ccgp-d-17-00003.1

Hower, J. C., Qian, D., Briot, N. J., Santillan-Jimenez, E., Hood, M. M., Taggart, R. K., & Hsu-Kim, H. (2019). Nano-scale rare earth distribution in fly ash derived from the combustion of the fire clay coal, kentucky. *Minerals*, *9*(4), 27–32. https://doi.org/10.3390/min9040206

Hower, J., Groppo, J., Joshi, P., Dai, S., Moecher, D., & Johnston, M. (2003). Location of Cerium in Coal-Combustion Fly Ashes: Implications for Recovery of Lanthanides. *Coal Combustion and Gasification Products*, *5*(1), 73–78. https://doi.org/10.4177/ccgp-d13-00007.1

Huang, K., Inoue, K., Harada, H., Kawakita, H., & Ohto, K. (2011). Leaching behavior of heavy metals with hydrochloric acid from fly ash generated in municipal waste incineration plants. *Transactions of Nonferrous Metals Society of China (English Edition)*, *21*(6), 1422–1427. https://doi.org/10.1016/S1003-6326(11)60876-5

Huang, Z., Fan, M., & Tian, H. (2019). Rare earth elements of fly ash from Wyoming's Powder River Basin coal. *Journal of Rare Earths*. https://doi.org/10.1016/j.jre.2019.05.004

Izquierdo, M., & Querol, X. (2012). Leaching behaviour of elements from coal combustion fly ash: An overview. *International Journal of Coal Geology*, *94*, 54–66. https://doi.org/10.1016/j.coal.2011.10.006

Jeffrey, L. (2005). Characterization of the coal resources of South Africa. *The Journal of The South African Institute of Mining and Metallurgy*, 97–101. https://www.saimm.co.za/Journal/v105n02p095.pdf

Jha, M. K., Kumari, A., Panda, R., Rajesh Kumar, J., Yoo, K., & Lee, J. Y. (2016). Review on hydrometallurgical recovery of rare earth metals. *Hydrometallurgy*, *165*, 2–26. https://doi.org/10.1016/j.hydromet.2016.01.035

Johnson, S. (2021). *Advantages & Disadvantages of XRD and XRF*. Sciencing.Com. https://sciencing.com/advantages-disadvantages-xrd-xrf-6054766.html

Kashiwakura, S., Kumagai, Y., Kubo, H., & Wagatsuma, K. (2013). Dissolution of Rare Earth Elements from Coal Fly Ash Particles in a Dilute Sulphuric Acid Solvent. *Open Journal of Physical Chemistry*, *03*(02), 69–75. https://doi.org/10.4236/ojpc.2013.32009

Kaußen, F. M., & Friedrich, B. (2016). Methods for Alkaline Recovery of Aluminum from Bauxite Residue. *Journal of Sustainable Metallurgy*, *2*(4), 353–364. https://doi.org/10.1007/s40831-016-0059-3

Ketris, M. P., & Yudovich, Y. E. (2009). Estimations of Clarkes for Carbonaceous biolithes: World averages for trace element contents in black shales and coals. *International Journal of Coal Geology*, *78*(2), 135–148. https://doi.org/10.1016/j.coal.2009.01.002

Khan, I., & Umar, R. (2019). Environmental risk assessment of coal fly ash on soil and groundwater quality, Aligarh, India. *Groundwater for Sustainable Development*, *8*, 346–357. https://doi.org/10.1016/J.GSD.2018.12.002

Kim, R., Cho, H., Han, K. N., Kim, K., & Mun, M. (2016). Optimization of acid leaching of rare-earth elements from mongolian apatite-based ore. *Minerals*, *6*(3). https://doi.org/10.3390/min6030063

King, J. F., Taggart, R. K., Smith, R. C., Hower, J. C., & Hsu-Kim, H. (2018). Aqueous acid and alkaline extraction of rare earth elements from coal combustion ash. *International Journal of Coal Geology*, *195*, 75–83. https://doi.org/10.1016/j.coal.2018.05.009

Kolker, A., Scott, C., Hower, J. C., Vazquez, J. A., Lopano, C. L., & Dai, S. (2017).

Distribution of rare earth elements in coal combustion fly ash, determined by SHRIMP-RG ion microprobe. *International Journal of Coal Geology*, *184*, 1–10. https://doi.org/10.1016/j.coal.2017.10.002

Koukouzas, N., Ward, C. R., Papanikolaou, D., Li, Z., & Ketikidis, C. (2009). Quantitative evaluation of minerals in fly ashes of biomass, coal and biomass-coal mixture derived from circulating fluidised bed combustion technology. *Journal of Hazardous Materials*, *169*, 100–107. https://doi.org/10.1016/j.jhazmat.2009.03.116

Kruskal, W. H., & Wallis, W. A. (1952). Use of Ranks in One-Criterion Variance Analysis. *Journal of the American Statistical Association*, *47*(260), 583–621. https://doi.org/10.1080/01621459.1952.10483441

Levenspiel, O. (1999). *Chemical reaction engineering. Ind. Eng. Chem. Res (Vol 38).*

Lichte, F. E., Meier, A. L., & Crock, J. G. (1987). Determination of the rare-earth elements in geological materials by inductively coupled plasma mass spectrometry. *Analytical Chemistry*, *59*(8), 1150–1157. https://pubs.er.usgs.gov/publication/70014731

Lidwala Consulting Engineers (SA) (Pty) Ltd. (2014). *Tutuka Continuous Ashing: Final EIA Report Chapter* (Issue December).

Lin, R., Soong, Y., Howard, B. H., Keller, M. J., Roth, E. A., Wang, P., & Granite, E. J. (2021). Leaching of rare earth elements and yttrium from a central appalachian coal and the ashes obtained at 550–950 oC2. *Journal of Rare Earths*.

Lin, R., Stuckman, M., Howard, B. H., Bank, T. L., Roth, E. A., Macala, M. K., Lopano, C., Soong, Y., & Granite, E. J. (2018). *Application of sequential extraction and hydrothermal treatment for characterization and enrichment of rare earth elements from coal fly ash*. https://doi.org/10.1016/j.fuel.2018.05.141

Liu, P., Huang, R., & Tang, Y. (2019). *Comprehensive Understandings of Rare Earth Element (REE) Speciation in Coal Fly Ashes and Implication for REE Extractability*. https://doi.org/10.1021/acs.est.9b00005

Maledi, N. . (2017). *Characterisation of Mineral Matter in South African Coals Using Micro-Raman Spectroscopy and Other Techniques Nthabiseng Beauty Maledi*. University of the Witwatersrand.

Mann, H. B., & Whitney, D. R. (1947). On a Test of Whether one of Two Random Variables

is Stochastically Larger than the Other. *The Annals of Mathematical Statistics*, *18*(1), 50–60. https://doi.org/10.1214/aoms/1177730491

Mayfield, D. B., & Lewis, A. S. (2013). Environmental Review of Coal Ash as a Resource for Rare Earth and Strategic Elements. *2013 World of Coal Ash (WOCA) Conference*, *May*, 22–25. https://www.researchgate.net/profile/David_Mayfield2/publication/256979903_Environmental_Review_of_Coal_Ash_as_a_Resource_for_Rare_Earth_and_Strategic_Elements/links/00b495241cad856612000000/Environmental-Review-of-Coal-Ash-as-a-Resource-for-Rare-Earth-an

Meier, A. L., Lichte, F. E., Briggs, P. H., & Bullock Jr., J. H. (1996). Coal ash by inductively coupled plasma-atomic emission spectrometry and inductively coupled plasma-mass spectrometry. *In: Arbogast, B.F. (Ed.), Analytical Methods Manual for the Mineral Resources Surveys Program. U.S. Geological Survey, Denver, CO*.

Meier, A. L., & Slowik, T. (2002). Rare earth elements by inductively coupled plasma-mass spectrometry. *In: Taggart Jr.J.E. (Ed.), Analytical Methods for Chemical Analysis of Geologic and Other Materials. U.S. Geological Survey (Version 5.0 Ed)*.

Methode Kalombe, R., Ojumu, T. V., Katambwe, V. N., Nzadi, M., Bent, D., Nieuwouldt, G., Madzivire, G., Kevern, J., & Petrik, L. F. (2020). *Treatment of acid mine drainage with coal fly ash in a jet loop reactor pilot plant*. https://doi.org/10.1016/j.mineng.2020.106611

Moolman, D. (2011). *Baseline Study of Kendal Power Station*. University of the Free State.

Munawer, M. E. (2018). Human health and environmental impacts of coal combustion and post-combustion wastes. In *Journal of Sustainable Mining* (Vol. 17, Issue 2, pp. 87–96). Central Mining Institute in Katowice. https://doi.org/10.1016/j.jsm.2017.12.007

Nemai Consulting. (2019). *Duvha Power Station Ash Dam, Raw and Ash Water Returns Dams Seepage Interception Drains in Mpumalanga Province Basic Assessment Report*. www.nemai.co.za

Norrish, K., & Hutton, J. T. (1969). An accurate X-ray spectrographic method for the analysis of geologic samples. *Geochemica et Cosmochimica Acta 33*, 431–454.

Pan, J., Hassas, V., Rezaee, M., Zhou, C., & Pisupati, S. V. (2020). Recovery of rare earth elements from coal fly ash through sequential chemical roasting, water leaching, and acid

leaching processes. *Journal of Cleaner Production*. https://doi.org/10.1016/j.jclepro.2020.124725

Pan, J., Nie, T., Hassas, B. V., Rezaee, M., Wen, Z., & Zhou, C. (2020). Recovery of rare earth elements from coal fly ash by integrated physical separation and acid leaching. *Chemosphere*, 126112. https://doi.org/10.1016/j.chemosphere.2020.126112

Pan, J., Zhou, C., Tang, M., Cao, S., Liu, C., Zhang, N., Wen, M., Luo, Y., Hu, T., & Ji, W. (2018). Study on the modes of occurrence of rare earth elements in coal fly ash by statistics and a sequential chemical extraction procedure. *Fuel*, *237*(2019), 555–565. https://doi.org/10.1016/j.fuel.2018.09.139

PerkinElmer. (2011). *The 30-minute Guide to ICP-MS*. https://doi.org/10.1016/j.pnucene.2012.01.005

Petrik, L. (2004). Simultaneous water recovery and utilization of two harmful effluents; fly ash leachate and acid mine drainage, for the production of high capacity inorganic ion exchange material useful for water beneficiation. *University of the Western Cape. COALTECH 2020*, *September*, 38–40.

Ray, H., & Ray, S. (2018). Chemically Controlled Reactions. In *Kinetics of Metallurgical Processes. Indian Institute of Metals Series*. Springer, Singapore. https://doi.org/https://doi.org/10.1007/978-981-13-0686-0_3

Reynolds-Clausen, K., & Singh, N. (2017). *Eskom's revised Coal Ash Strategy and Implementation Progress*.

Reynolds-Clausen, K., & Singh, N. (2019). South Africa's Power Producer's Revised Coal Ash Strategy and Implementation Progress. *Coal Combustion and Gasification Products*, 10. https://doi.org/10.4177/CCGP-D-18-00015.1

Ripfumelo, M. A. (2012). *Consideration Of Rare Earth Elements (REE'S) Associated with Coal and Coal Ash in South Africa*. University of Johannesburg.

Rybak, A., & Rybak, A. (2021). Characteristics of some selected methods of rare earth elements recovery from coal fly ashes. *Metals*, *11*(1), 1–27. https://doi.org/10.3390/met11010142

SACAA. (2020). *Ash Benefits and Uses*. http://coalash.co.za/about-us/ash-benefits-uses

Seaman, J. (2010). *Rare Earths and Clean Energy: Analyzing China's Upper Hand*.

Seidel, A., & Zimmels, Y. (1998). Mechanism and kinetics of aluminum and iron leaching from coal fly ash by sulfuric acid. *Chemical Engineering Science*. https://doi.org/10.1016/S0009-2509(98)00201-2

Seredin, V. V., & Dai, S. (2012). Coal deposits as potential alternative sources for lanthanides and yttrium. In *International Journal of Coal Geology* (Vol. 94, pp. 67–93). Elsevier. https://doi.org/10.1016/j.coal.2011.11.001

Shapiro, S. S., & Wilk, M. B. (1965). An analysis of variance test for normality (complete samples). *Biometrika*, *52*(3–4), 591–611. https://doi.org/doi.org/10.1093/biomet/52.3-4.591

Shemi, A. (2013). *Extraction of Aluminium from Coal Fly Ash using a Two-Step Acid Leach Process*. University of Witwatersrand.

Sheskin, D. J. (2011). Parametric Versus Nonparametric Tests. *In: Lovric M. (Eds) International Encyclopedia of Statistical Science*. https://doi.org/https://doi.org/10.1007/978-3-642-04898-2_440

South African Department of Energy. (2019). *Directorate: Energy data collection, management and analysis. The South African energy sector report 2019*.

Taggart, R. K. (2017). *Recovery of Rare Earth Elements from Coal Combustion Ash: Survey, Extraction, and Speciation*.

Taggart, R. K., Hower, J. C., Dwyer, G. S., & Hsu-Kim, H. (2016). Trends in the Rare Earth Element Content of U.S.-Based Coal Combustion Fly Ashes. *Environmental Science and Technology*, *50*(11), 5919–5926. https://doi.org/10.1021/acs.est.6b00085

Taggart, R. K., Hower, J. C., & Hsu-Kim, H. (2018). Effects of roasting additives and leaching parameters on the extraction of rare earth elements from coal fly ash. *International Journal of Coal Geology*, *196*(2018), 106–114. https://doi.org/10.1016/j.coal.2018.06.021

Tang, M., Zhou, C., Pan, J., Zhang, N., Liu, C., Cao, S., Hu, T., & Ji, W. (2019). Study on extraction of rare earth elements from coal fly ash through alkali fusion – Acid leaching. *Minerals Engineering*, *136*(March), 36–42. https://doi.org/10.1016/j.mineng.2019.01.027

Taylor, S. R., & McLennan, S. M. (1985). *The Continental Crust: its Composition and Evolution*. Blackwell.

U.S. Geological Survey. (2018). Mineral commodity summaries 2018. In *Geological Survey*. https://doi.org/doi.org/10.3133/70194932.

US Department of Energy. (2017). *Report on Rare Earth Elements from Coal and Coal Byproducts*. *January*, 1–49. https://edx.netl.doe.gov/ree/.%0Ahttps://www.energy.gov/sites/prod/files/2018/01/f47/EXEC-2014-000442 - for Conrad Regis 2.2.17.pdf

Vadapalli, V. R. K., Gitari, M. W., Petrik, L. F., Etchebers, O., & Ellendt, A. (2012). Integrated acid mine drainage management using fly ash. *Journal of Environmental Science and Health - Part A Toxic/Hazardous Substances and Environmental Engineering*, *47*(1), 60–69. https://doi.org/10.1080/10934529.2012.629582

Wagner, N. J., & Matiane, A. (2018). Rare earth elements in select Main Karoo Basin (South Africa) coal and coal ash samples. *International Journal of Coal Geology*, *196*(February), 82–92. https://doi.org/10.1016/j.coal.2018.06.020

Walawalkar, M., Nichol, C. K., & Azimi, G. (2016). Process investigation of the acid leaching of rare earth elements from phosphogypsum using HCl, HNO3, and H2SO4. *Hydrometallurgy*, *166*, 195–204. https://doi.org/10.1016/j.hydromet.2016.06.008

Wang, Q., Song, X., & Liu, Y. (2020). China's coal consumption in a globalizing world: Insights from Multi-Regional Input-Output and structural decomposition analysis. *Science of the Total Environment*, *711*, 134790. https://doi.org/10.1016/j.scitotenv.2019.134790

Wang, Z., Dai, S., Zou, J., French, D., & Graham, I. T. (2019). Rare earth elements and yttrium in coal ash from the Luzhou power plant in Sichuan, Southwest China: Concentration, characterization and optimized extraction. *International Journal of Coal Geology*, *203*, 1–14. https://doi.org/10.1016/j.coal.2019.01.001

Ward, C. R., French, D., Jankowski, J., Dubikova, M., Li, Z., & Riley, K. W. (2009). Element mobility from fresh and long-stored acidic fly ashes associated with an Australian power station. *International Journal of Coal Geology*, *80*, 224–236. https://doi.org/10.1016/j.coal.2009.09.001

Weltje, G. J., & Tjallingii, R. (2008). Calibration of XRF core scanners for quantitative geochemical logging of sediment cores: Theory and application. *Earth and Planetary Science Letters*, *274*(3–4), 423–438. https://doi.org/10.1016/j.epsl.2008.07.054

Wen, C. Y. (1968). Non-catalytic Heterogeneous Solid-fluid Reaction Models. *Industrial and Engineering Chemistry*, *60*(9), 34–54. https://doi.org/10.1021/ie50705a007

Wilschefski, S. C., & Baxter, M. R. (2019). Inductively Coupled Plasma Mass Spectrometry: Introduction to Analytical Aspects. *Clinical Biochemist Reviews*, *40*(3), 115–133. https://doi.org/10.33176/AACB-19-00024

Xia, Y. (2020). The Microbiome in Health and Disease. *Progress in Molecular Biology and Translational Science*.

Yang, X. (2019). *Leaching Characteristics of Rare Earth Elements From Bituminous Coal-Based Sources*.

Yao, Z., Ji, X., Sarker, P., Tang, J., Ge, L., Xia, M., & Xi, Y. (2014). *A comprehensive review on the applications of coal fly ash*. https://doi.org/10.1016/j.earscirev.2014.11.016

Zhang, W., & Honaker, R. (2020). Characterization and recovery of rare earth elements and other critical metals (Co, Cr, Li, Mn, Sr, and V) from the calcination products of a coal refuse sample. *Fuel*, *267*, 117236. https://doi.org/10.1016/J.FUEL.2020.117236

Zithole Consulting. (2000). *Report on Kendal Power Station: 30 Year Ash Disposal Facility Project Conceptual Engineering Report No : 12935-45-Rep-001-*.

8   Appendices

118

Appendix A:

Sample Characterization

Table A1: Major elements of CFA in the study as determined by XRF.

Content (wt%)	Tutuka CFA	Duvha CFA	Kendal CFA
SiO_2	52.22	54.25	52.48
Al_2O_3	27.47	28.65	29.57
Fe_2O_3	5.18	4.07	4.64
MnO	0.06	0.04	0.05
MgO	1.53	0.94	1.53
CaO	4.87	3.57	5.59
Na_2O	0.29	0.06	0.18
K_2O	0.83	0.63	0.86
TiO_2	1.44	1.72	1.57
P_2O_5	0.42	0.65	0.50
Cr_2O_3	0.03	0.03	0.03
NiO	0.01	0.01	0.00
LOI	5.22	5.18	2.59
Total	99.57	99.80	99.61

LOI = Loss of Ignition

Table A2: Concentration of REEs in ppm for Tutuka, Kendal and Duvha CFA as determined by the ICP-MS analytical technique

REEs	Tutuka	Kendal	Duvha
Sc	24.20	25.58	27.52
La	95.19	104.52	99.41
Ce	194.53	216.56	216.98
Pr	20.01	22.00	21.59
Nd	74.98	79.58	76.67
Sm	14.43	15.24	14.64
Y	56.59	56.65	69.89
Eu	2.69	2.77	2.68
Gd	13.27	13.71	13.15
Tb	1.92	2.01	2.06
Dy	11.62	12.07	12.27
Ho	2.32	2.37	2.37
Er	6.42	6.54	6.73
Tm	0.90	0.92	0.93
Yb	6.44	6.36	6.03
Lu	0.83	0.80	0.87
TREE	526.35	567.68	573.77
LREEs	399.14	437.91	429.28
MREEs	86.10	87.21	100.05
HREEs	16.91	16.98	16.92
Critical	154.22	159.61	170.29
Uncritical	142.90	155.48	148.78
Excessive	205.03	227.01	227.17
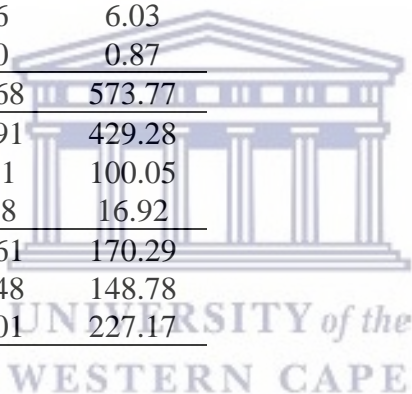
Table A3: Primary minerals in Tutuka, Kendal and Duvha CFA as determined by the TIMA analytical technique.

Primary phases Content (%)	Tutuka CFA	Kendal CFA	Duvha CFA
Actinolite	0.0734	0.0106	0.0004
Al2SiO5 polymorphs	0.0081	0.0029	0.0032
Albite	0.0788	0.0132	0.0115
Allanite-(Ce)	0.0255	0.0238	0.0073
Almandine_spessartine	1.1327	0.2699	0.5975
Alumosilicates mixture	0.3833	0.5748	1.1841
Andradite	0.0921	0.0288	0.0173
Ankerite	0.0616	0.0512	0.1282
Apatite	0.0064	0.0154	0.0146
Baryte	0.0005	0.0000	-
Beryl	0.2729	0.2312	0.5007
Biotite	0.4335	0.0166	0.0546
Calcite	0.0796	0.1092	0.2071
Cerussite	0.0003	0.0000	0.0008
Chlorite - Chamosite	0.0394	0.0116	0.0252
Chlorite - Clinochlore	0.8451	0.0129	0.0728
Chromite	0.0038	0.0212	0.0062
Corundum	0.0063	0.0000	0.0075
Cuprite	0.0062	0.0000	0.0129
Diopside	0.0452	0.0011	0.0105
Dolomite	0.0007	0.0018	0.0158
Enstatite	0.0006	0.0000	0.0063
Epidote	0.0083	0.0000	0.0009
Ferro-Actinolite	0.0048	0.0038	0.0047
Ferrogedrite	0.0055	-	-
Goethite	0.1793	0.0740	0.1095
Grossular	0.1892	0.1184	0.1191
Hematite/Magnetite	1.4714	0.5411	0.9213
Ilmenite	0.0250	0.0000	0.0059
Kaersutite	0.2736	0.0174	0.0083
Kaolinite	13.5270	25.1304	23.0141
Monazite	0.0066	0.0000	0.0012
Muscovite	0.1632	0.0567	0.0579
Nepheline	0.0010	0.0000	0.0048
Olivine	0.0110	0.0059	0.0017
Orthoclase	0.6165	0.0437	0.1185
Plagioclase	13.5657	13.3702	2.0051
Pyrope	0.0522	0.0233	0.0092
Quartz	9.0984	6.1490	6.6314
Romanechite	0.0034	-	-
Rutile	0.0527	0.0283	0.0533

Primary phases Content (%)	Tutuka CFA	Kendal CFA	Duvha CFA
Sillenite	0.0001	0.0000	-
Sphalerite	0.0005	-	-
Tantalite-(Fe)	0.0161	0.0000	0.0374
Tantalite-(Mn)	0.0074	0.0000	0.0235
Titanite	0.0028	-	-
Topaz	0.0003	-	-
Zircon	0.0233	0.0091	0.0212
Zoisite	0.7151	0.3936	0.2911
Florencite-(La)	-	0.0000	-
Hemimorphite	-	0.0000	-
Xenotime-(Y)	-	0.0000	0.0003
Gypsum	-	-	0.0001
Baddeleyite	-	-	0.0003
The rest	**0.0001**	**51.6725**	**0.0001**

Table A4: Elemental percentage of EDX spectrum of Ilmenite as determined by the TIMA analytical technique.

Element	weight %
Ti	34.7427
Fe	31.4348
O	30.0264
Al	1.2707
Si	1.1834
Ce	0.6278
La	0.4692
Pr	0.2449
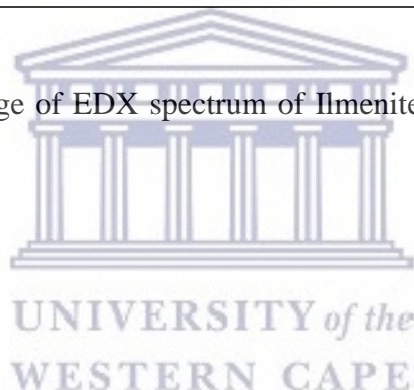
Table A5: Elemental percentage of EDX spectrum of hematite as determined by the TIMA analytical technique.

Element	weight %
Fe	59.3498
O	30.2972
Eu	3.8466
Ca	2.2698
Si	2.1823
Al	1.7989
Lu	0.2554

Table A6: Elemental percentage of EDX spectrum of zircon as determined by the TIMA analytical technique

Element	weight %
Zr	43.0006
O	35.8101
Si	13.6893
Fe	3.0915
Ca	2.9435
Y	1.4649

Table A7: Elemental percentage of EDX spectrum of calcite as determined by the TIMA analytical technique

Element	weight %
Ca	52.9556
O	37.2971
Al	6.4558
Si	2.328
Sc	0.9635

UNIVERSITY *of the*
WESTERN CAPE

Appendix B:

Sample Calculations
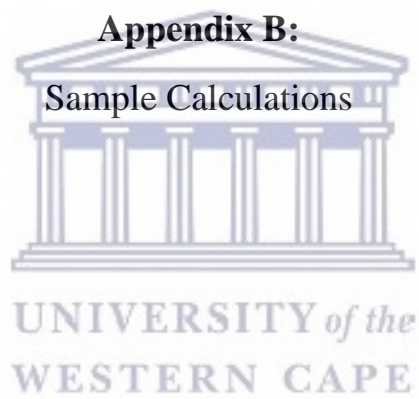
B.1 Acid preparation equation

$$C_1 V_1 = C_2 V_2 \qquad \textit{(A-1)}$$

$$V_1 = \frac{C_2 V_2}{C_1} \qquad \textit{(A-2)}$$

C_1 = concentration of the stock acid in mol/L

V_1 = volume of acid that was added to the solvent (deionised water) in ml

C_2 = concentration of the solution after dilution mol/L

V_2 = the volume of the flask that will contain the solution ml

Calculating volume of solvent required to prepare 1 mol/L of HCl

$$V_1 = \frac{C_2 V_2}{C_1}$$
$$V_1 = \frac{(1 \, mol/l)(500 \, ml)}{(10.2 \, mol/l)} = 49.02 \, ml$$

2 mol/L HCl preparation:

$$V_1 = \frac{(2 \, mol/l)(500 \, ml)}{(10.2 \, mol/l)} = 98.04 \, ml$$

3 mol/L HCl preparation :

$$V_1 = \frac{(3 \, mol/l)(500 \, ml)}{(10.2 \, mol/l)} = 147.06 \, ml$$

Appendix C:

Rare earth element extraction
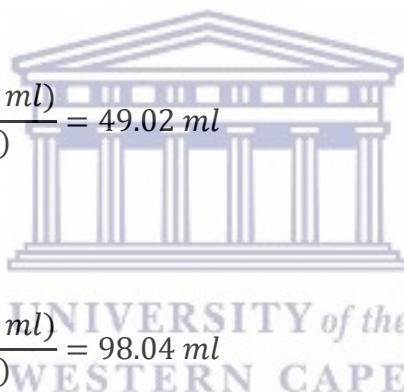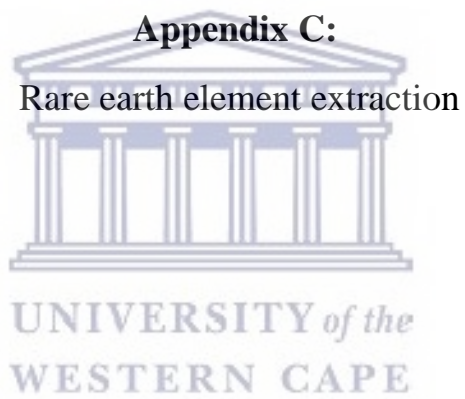
Table C1: Effect of acid concentration (at 1, 2 and 3 mol/L HCl) on the extraction of REEs (in ppm) from Tutuka, Kendal and Duvha CFA as determined by ICP-MS.

Elements	T1M	K1M	D1M	T2M	K2M	D2M	T3M	K3M	D3M
Sc	0.001	0.000	0.001	0.285	0.160	0.480	0.744	0.746	0.256
Y	0.010	0.002	0.055	2.702	2.938	3.461	1.949	1.890	0.705
La	0.000	0.000	0.000	3.659	4.115	4.212	2.854	2.952	1.032
Ce	0.000	0.000	0.000	4.065	4.891	4.195	4.796	4.916	1.733
Pr	0.000	0.000	0.000	0.773	0.849	0.947	0.602	0.620	0.213
Nd	0.000	0.000	0.000	2.961	3.182	3.439	2.323	2.300	0.780
Sm	0.000	0.000	0.000	0.591	0.597	0.597	0.461	0.449	0.160
Eu	0.000	0.000	0.000	0.109	0.109	0.105	0.081	0.081	0.028
Gd	0.000	0.000	0.001	0.569	0.574	0.572	0.425	0.428	0.150
Tb	0.000	0.000	0.000	0.090	0.093	0.092	0.067	0.067	0.023
Dy	0.000	0.000	0.000	0.558	0.564	0.601	0.400	0.412	0.141
Ho	0.000	0.000	0.000	0.111	0.115	0.122	0.080	0.080	0.028
Er	0.000	0.000	0.000	0.323	0.332	0.330	0.230	0.228	0.083
Tm	0.000	0.000	0.000	0.045	0.047	0.045	0.033	0.033	0.012
Yb	0.000	0.000	0.000	0.290	0.286	0.287	0.215	0.201	0.075
Lu	0.000	0.000	0.000	0.041	0.041	0.043	0.030	0.029	0.011
Note:	T =Tutuka, K=Kendal, D=Duvha , M=mol/L								

Table C2: Effect of acid concentration on the extraction of LREEs, MREEs and HREEs from Tutuka, Kendal and Duvha CFA.

CFA	Class	1 mol/L	2 mol/L	3 mol/L
Tutuka	LREEs	0.00	12.05	11.04
	MREEs	0.01	4.03	2.92
	HREEs	0.00	0.81	0.59
Kendal	LREEs	0.00	13.63	11.24
	MREEs	0.00	4.28	2.88
	HREEs	0.00	0.82	0.57
Duvha	LREEs	0.00	13.39	3.92
	MREEs	0.06	4.83	1.05
	HREEs	0.00	0.83	0.21

Table C3: The effect of acid concentration on TREE extraction from Tutuka, Kendal and Duvha CFA.

CFA	1 mol/L	2 mol/L	3 mol/L
Tutuka	0.01	17.17	15.29
Kendal	0.00	18.89	15.43
Duvha	0.06	19.53	5.43

UNIVERSITY *of the*

WESTERN CAPE

Appendix D:

Rare earth element recovery

Table D1: Effect of acid concentration (1, 2 and 3 mol/L) on recovery of individual REEs from Tutuka, Kendal and Duvha CFA

		Tutuka CFA			Kendal CFA			Duvha CFA		
	REEs	1 mol/L	2 mol/L	3 mol/L	1 mol/L	2 mol/L	3 mol/L	1 mol/L	2 mol/L	3 mol/L
	Sc	0.026	11.78	30.73	0.02	6.25	29.16	0.05	17.45	9.31
LREEs	La	0.000	38.44	29.98	0.00	39.37	28.24	0.00	42.37	10.38
	Ce	0.000	20.90	24.65	0.00	22.58	22.70	0.00	19.33	7.98
	Pr	0.000	38.61	30.08	0.00	38.61	28.18	0.00	43.86	9.85
	Nd	0.002	39.50	30.98	0.00	39.98	28.90	0.01	44.85	10.18
	Sm	0.001	40.95	31.93	0.00	39.15	29.49	0.00	40.77	10.90
MREEs	Y	0.185	47.74	34.43	0.03	51.87	33.37	0.78	49.53	10.09
	Eu	0.000	40.44	30.01	0.00	39.27	29.30	0.01	39.37	10.46
	Gd	0.013	42.89	32.02	0.00	41.85	31.23	0.09	43.47	11.39
	Tb	0.000	46.72	34.72	0.00	46.37	33.16	0.00	44.60	11.28
	Dy	0.000	48.04	34.44	0.00	46.75	34.17	0.00	48.95	11.48
HREEs	Ho	0.000	47.63	34.50	0.00	48.59	33.93	0.01	51.72	11.99
	Er	0.003	50.36	35.87	0.00	50.76	34.84	0.01	49.02	12.39
	Tm	0.009	49.85	36.84	0.00	50.80	35.93	0.01	48.89	12.64
	Yb	0.008	44.96	33.41	0.00	44.95	31.57	0.02	47.67	12.40
	Lu	0.008	50.04	35.98	0.00	51.72	36.45	0.02	49.24	12.28

Table D2: The effect of acid concentration on the recovery of LREEs, MREEs HREEs and TREEs from Tutuka, Kendal and Duvha CFA

CFA	Class	1 mol/L	2 mol/L	3 mol/L
Tutuka	LREEs	0.00	30.19	27.65
	MREEs	0.12	46.78	33.93
	HREEs	0.01	47.89	34.80
Kendal	LREEs	0.00	31.13	25.66
	MREEs	0.02	49.06	33.01
	HREEs	0.00	48.33	33.62
Duvha	LREEs	0.00	31.19	9.12
	MREEs	0.56	48.29	10.46
	HREEs	0.01	48.92	12.34

Table D3: The effect of acid concentration on TREE recovery from Tutuka, Kendal and Duvha CFA.

CFA	1 mol/L	2 mol/L	3 mol/L
Tutuka	0.02	32.62	29.05
Kendal	0.00	33.28	27.19
Duvha	0.10	34.03	9.46

Appendix E:

Statistical analysis

Table E1: Summary of descriptive statistics, including skewness, kurtosis and the Shapiro-Wilk Test of REE recovery data at different acid concentrations for Tutuka, Kendal and Duvha CFA. The skewness and kurtosis values of normally distributed data should be between -1.96 to +1.96 and the Shapiro-Wilk test and the alpha (α) level $p < 0.05$.

Acid concentration	Description	Statistic	Standard deviation
Tutuka CFA			
1 mol/L	Skewness	3.846	0.564
	Kurtosis	15.083	1.091
	Shapiro-Wilk (*p*)	< 0.001	
2 mol/L	Skewness	-1.912	0.564
	Kurtosis	3.506	1.091
	Shapiro-Wilk (*p*)	< .001	
3 mol/L	Skewness	-0.901	0.564
	Kurtosis	1.233	1.091
	Shapiro-Wilk (*p*)	0.180	
Kendal CFA			
1 mol/L	Skewness	2.722	0.564
	Kurtosis	6.643	1.091
	Shapiro-Wilk (*p*)	< .001	
2 mol/L	Skewness	-1.999	0.564
	Kurtosis	4.531	1.091
	Shapiro-Wilk (*p*)	0.001	
3 mol/L	Skewness	-0.636	0.564
	Kurtosis	0.563	1.091
	Shapiro-Wilk (*p*)	0.354	
Duvha CFA			
1 mol/L	Skewness	3.902	0.564
	Kurtosis	15.416	1.091
	Shapiro-Wilk (*p*)	< 0.001	
2 mol/L	Skewness	-1.947	0.564
	Kurtosis	3.138	1.091
		< 0.001	
3 mol/L	Skewness	-0.627	0.564
	Kurtosis	0.138	1.091
	Shapiro-Wilk (*p*)	0.439	

Table E2: The Kruskal-Wallis test was used to determine whether statistically significant differences ($p < 0.05$) in TREE recovery (%) at different acid concentrations for the Tutuka, Kendal and Duvha CFA.

Tutuka CFA				
H	**df**	**P**	**Acid concentration**	**Mean rank**
37.340	2	<.000	1 mol/L	8.50
			2 mol/L	38.50
			3 mol/L	26.50
Kendal CFA				
38.167	2	<.000	1 mol/L	8.50
			2 mol/L	38.50
			3 mol/L	26.50
Duvha CFA				
41.923	2	<.000	1 mol/L	8.50
			2 mol/L	40.50
			3 mol/L	24.50

Table E3: The Mann-Whitney U test was used for multiple comparisons to determine if each specific pair of acid concentrations differed significantly (defined as $p < 0.05$) concerning TREEs (%).

Acid concentration pairs	W (test statistic)	P (significance)	Mean ranks
Tutuka CFA			
1-2 mol/L	.000	<.000	8.50-24.50
2-3 mol/L	32.000	<.000	22.50-10.50
3-1 mol/L	.000	<.000	24.50-8.50
Kendal CFA			
1-2 mol/L	.000	<.000	8.50-24.50
2-3 mol/L	32.000	<.000	22.50-10.50
3-1 mol/L	.000	<.000	24.50-8.50
Duvha CFA			
1-2 mol/L	.000	<.000	8.50-24.50
2-3 mol/L	.000	<.000	24.50-8.50
3-1 mol/L	.000	<.000	24.50-8.50

Appendix F:

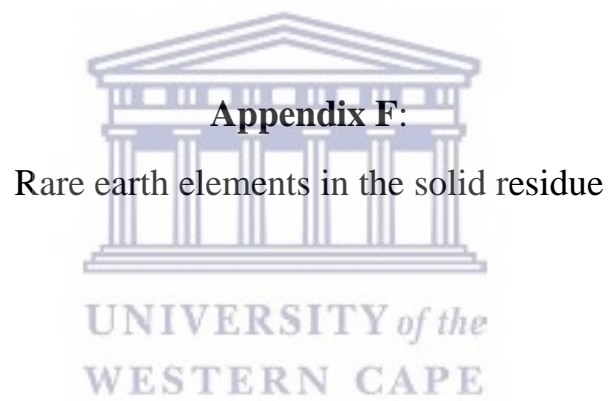Rare earth elements in the solid residue

Table F1: Primary minerals in Tutuka, Kendal and Duvha leached residues as determined by the TIMA analytical technique.

Primary phases Concentration (%)	Tutuka leached residue	Kendal leached residue	Duvha leached residue
Actinolite	0.0112	0.0014	-
Al2SiO5 polymorphs	0.0071	0.0095	0.01
Albite	0.0047	0.0033	0.02
Allanite-(Ce)	0.0002	0.0004	-
Almandine_spessartine	0.2351	0.3249	0.24
Alumosilicates mixture	42.9903	48.1592	-
Andradite	0.0018	0.0004	-
Apatite	0.0000	-	-
Baryte	0.0000	0.0004	-
Beryl	0.1607	0.2813	0.47
Biotite	0.0174	0.0054	0.01
Calcite	0.0071	0.0039	-
Chalcopyrite	0.0001	-	-
Chlorite - Chamosite	0.0078	0.0081	-
Chlorite - Clinochlore	0.0163	0.0268	0.03
Chromite	0.0017	0.0013	-
Corundum	0.0710	0.0501	0.01
Cuprite	0.0123	0.0219	-
Diopside	0.0028	0.0033	-
Dolomite	0.0001	0.0000	-
Enstatite	0.0015	0.0005	-
Epidote	0.0004	0.0002	-
Ferro-Actinolite	0.0002	0.0003	-
Goethite	0.0407	0.0621	0.04
Grossular	0.0060	0.0046	-
Gypsum	0.0006	0.0003	-
Hematite/Magnetite	0.4054	0.3443	0.37
Ilmenite	0.0162	0.0007	-
Kaersutite	0.0207	0.0041	-
Kaolinite	0.6772	1.4459	4.51
Monazite	0.0001	-	-
Muscovite	0.0158	0.0029	0.02
Nepheline	0.0006	0.0004	-
Olivine	0.0312	0.0086	-
Orthoclase	0.0349	0.0165	0.04
Plagioclase	2.0027	4.0909	0.94
Plumalsite	0.0005	0.0002	-
Pyrite	0.0001	-	-
Pyrope	0.0109	0.0023	-

Continued

Primary phases Concentration (%)	Tutuka leached residue	Kendal leached residue	Duvha leached residue
Pyrrhotite	0.0003	-	-
Quartz	1.8024	1.9974	5.37
Rutile	0.0326	0.0160	0.04
Schorl	0.3565	0.6637	0.12
Tantalite-(Fe)	0.0406	0.0241	0.02
Tantalite-(Mn)	0.0305	0.0200	0.02
Titanite	0.0004	0.0001	-
Topaz	0.0013	-	-
Wolframite	0.0000	0.0002	-
Zircon	0.0072	0.0117	0.02
Zoisite	0.0589	0.0811	-
Cerussite	-	0.0003	-
Xenotime-(Y)	-	0.0001	-
The rest	**0.0001**	**0.0003**	**0.06**

Table F2: Elemental percentage of EDX spectrum of rutile as determined by the TIMA analytical technique.

Element	weight %
Ti	51.9261
O	39.2805
Si	3.382
Al	1.3775
Ce	1.079
La	0.9323
Ca	0.9006
Cl	0.7743
Pr	0.3477

Table F3: Elemental percentage of EDX spectrum of hematite as determined by the TIMA analytical technique

Element	weight %
Fe	60.1906
O	29.0195
Sm	3.8861
Tb	2.3298
Eu	1.5906
Si	1.4526
Al	0.6387
Er	0.4036
Gd	0.3901
Dy	0.0983

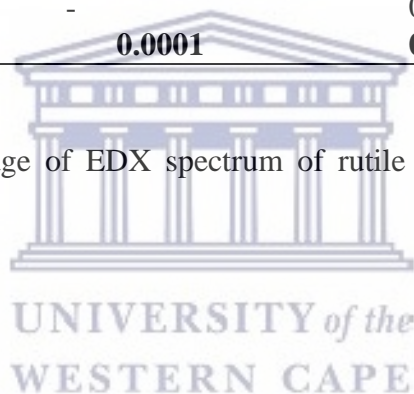**Table F4:** Elemental percentage of EDX spectrum of hematite as determined by the TIMA analytical technique

Element	weight %
Zr	46.476
O	38.3241
Si	14.7655
Y	0.4344

Table F5: Concentration of REEs in solid residue, lixiviant and leached residue of Tutuka, Kendal and Duvha CFA.

REEs	Tutuka CFA	Lixiviant	Residue	Kendal CFA	Lixiviant	Residue	Duvha CFA	Lixiviant	Residue
Sc	24.204	0.285	13.476	25.577	0.160	13.77	27.524	0.480	14.03
Y	56.591	2.702	15.714	56.647	2.938	17.01	69.89	3.461	18.03
La	95.189	3.659	27.795	104.524	4.115	32.53	99.408	4.212	36.22
Ce	194.53	4.065	90.582	216.562	4.891	98.10	216.978	4.195	115.78
Pr	20.014	0.773	5.777	22.001	0.849	6.72	21.588	0.947	7.89
Nd	74.975	2.961	21.220	79.579	3.182	24.40	76.668	3.439	28.65
Sm	14.427	0.591	3.968	15.243	0.597	4.58	14.637	0.597	4.97
Eu	2.69	0.109	0.699	2.769	0.109	0.78	2.676	0.105	0.86
Gd	13.274	0.569	3.743	13.714	0.574	4.20	13.149	0.572	4.79
Tb	1.919	0.090	0.540	2.012	0.093	0.62	2.058	0.092	0.68
Dy	11.622	0.558	3.162	12.066	0.564	3.65	12.274	0.601	4.08
Ho	2.32	0.111	0.628	2.368	0.115	0.71	2.366	0.122	0.83
Er	6.418	0.323	1.757	6.535	0.332	1.97	6.728	0.330	2.19
Tm	0.904	0.045	0.257	0.92	0.047	0.29	0.929	0.045	0.32
Yb	6.444	0.290	1.632	6.358	0.286	1.81	6.03	0.287	2.00
Lu	0.826	0.041	0.230	0.802	0.041	0.25	0.866	0.043	0.28

Appendix G:

Trace element concentrations in lixiviant and solid residue

140

Table G1: Recovery of trace elements compared to the recovery of REEs from Tutuka Kendal and Duvha CFA using the alkali fusion-acid leaching method.

Elements	Tutuka CFA	Kendal CFA	Duvha CFA
V	0.13	0.56	1.63
Cr	17.54	21.01	12.17
Co	29.05	25.98	14.94
Ni	24.08	22.20	12.30
Cu	35.68	38.19	20.37
Zn	32.65	30.51	17.19
Sr	49.49	40.22	22.39
Sn	0.03	0.08	1.05
Sb	0.17	0.22	1.79
Ba	2.71	8.10	2.07
Pb	45.44	36.98	20.61
Th	0.07	0.89	18.24
U	15.50	39.49	30.25
TREE	32.62	33.28	34.03